Imperial College London

Engineering and Physical Sciences Research Council

Exploiting the Resilience of Masonry Arch Bridge Infrastructure
Workshop, London 5-6 Sept. 2023

High-fidelity Simulation of Masonry Arch Bridges

M. El Ashri, S. Grosman,
L. Macorini and B.A. Izzuddin

Computational Structural Mechanics Group
Department of Civil and Environmental Engineering
Imperial College London
www.imperial.ac.uk/csm

ERMABI project context

Understanding:

Practical tools:

Impact:

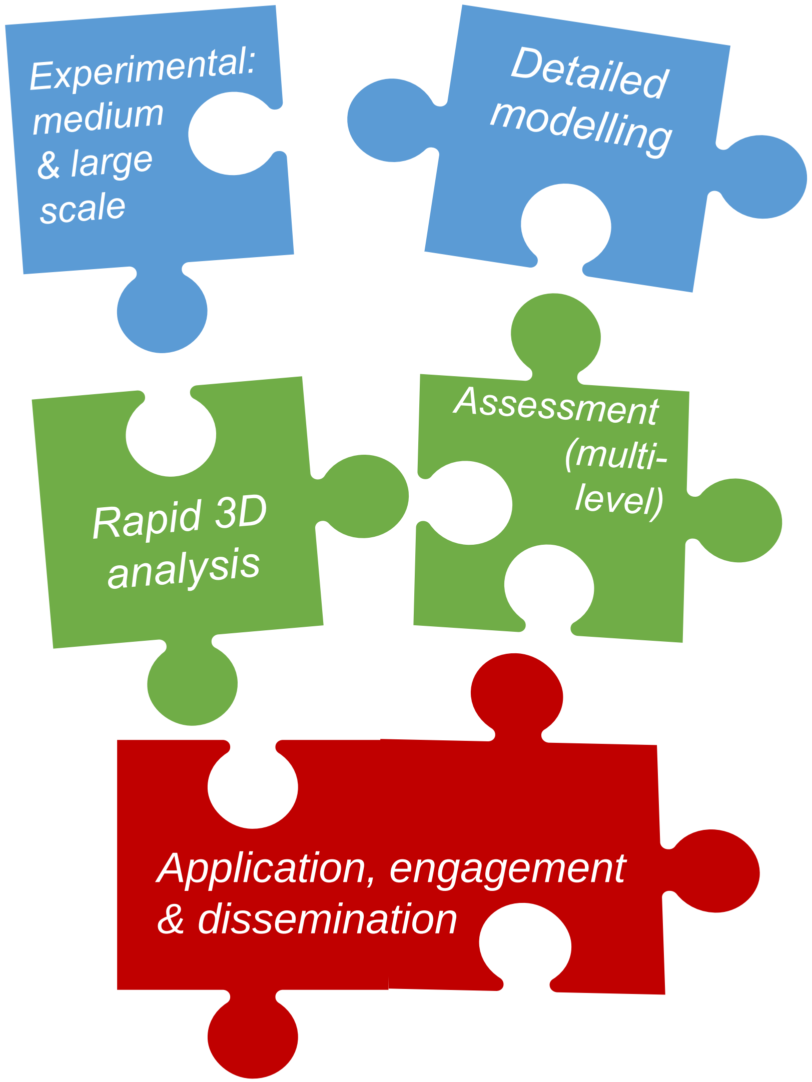

Engineering and Physical Sciences Research Council

ERMABI project context

Understanding:

Practical tools:

Impact:

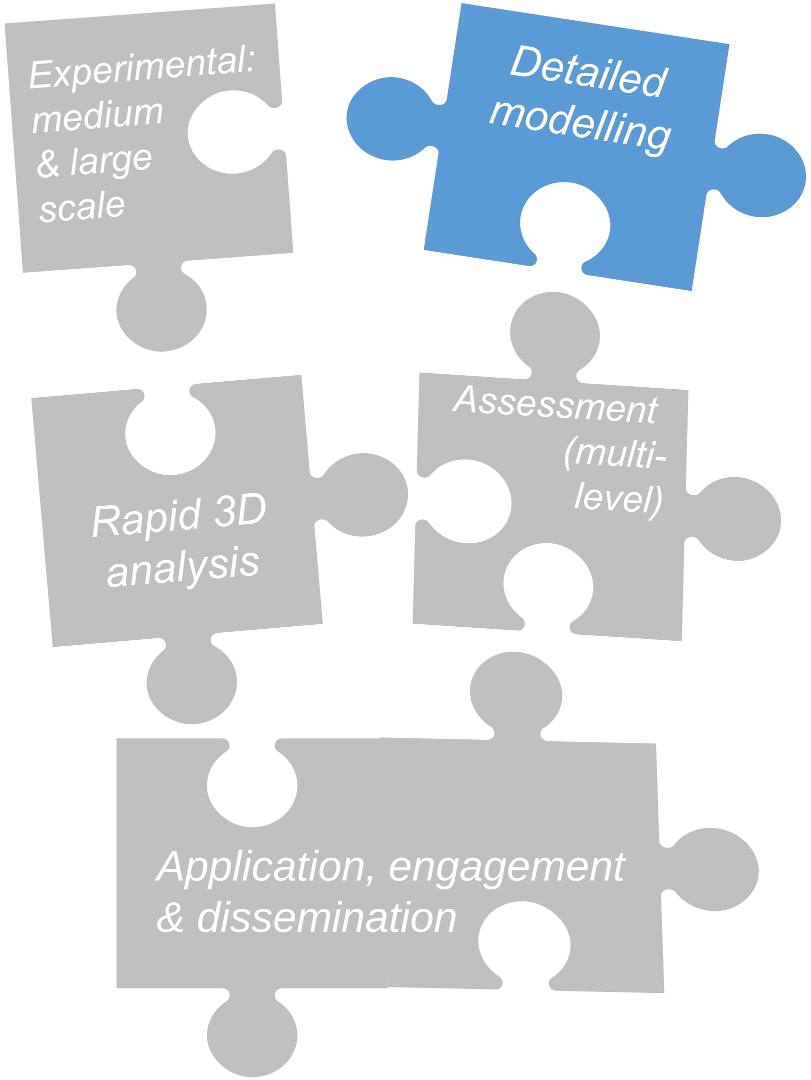

Engineering and Physical Sciences Research Council

Outline

- Masonry modelling capabilities
- Calibration of Material Parameters
- Validation of Numerical Models
  - Investigation of 3D Failure Modes
- Fatigue in Masonry
- Conclusions

Masonry modelling capabilities

Developments - CSM Group

3D mesoscale high-fidelity models

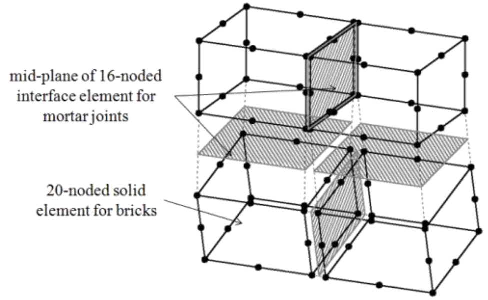

Masonry Modelling Capabilities

Engineering and Physical Sciences Research Council

Developments - CSM Group

3D mesoscale high-fidelity models

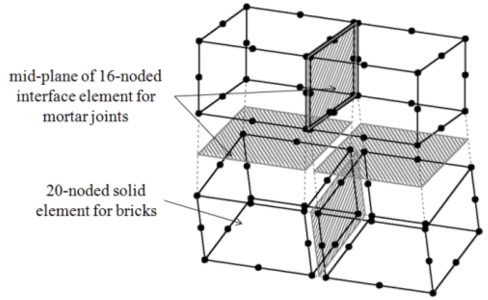

Plasticity damage formulation

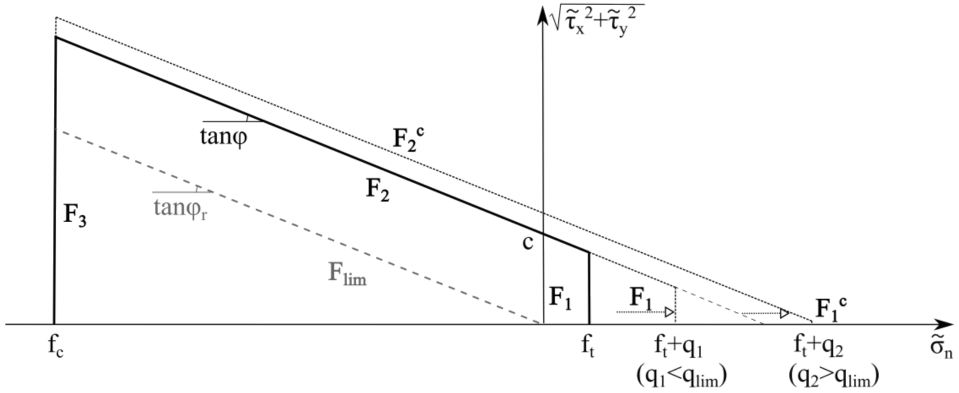

Minga et al. 2018

Masonry Modelling Capabilities

Developments - CSM Group

3D mesoscale high-fidelity models

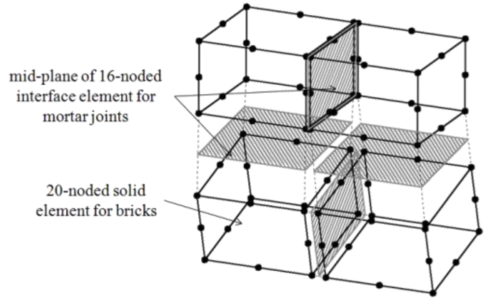

Yield functions

Cap in tension

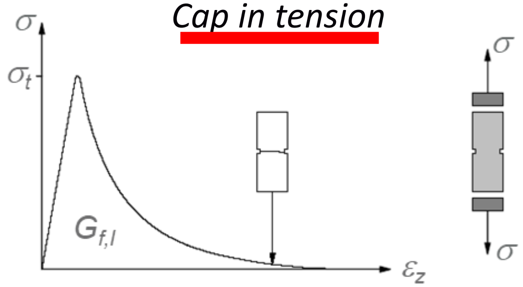

Plasticity damage formulation

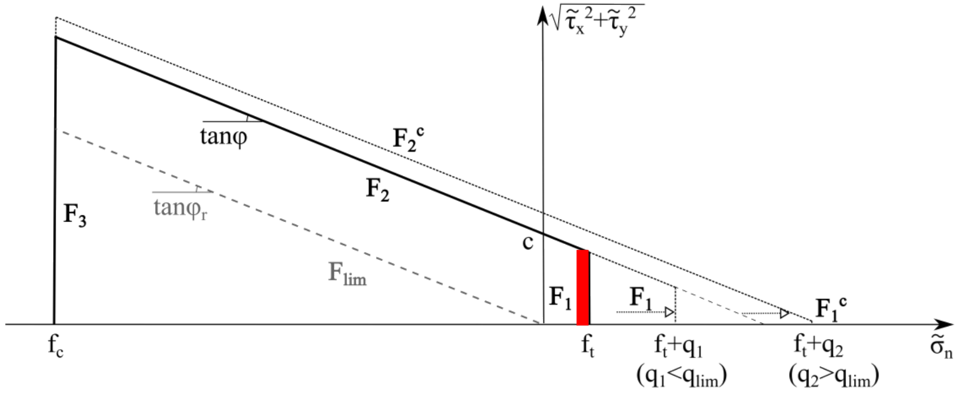

Minga et al. 2018

Masonry Modelling Capabilities

Developments - CSM Group

3D mesoscale high-fidelity models

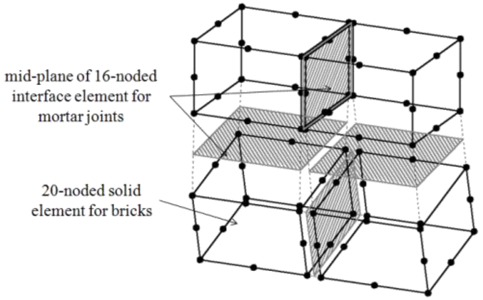

Plasticity damage formulation

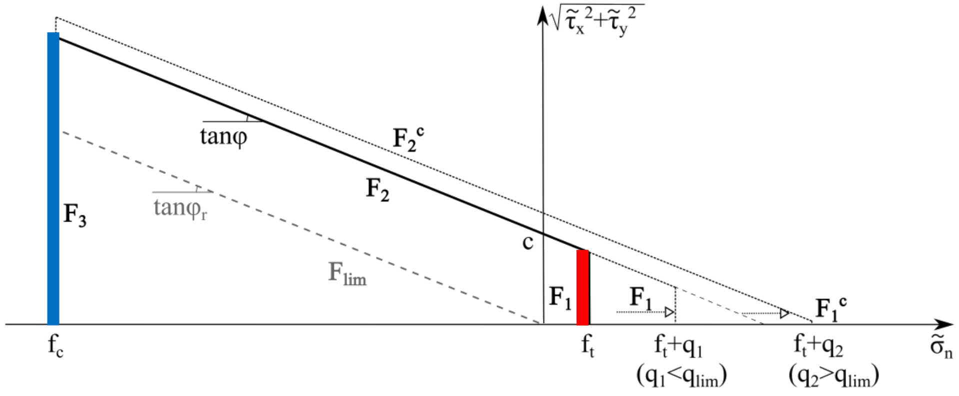

Yield functions

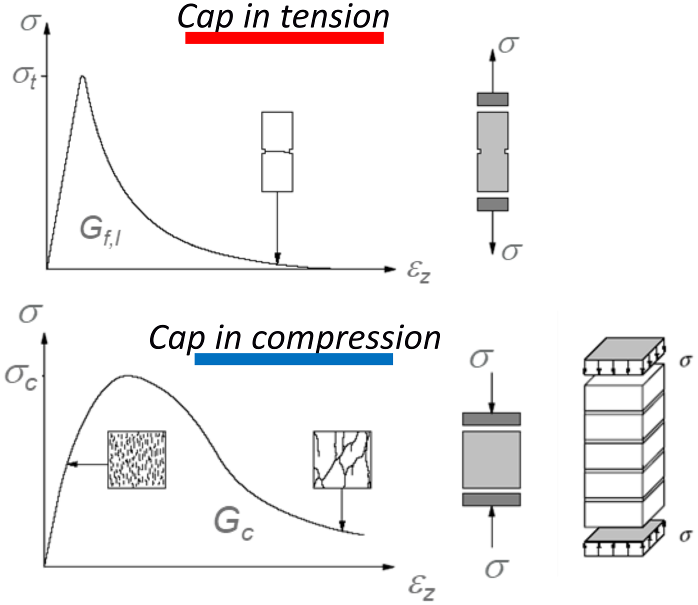

Masonry Modelling Capabilities

Developments - CSM Group

3D mesoscale high-fidelity models

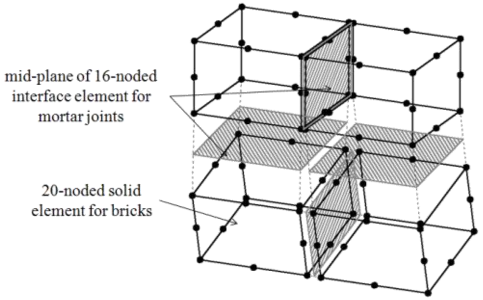

Plasticity damage formulation

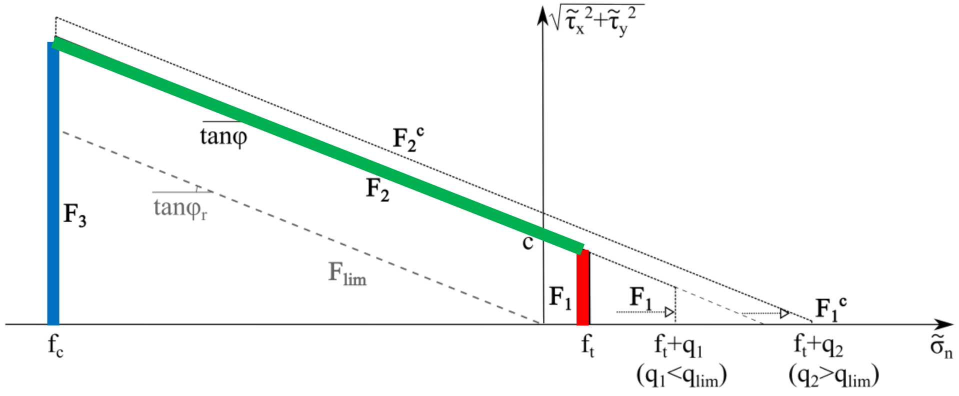

Minga et al. 2018

Yield functions

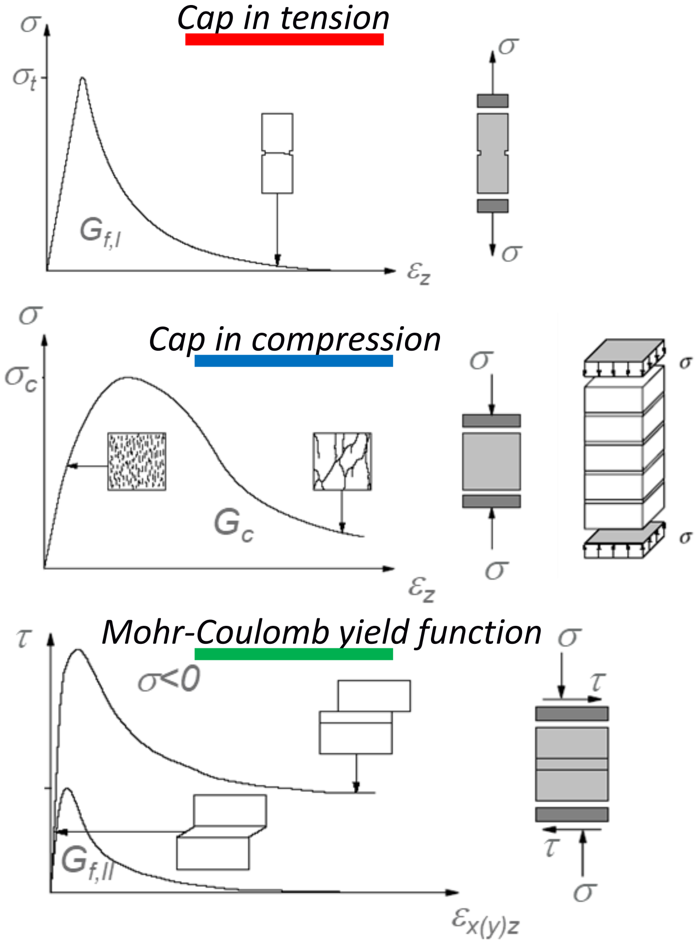

Masonry Modelling Capabilities

Developments - CSM Group

3D mesoscale high-fidelity models

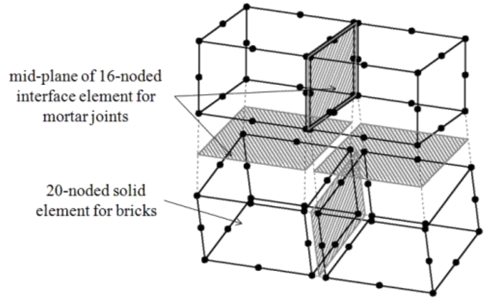

Plasticity damage formulation

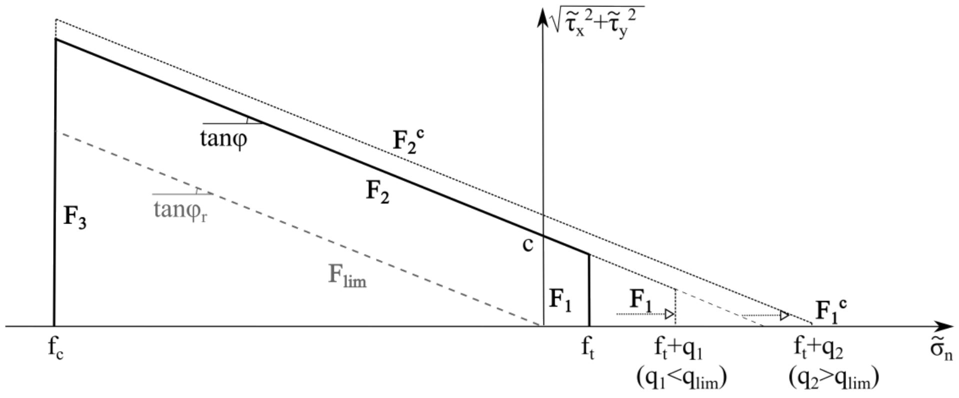

Minga et al. 2018

Yield functions

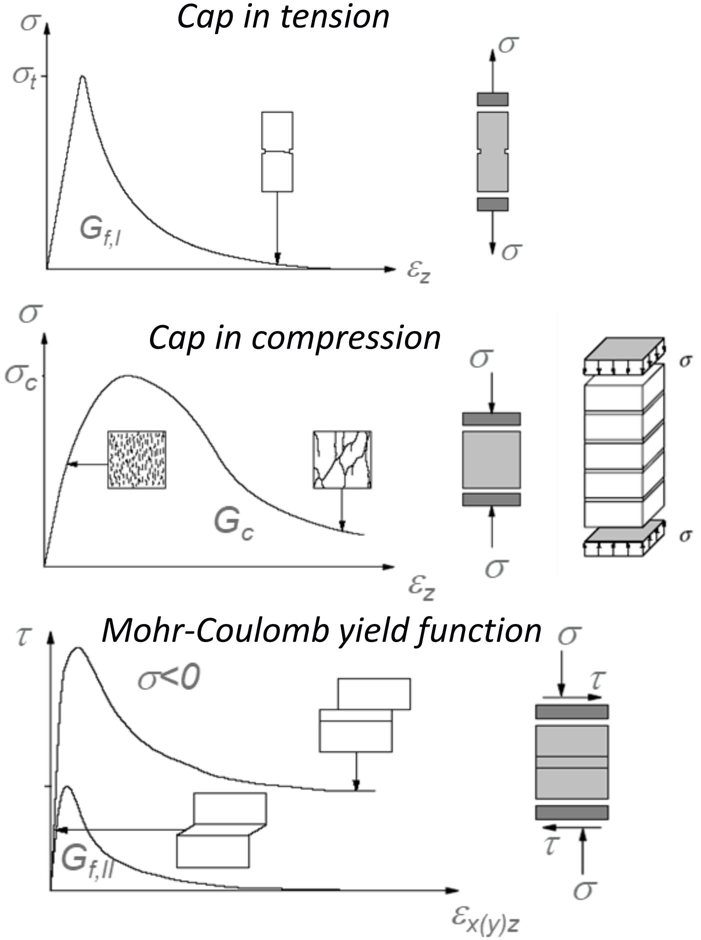

Cyclic behaviour

Normal direction

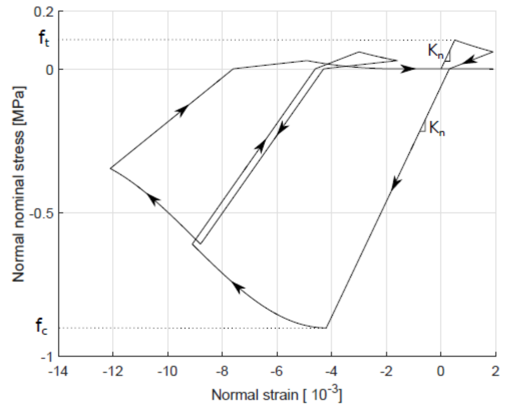

Tangential direction

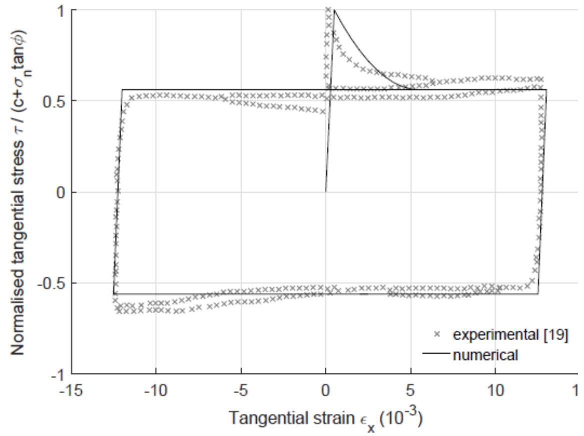

Developments - CSM Group

Nonlinear numerical analysis

ADAPTIC

Imperial College London

Masonry Modelling Capabilities

Engineering and Physical Sciences Research Council

Developments - CSM Group

Nonlinear numerical analysis

ADAPTIC

Parametric modelling tool

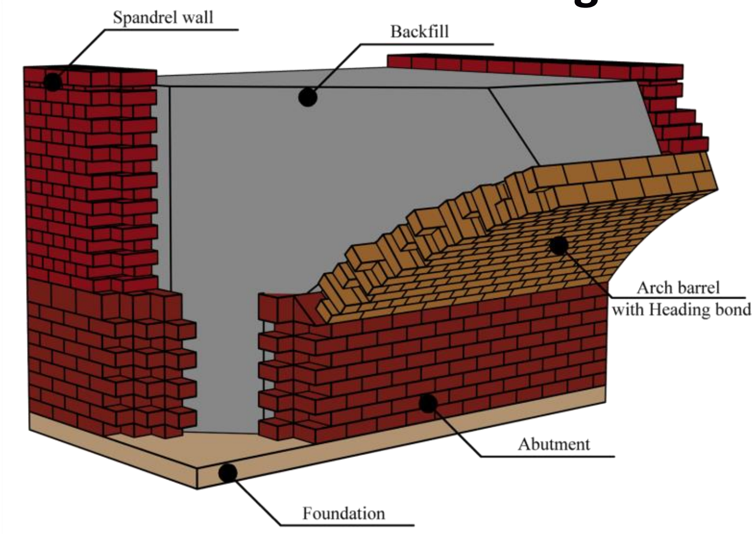

Masonry Modelling Capabilities

Developments - CSM Group

Nonlinear numerical analysis

ADAPTIC

Parametric modelling tool

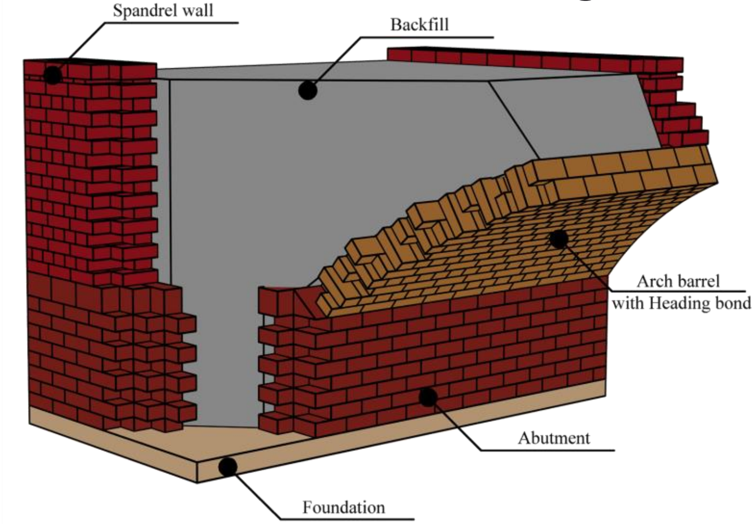

Bond pattern generation

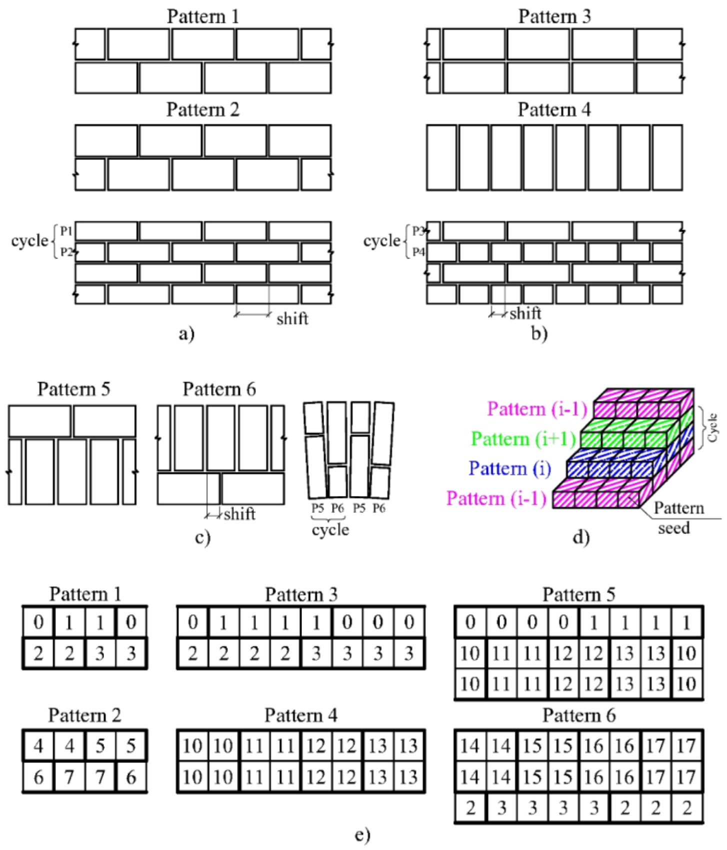

Grosman, Macorini & Izzuddin, B.A. (2023)

Masonry Modelling Capabilities

Developments - CSM Group

Nonlinear numerical analysis

ADAPTIC

Parametric modelling tool

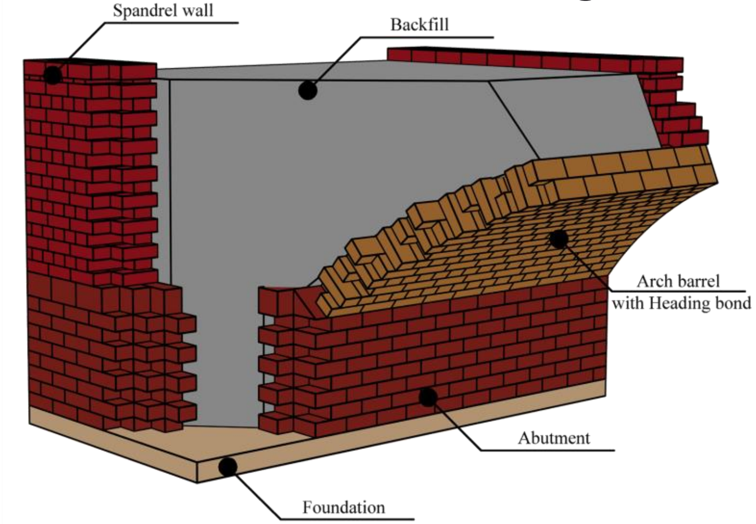

Bond pattern generation

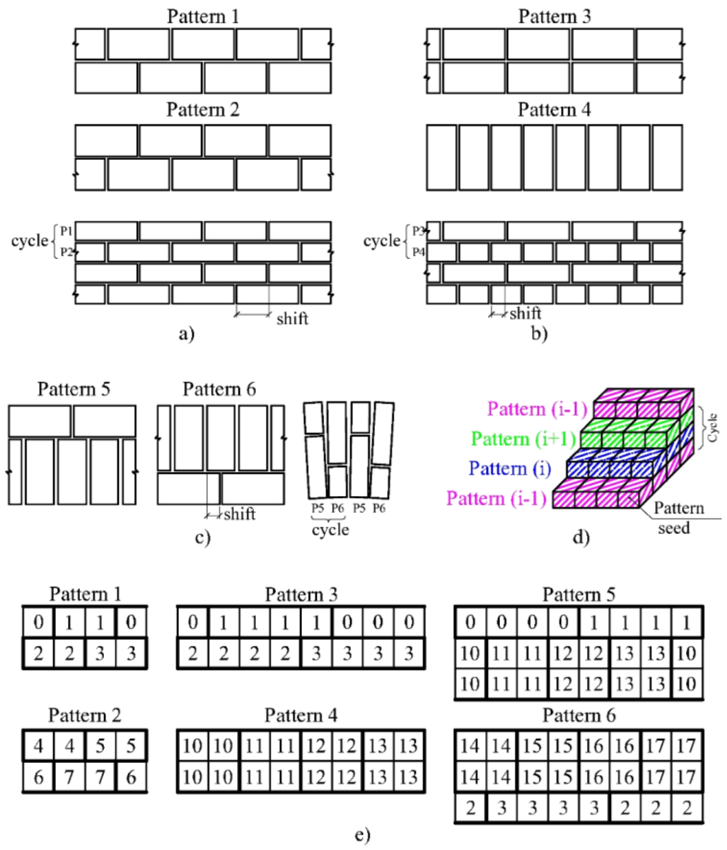

Grosman, Macorini & Izzuddin, B.A. (2023)

Domain partitioning approach

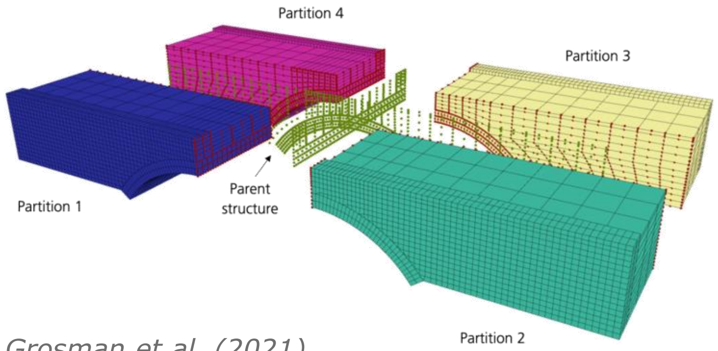

Grosman et al. (2021)

- Parallel computation
- Improved computational efficiency

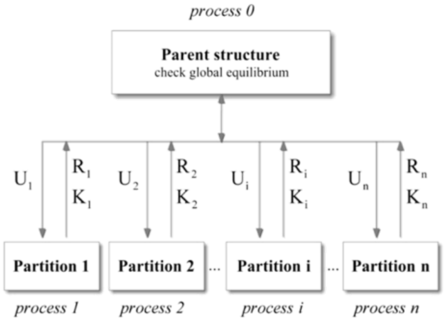

Jokhio & Izzuddin (2015)

Calibration of Material Parameters

Calibration of Material Parameters

Engineering and Physical Sciences Research Council

Mesoscale Models

- **Brick Units:**
  - *Modelled using "Elastic" solid elements, requiring only "Linear" parameters (E, ν)*
    - *Young's Modulus:* $E_b = (200{:}\,1000) f_c$
    - *Poisson's ratio:* $\nu = 0.15{:}\,0.25$
- **Mortar Joints:**
  - *Modelled using "Non-linear" interface elements, at which all material non-linearity is lumped*
  - *Linear Parameters:*
    - *Normal Stiffness:* $k_n = \dfrac{E_b E_M}{(h_b + h_m)\,(E_b - E_M)}$
    - *Tangential Stiffness:* $k_t = 0.4\, k_n$

Source: Lourenço, P. and Gaetani, A. (2022) Finite Element Analysis for Building Assessment: Advanced Use and Practical Recommendations. 1st edn. CRC Press.

Calibration of Material Parameters

Mesoscale Models

- **Mortar Joints:**
  - *Nonlinear Parameters*
    - *Bond Tensile Strength:* f_t = *c/1.4*
    - *Cohesion: c = (0.15: 0.25) MPa*
    - *Friction Coefficient: tanϕ = (0.60: 0.75)*
    - *Dilatancy Coefficient: tanψ = 0.00*
    - *Mode I Fracture Energy:* G_f^I *= 0.01 N/mm*
    - *Mode II Fracture Energy:* G_f^{II} *= 0.1 c*

Source: Lourenço, P. and Gaetani, A. (2022) Finite Element Analysis for Building Assessment: Advanced Use and Practical Recommendations. 1st edn. CRC Press.

Validation of Numerical Models

Validation of Numerical Models

Square Bridge

Validation: Square Bridge

Bolton Square Bridge 3-3

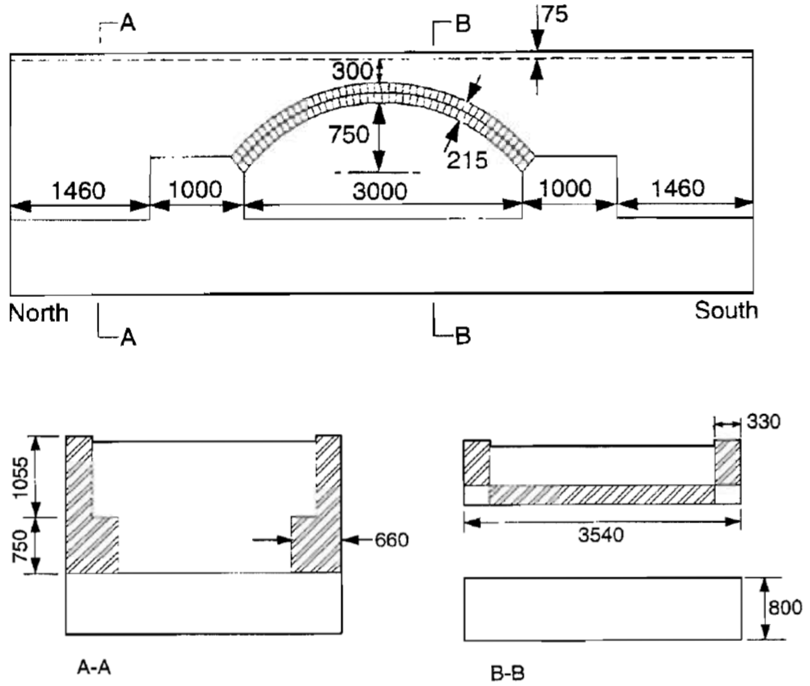

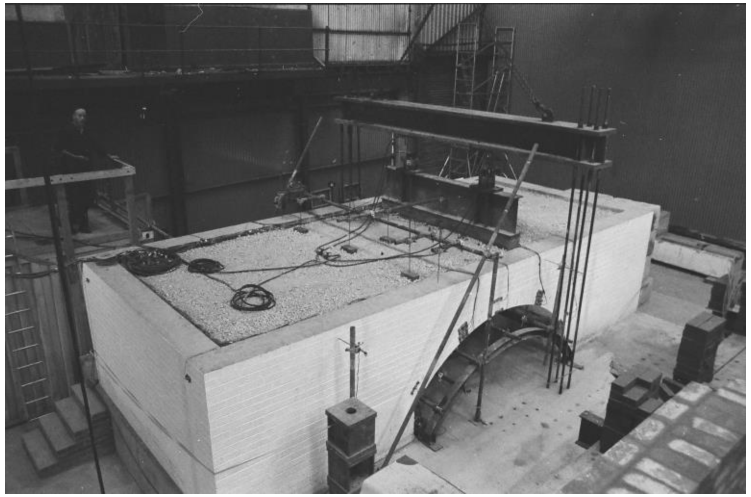

Bridge 3-3 Characteristics:
- Span = 3m
- Width = 3.54m
- Rise = 0.75m
- 2 Rings

(Melbourne & Gilbert, 1995)

Validation: Square Bridge

Bolton Square Bridge 3-3

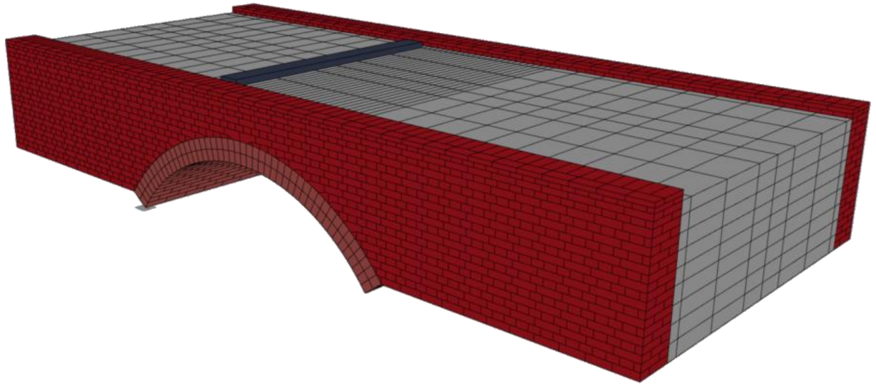

- Line load at quarter span increased up to collapse

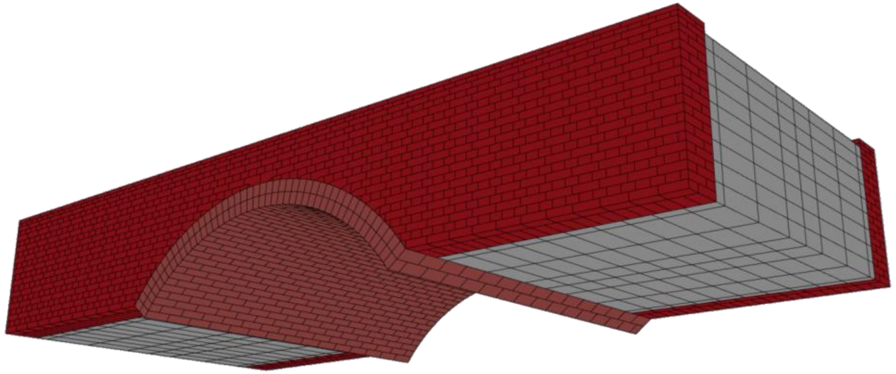

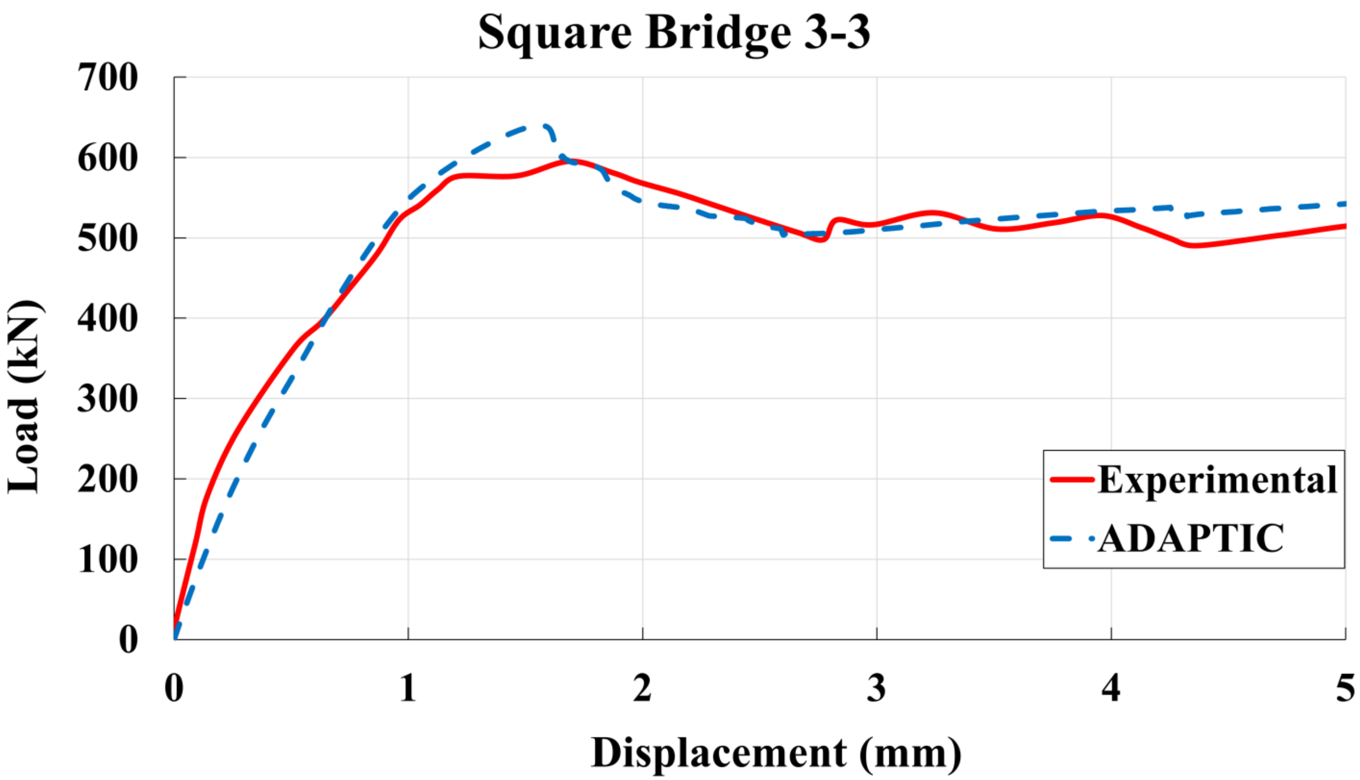

(Melbourne & Gilbert, 1995)

Validation: Square Bridge

Bolton Square Bridge 3-3

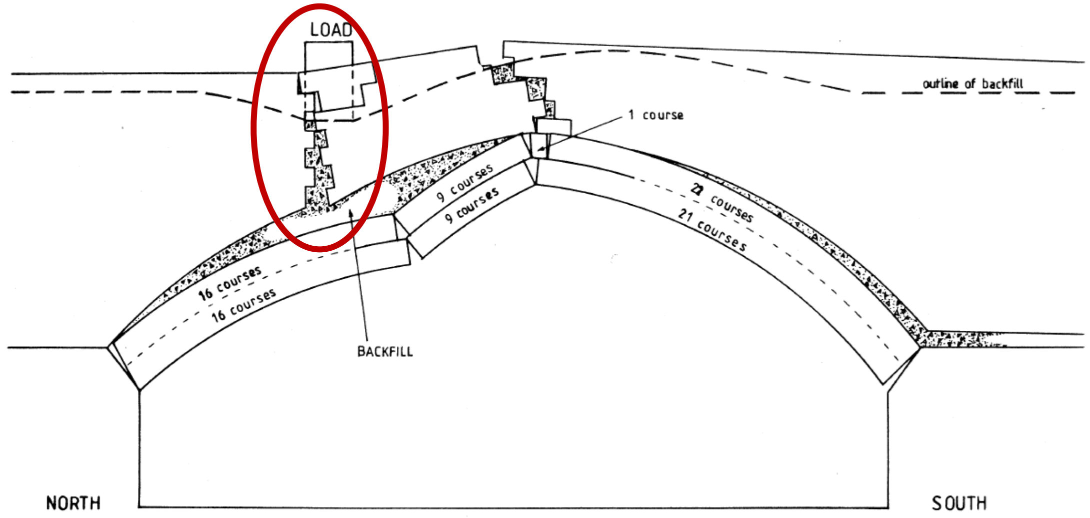

Experimental Crack Pattern
(Melbourne & Gilbert, 1995)

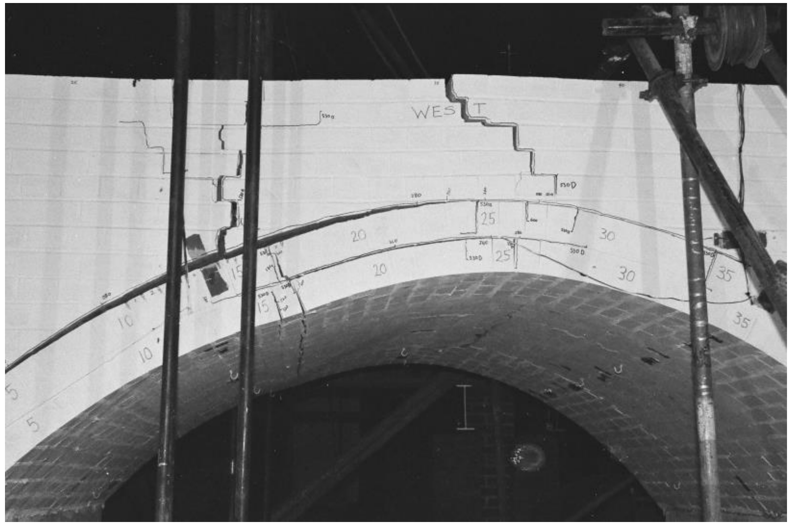

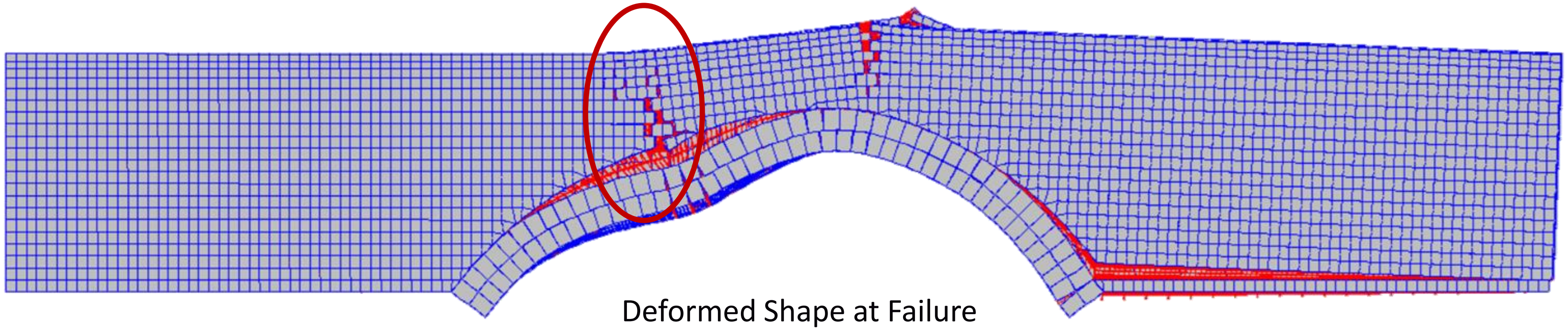

Deformed Shape at Failure

West Elevation

Validation: Square Bridge

Bolton Square Bridge 3-3

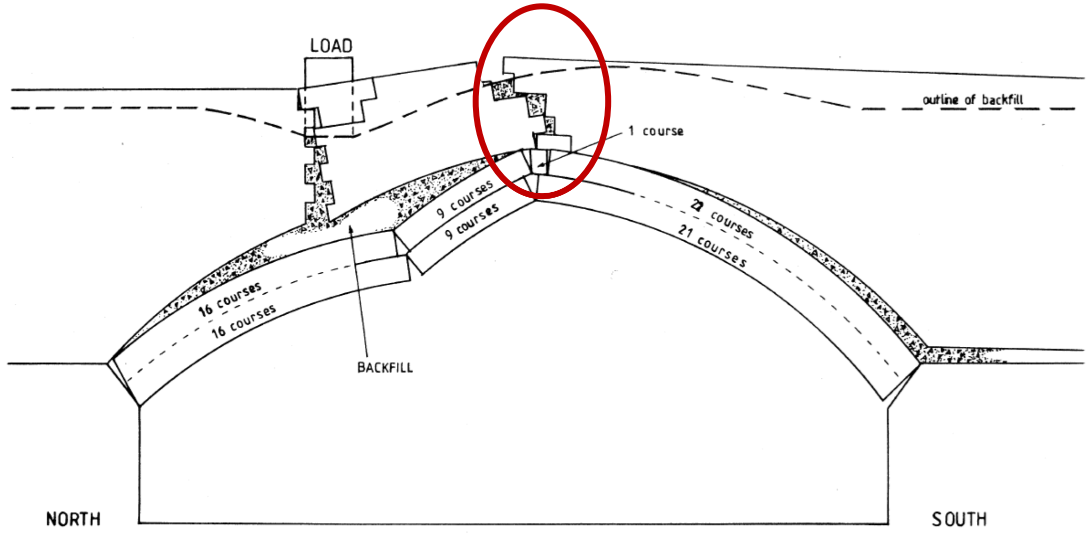

Experimental Crack Pattern
(Melbourne & Gilbert, 1995)

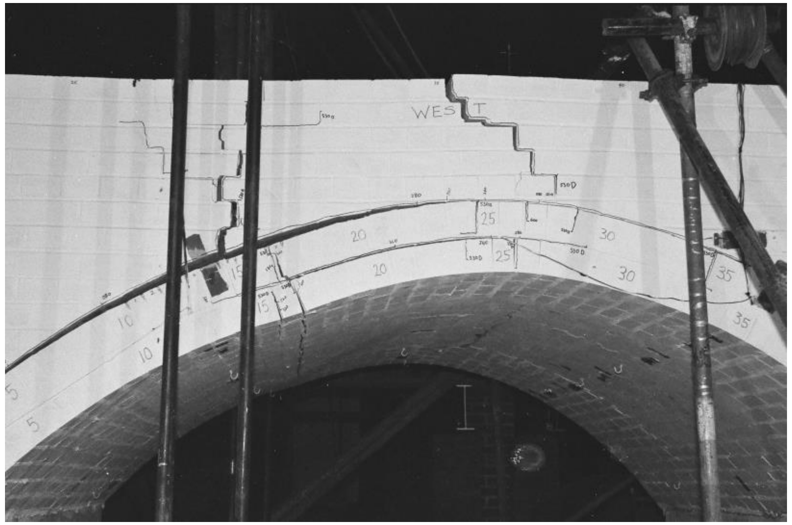

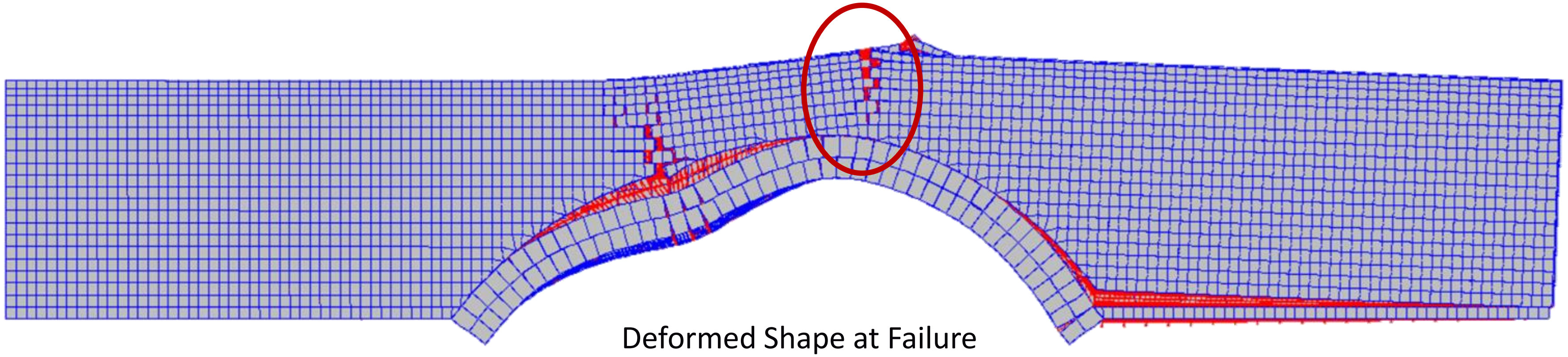

Deformed Shape at Failure

West Elevation

Validation: Square Bridge

Bolton Square Bridge 3-3

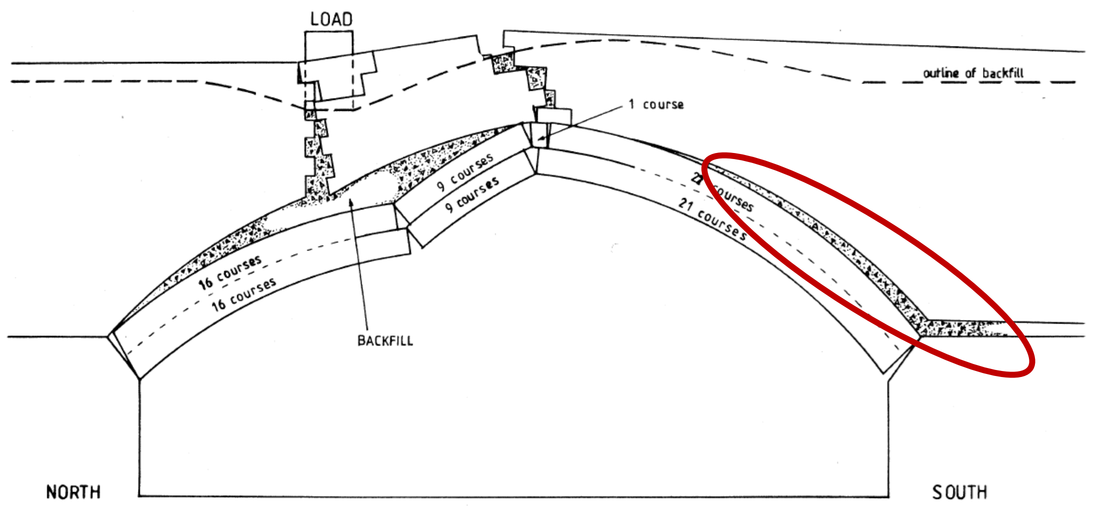

Experimental Crack Pattern
(Melbourne & Gilbert, 1995)

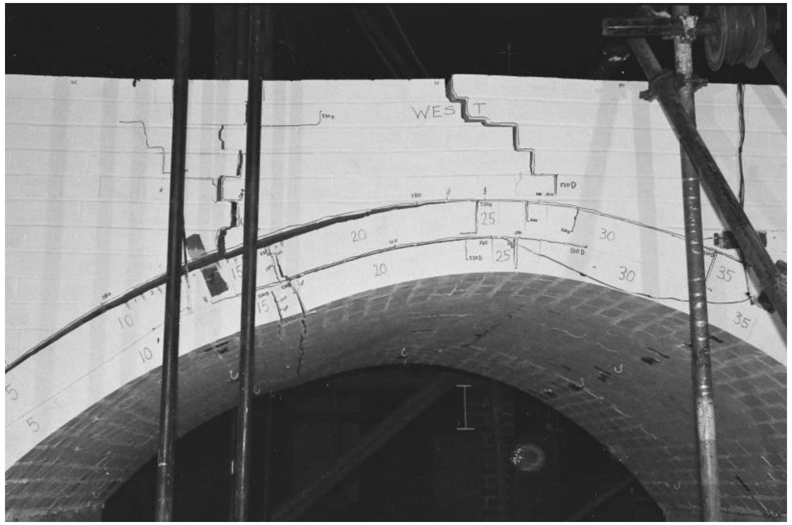

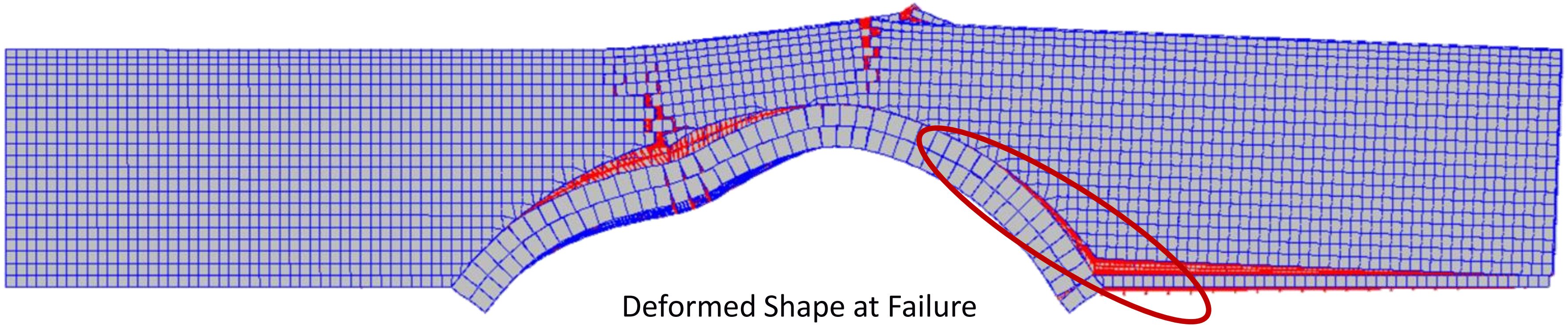

Deformed Shape at Failure

West Elevation

Validation: Square Bridge

Bolton Square Bridge 3-3

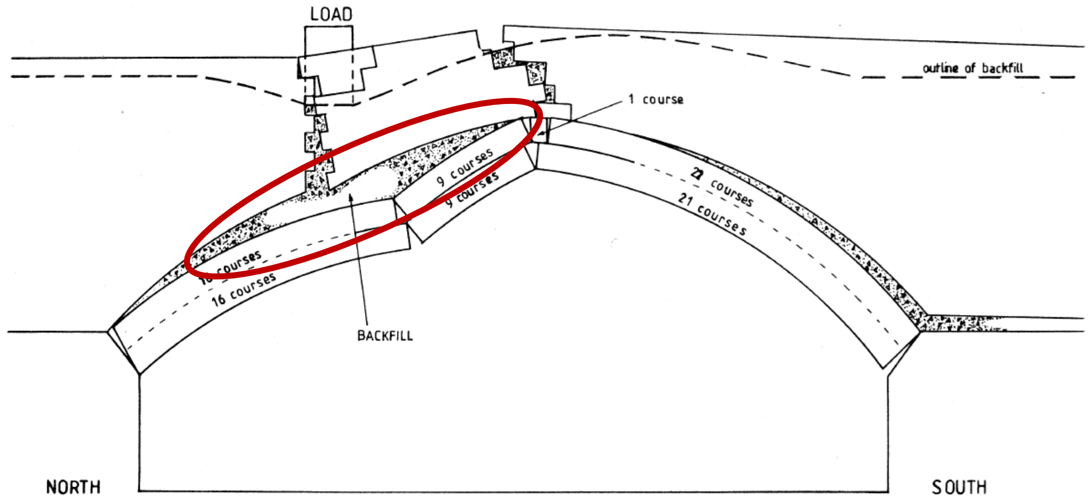

Experimental Crack Pattern
(Melbourne & Gilbert, 1995)

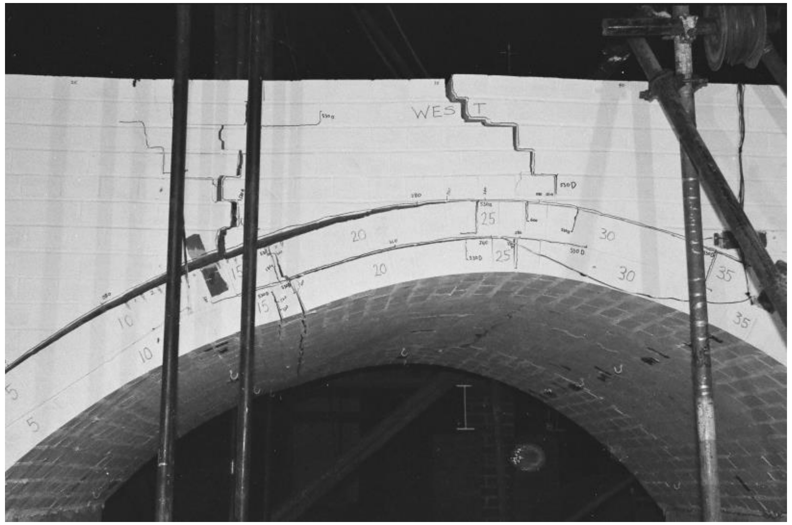

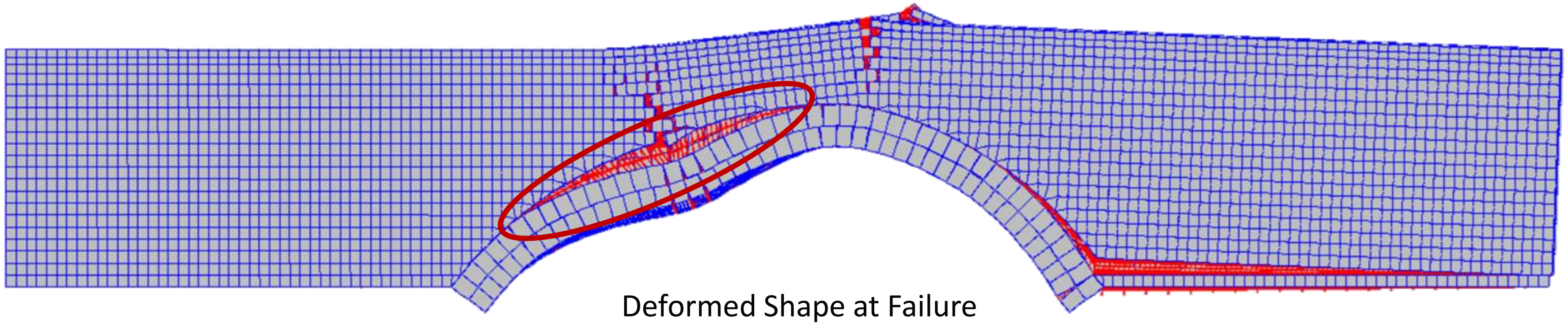

Deformed Shape at Failure

West Elevation

Validation: Square Bridge

Bolton Square Bridge 3-3

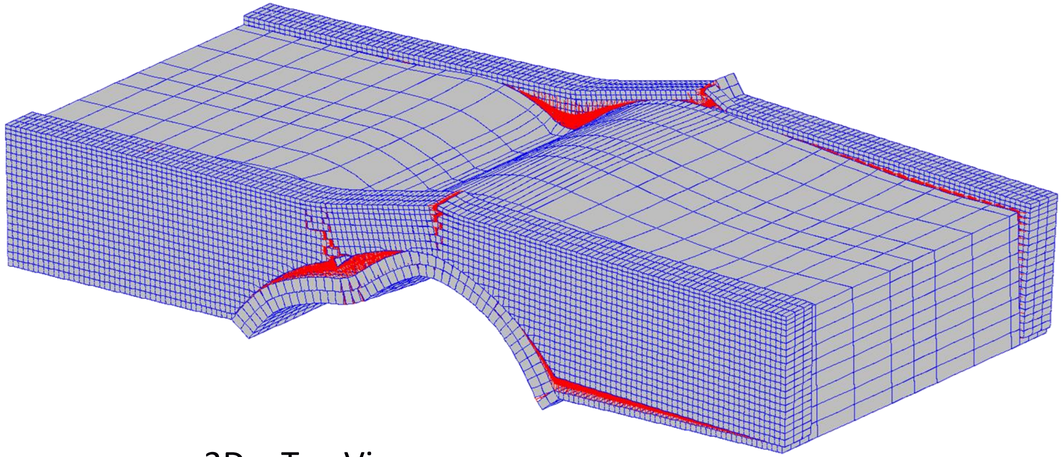

3D – Top View

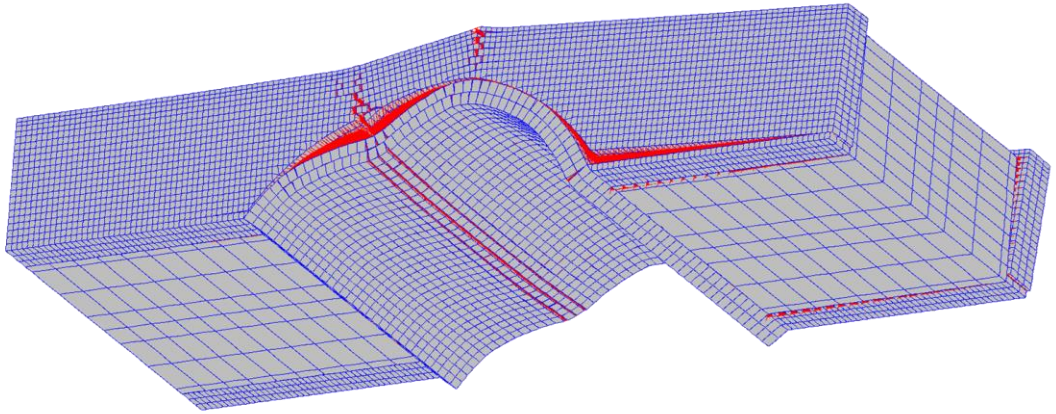

3D – Bottom View

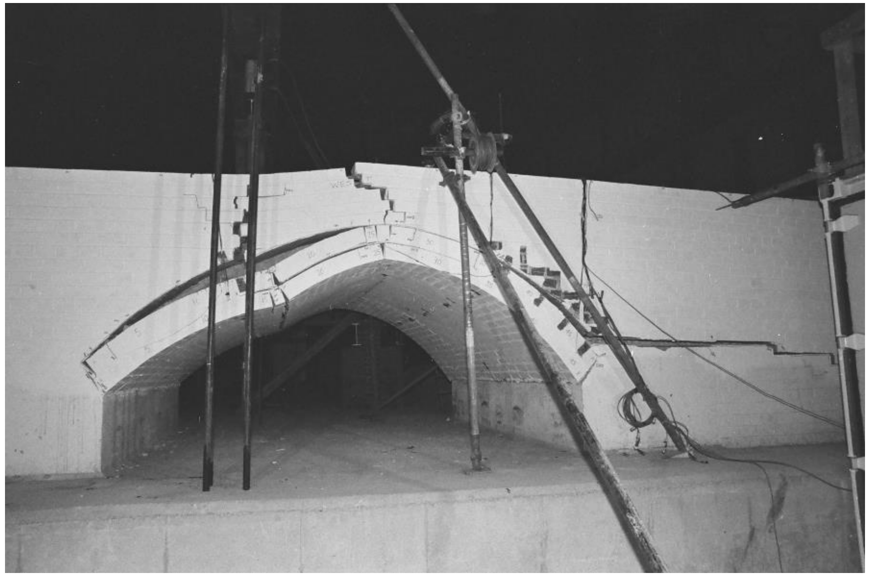

(Melbourne & Gilbert, 1995)

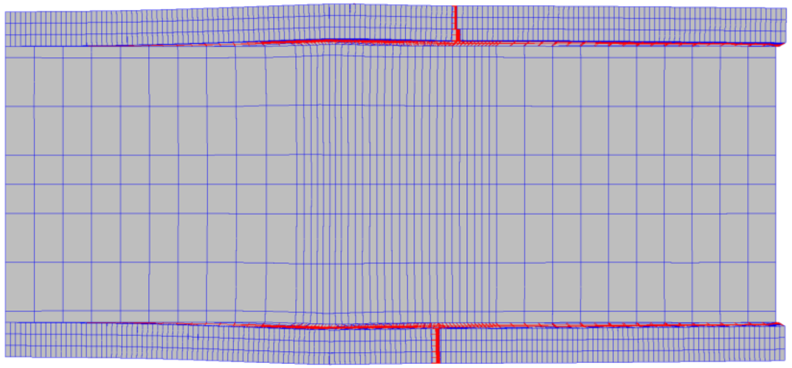

Top Plan View

Validation: Square Bridge

Bolton Square Bridge 3-3

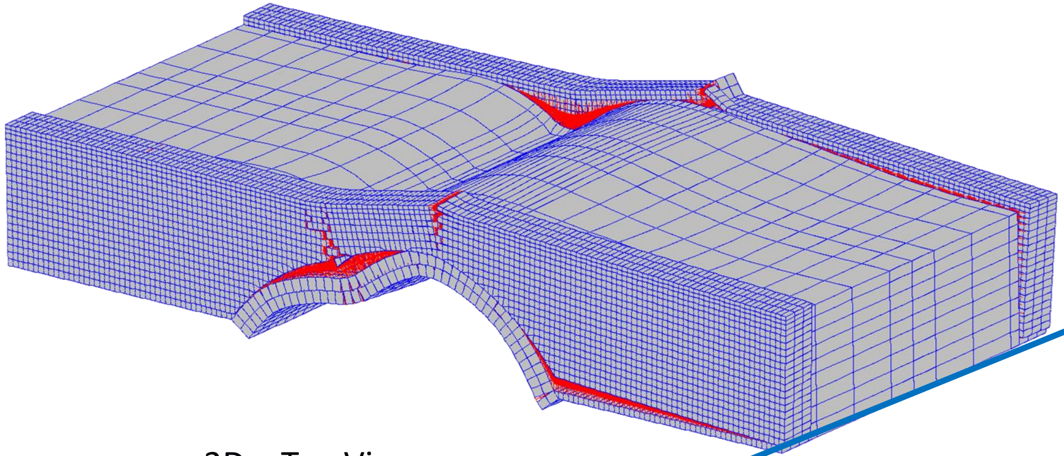

3D – Top View

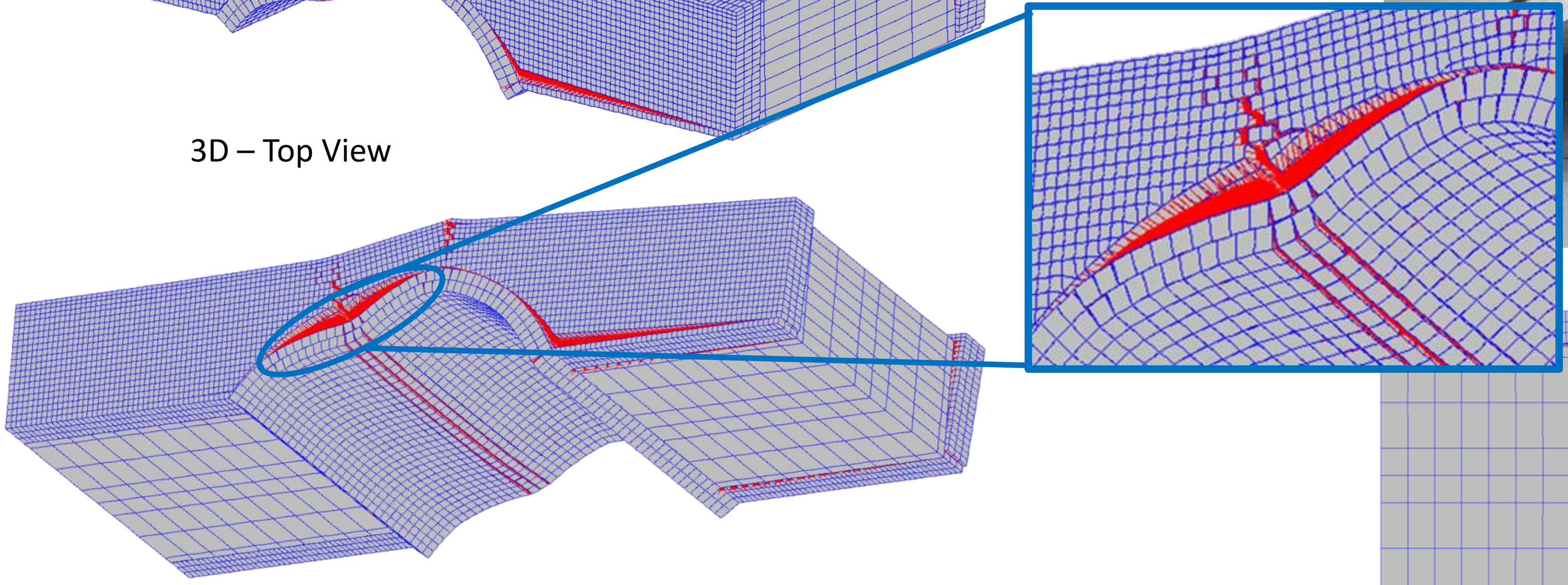

3D – Bottom View

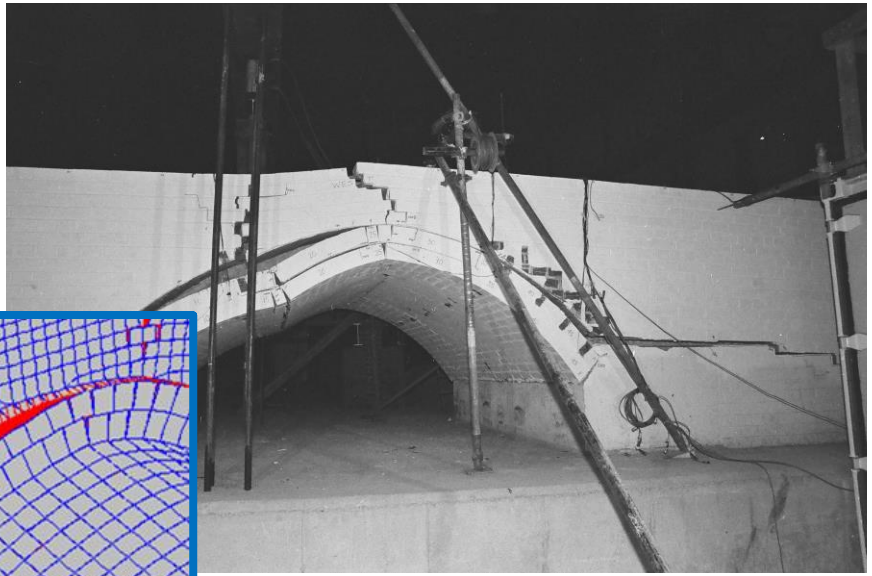

(Melbourne & Gilbert, 1995)

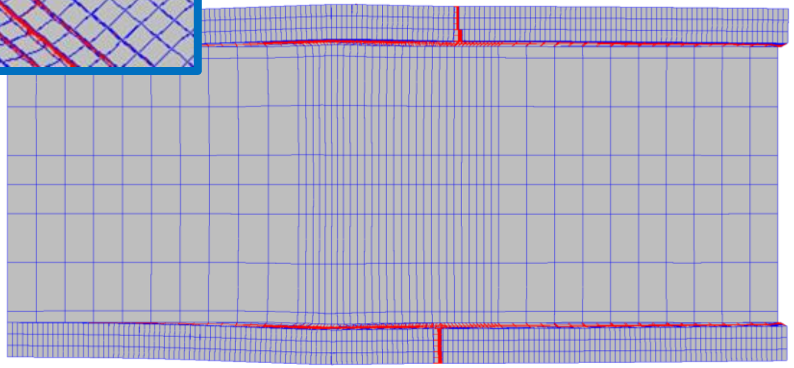

Top Plan View

Validation of Numerical Models

Skew Bridge

Validation: Skew Bridge

Hodgson's Skew Bridge 3-3

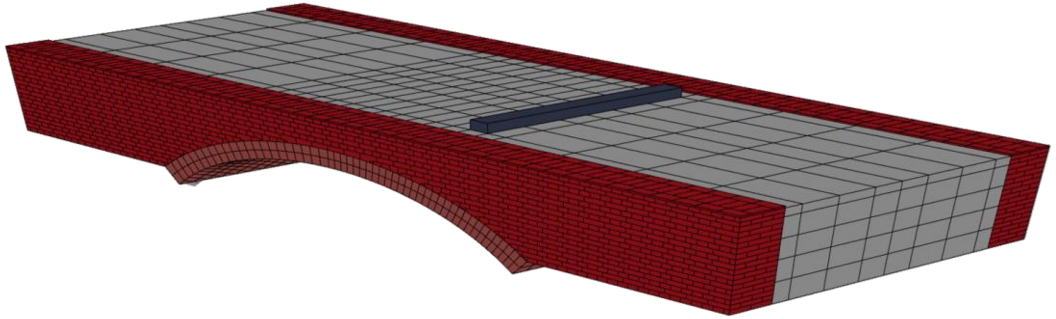

- Line load at quarter span increased up to collapse

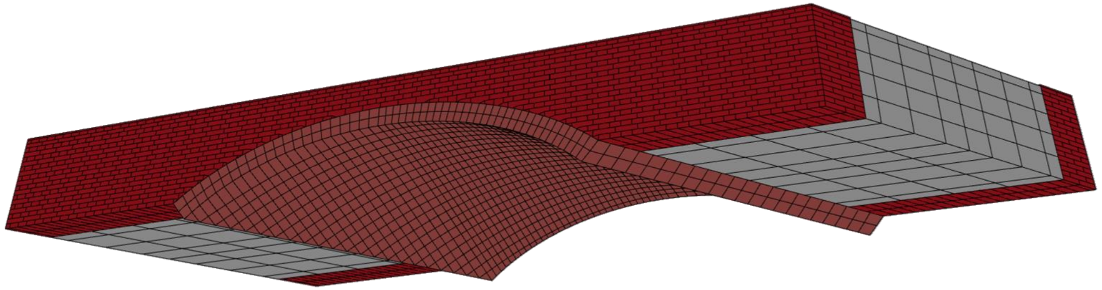

3D Model for Skew Bridge 3-3

Bridge 3-3 Characteristics:

- Span = 3m
- Width = 3.5m
- Rise = 0.75m
- 2 Rings
- 45° Skew

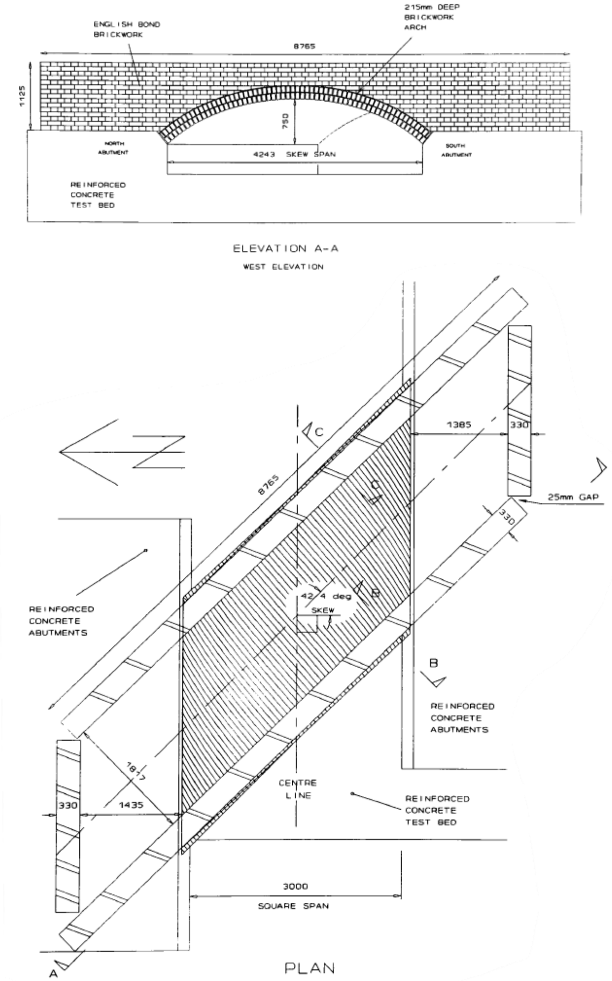

(Hodgson, 1996)

Validation: Skew Bridge

Hodgson's Skew Bridge 3-3

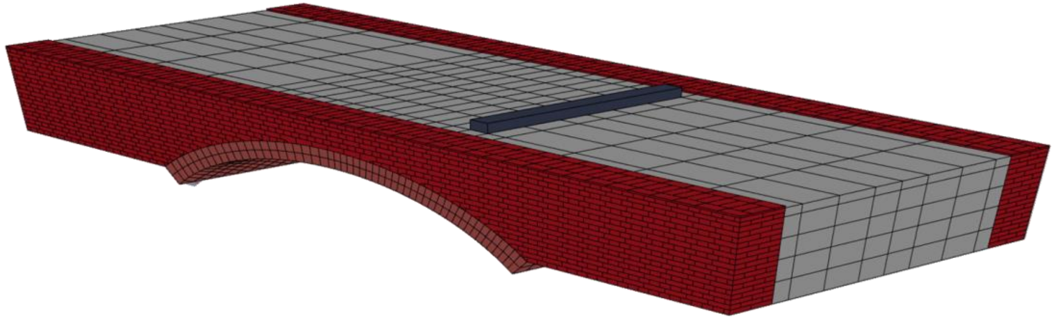

- Line load at quarter span increased up to collapse

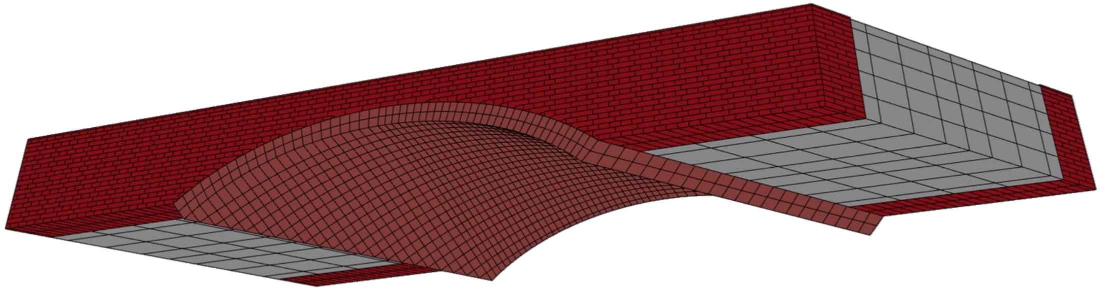

3D Model for Skew Bridge 3-3

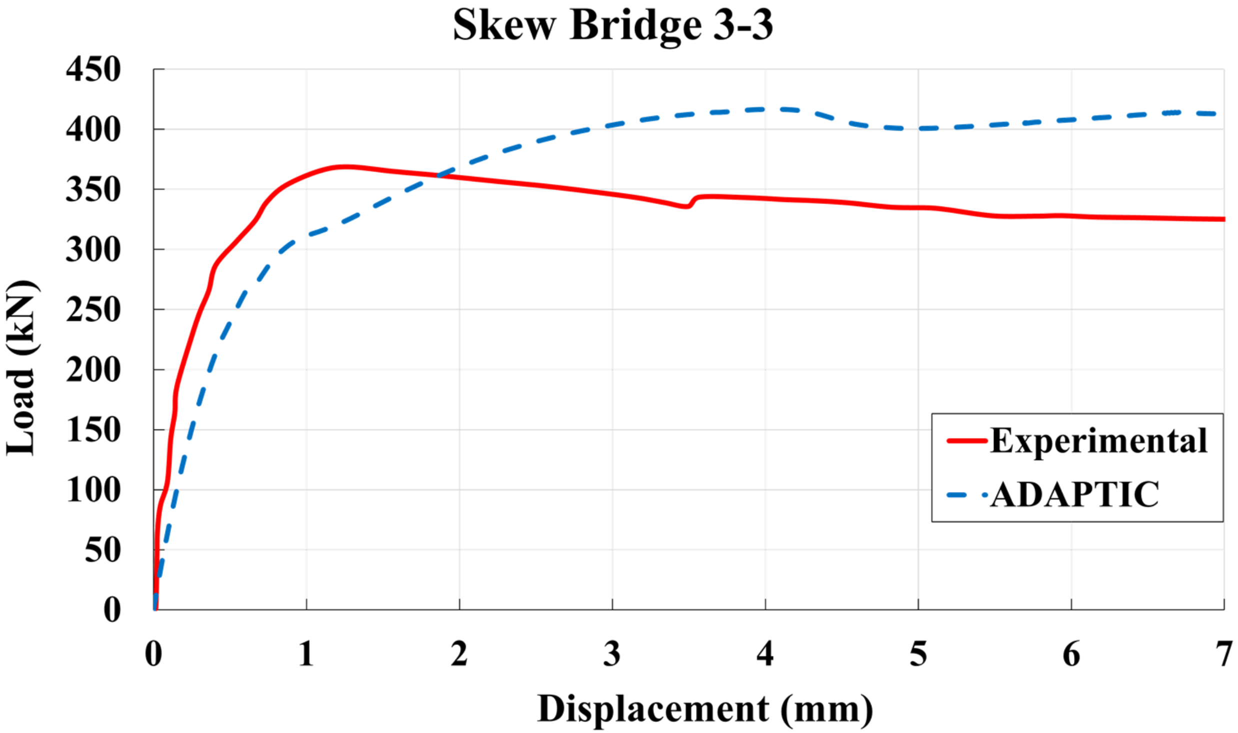

Validation: Skew Bridge

Hodgson's Skew Bridge 3-3

Arch Intrados

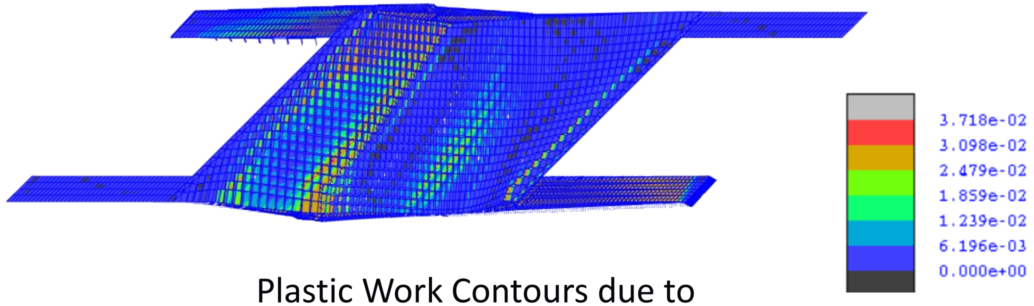

Plastic Work Contours due to Tension for Interface Elements

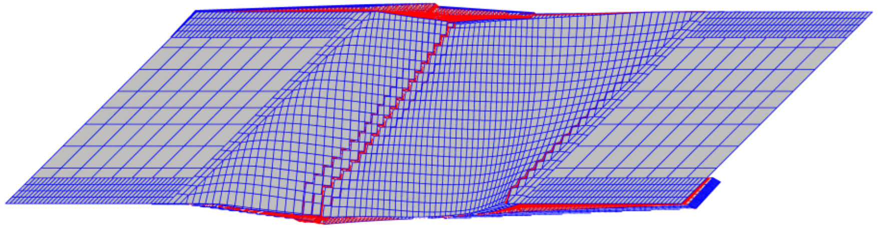

Deformed Shape at Failure

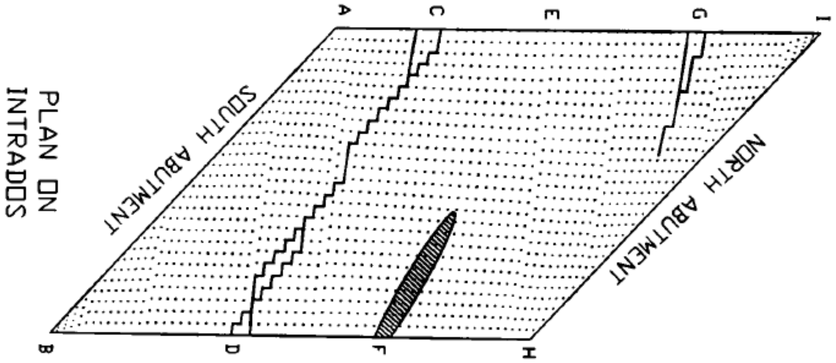

Experimental Crack Pattern (Hodgson, 1996)

Validation: Skew Bridge

Hodgson's Skew Bridge 3-3

Arch Intrados

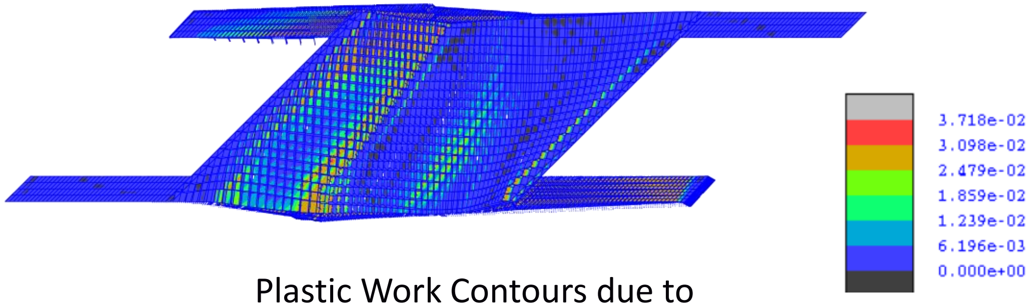

Plastic Work Contours due to Tension for Interface Elements

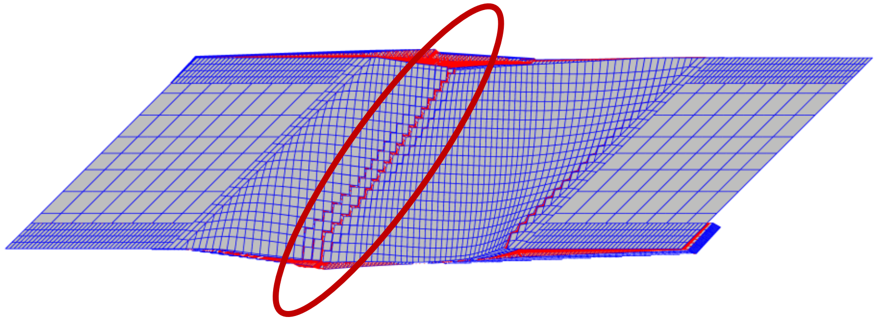

Deformed Shape at Failure

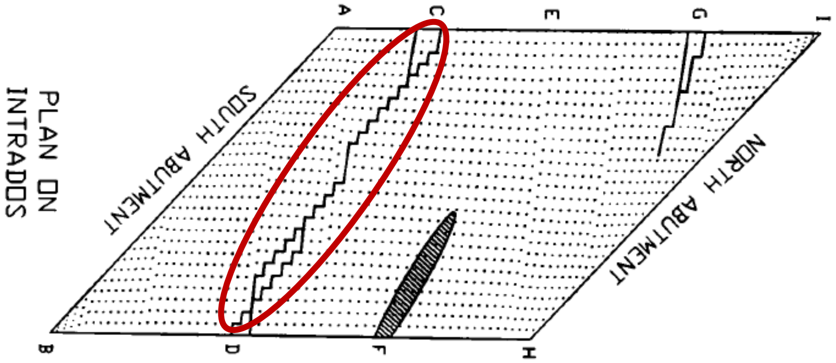

Experimental Crack Pattern (Hodgson, 1996)

Validation: Skew Bridge

Hodgson's Skew Bridge 3-3

Arch Intrados

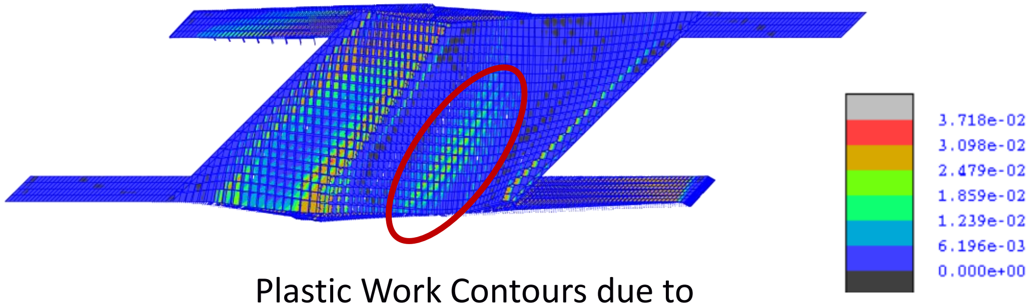

Plastic Work Contours due to Tension for Interface Elements

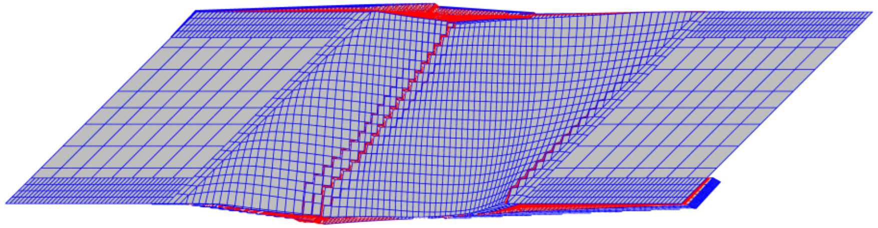

Deformed Shape at Failure

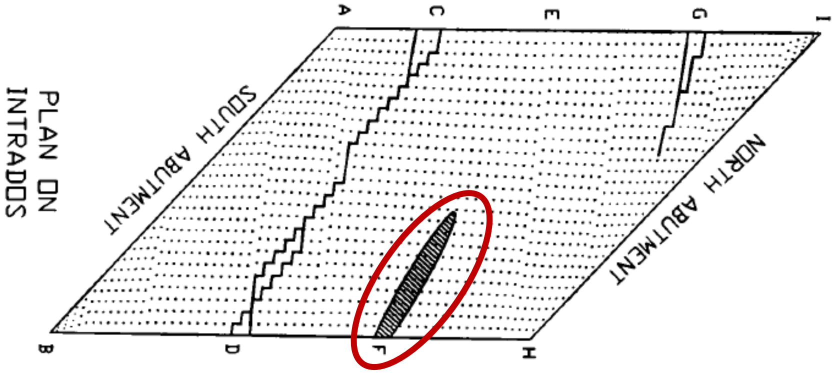

Experimental Crack Pattern (Hodgson, 1996)

Validation: Skew Bridge

Hodgson's Skew Bridge 3-3

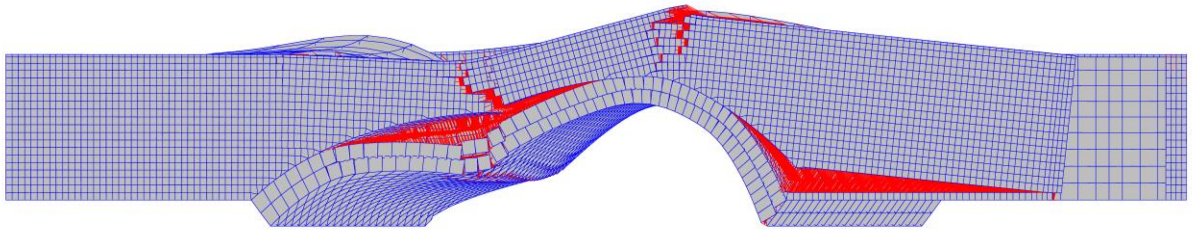

East Elevation

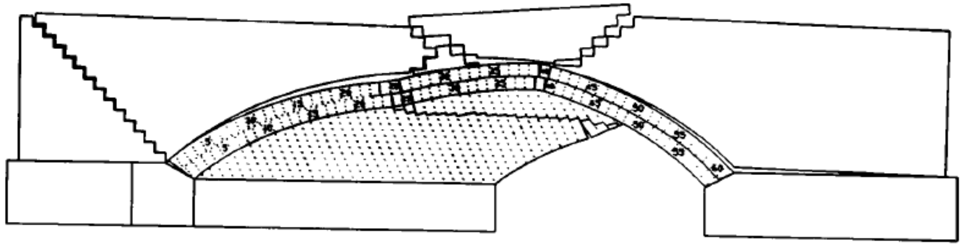

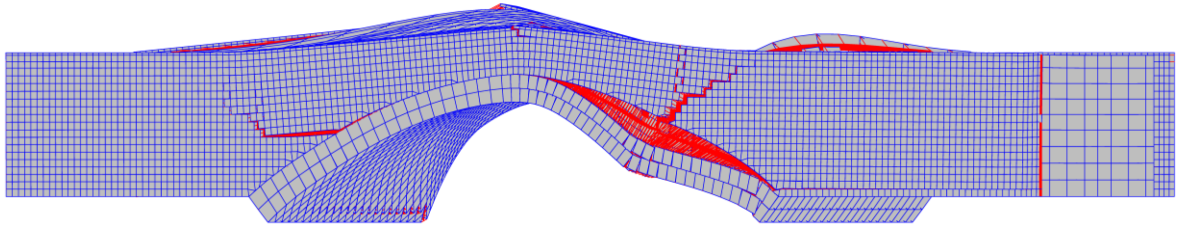

West Elevation

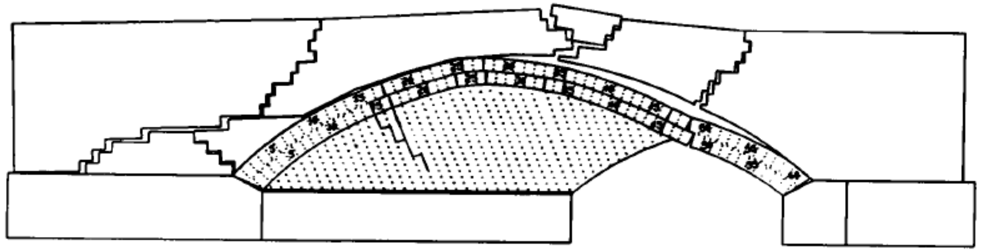

Deformed Shape at Failure

Experimental Failure Mode
(Hodgson, 1996)

Validation: Skew Bridge

Hodgson's Skew Bridge 3-3

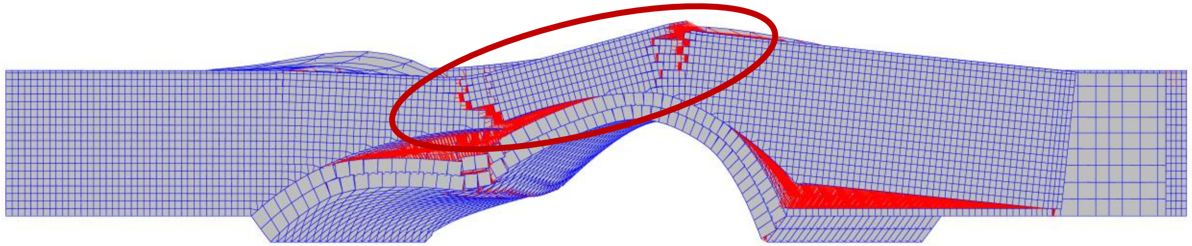

East Elevation

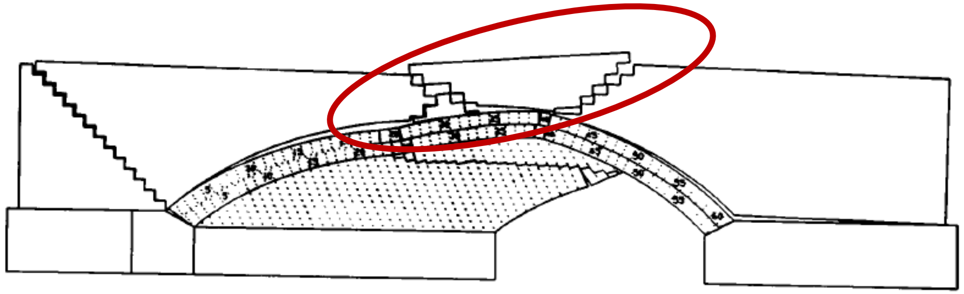

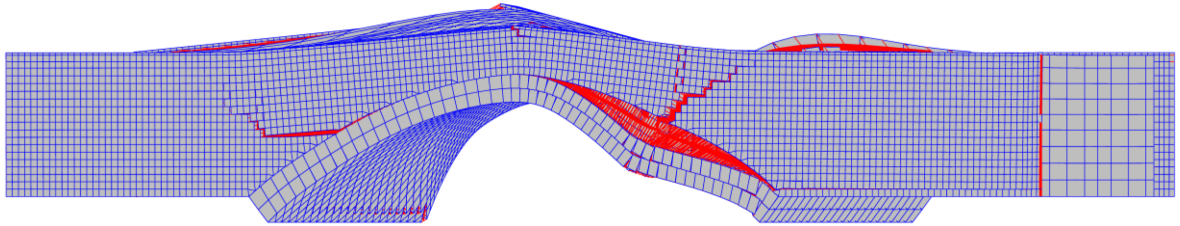

West Elevation

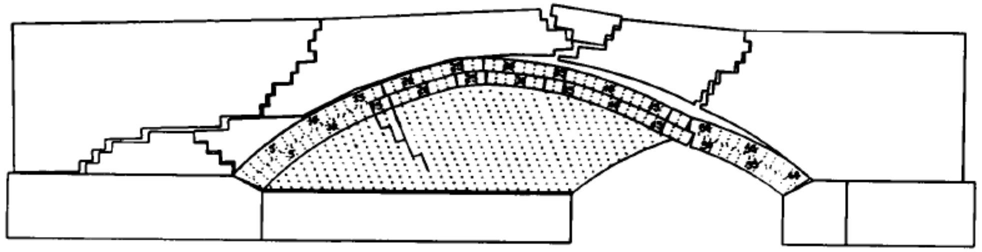

Deformed Shape at Failure

Experimental Failure Mode
(Hodgson, 1996)

Validation: Skew Bridge

Hodgson’s Skew Bridge 3-3

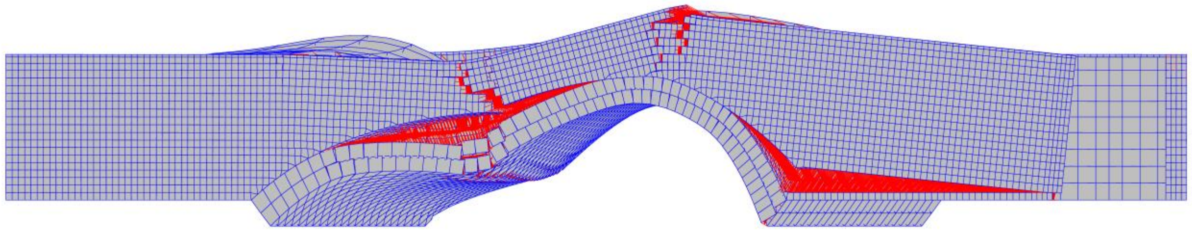

East Elevation

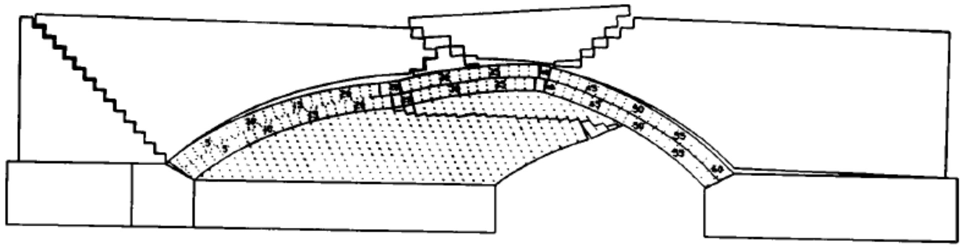

EAST ELEVATION

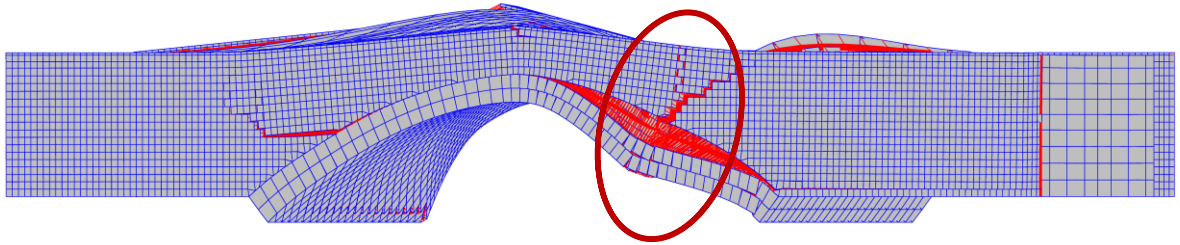

West Elevation

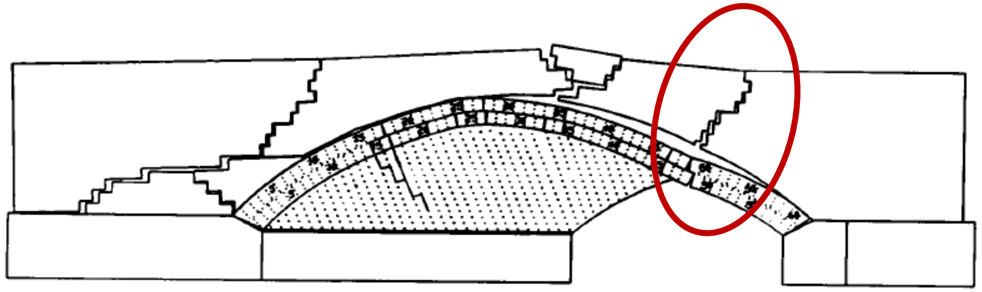

WEST ELEVATION

Deformed Shape at Failure

Experimental Failure Mode
(Hodgson, 1996)

Validation: Skew Bridge

Hodgson’s Skew Bridge 3-3

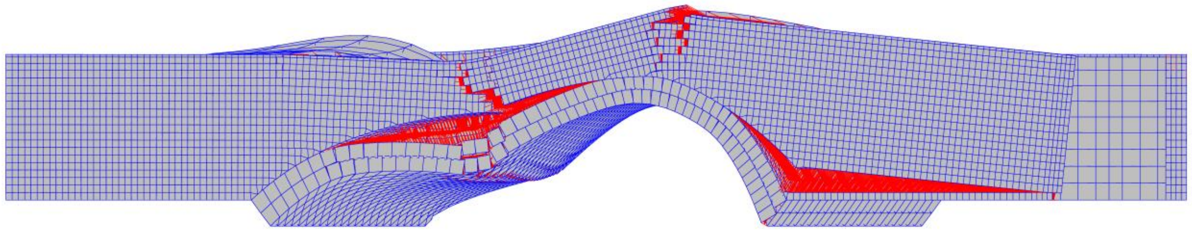

East Elevation

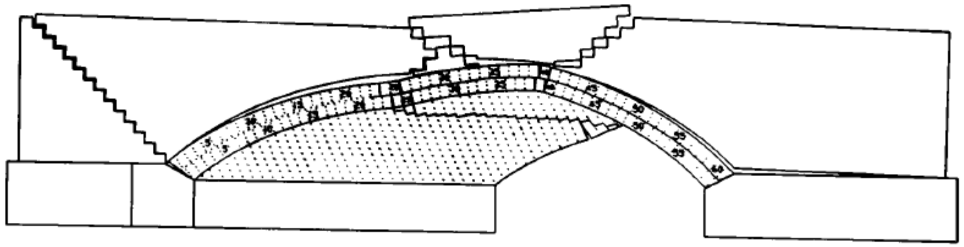

EAST ELEVATION

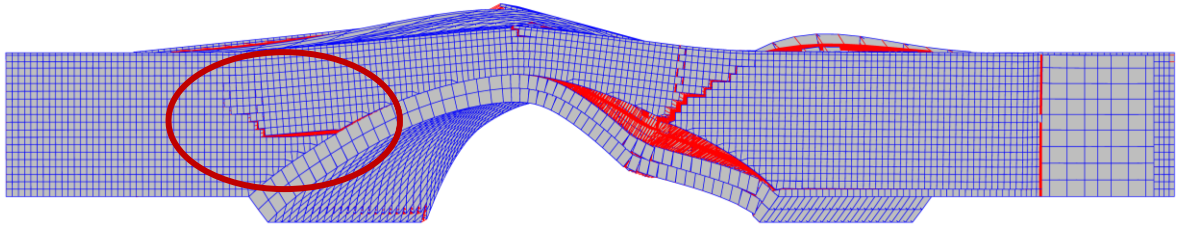

West Elevation

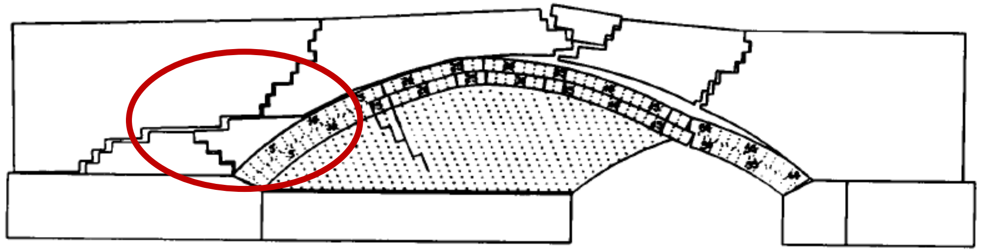

WEST ELEVATION

Deformed Shape at Failure

Experimental Failure Mode
(Hodgson, 1996)

Investigation of 3D Failure Modes

Investigation of 3D Failure Modes

Patch Load

Patch Size (500mm×600mm)

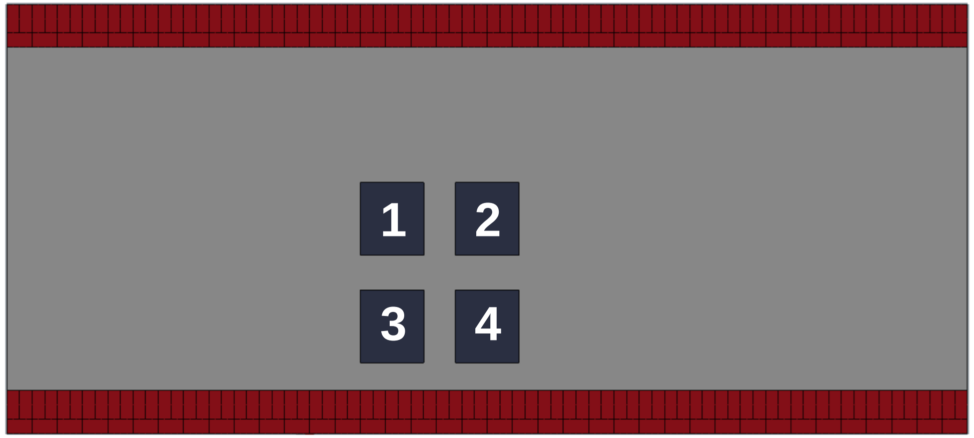

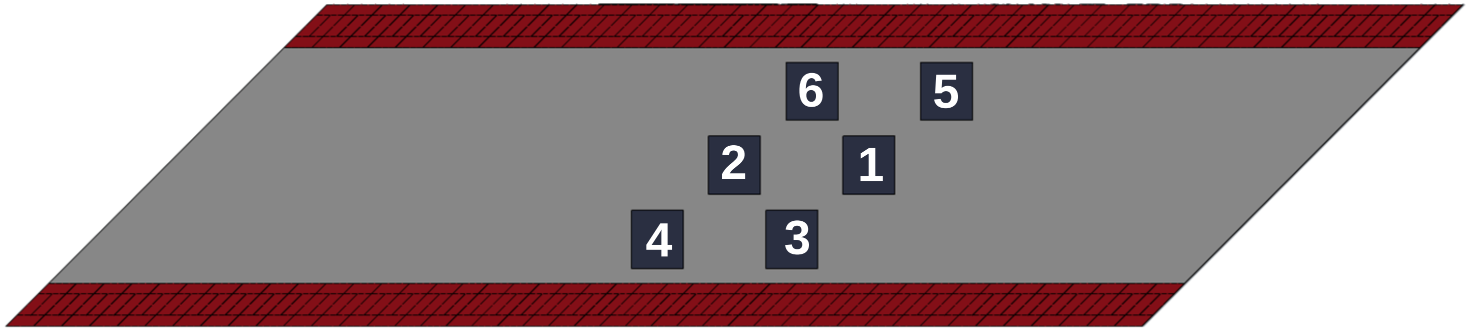

1 – ¼ Span; ½ Width
2 – ½ Span; ½ Width
3 – ¼ Span; ¼ Width
4 – ½ Span; ¼ Width
5 – ¼ Span; ¾ Width
6 – ½ Span; ¾ Width

Investigation of 3D Failure Modes

Patch Load

½ Span;
½ Width

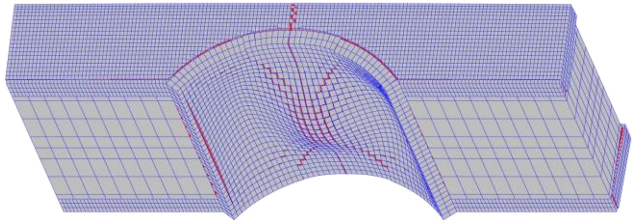

West Elevation

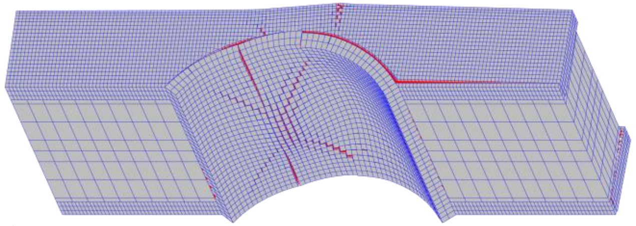

¼ Span;
½ Width

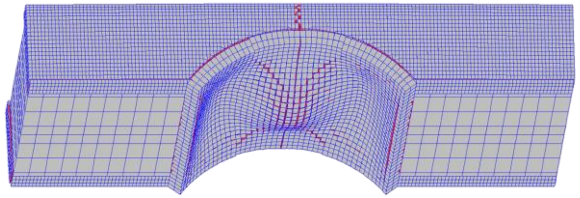

East Elevation

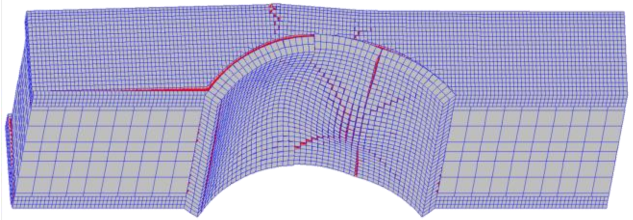

½ Span;
¼ Width

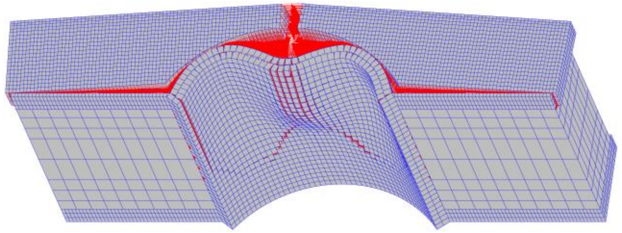

West Elevation

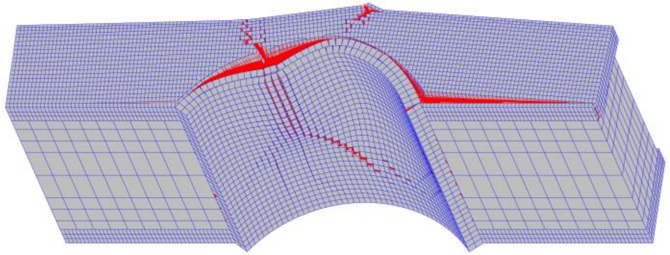

¼ Span;
¼ Width

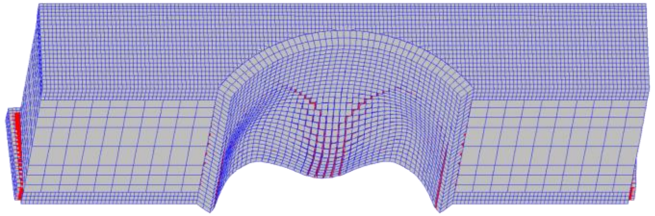

East Elevation

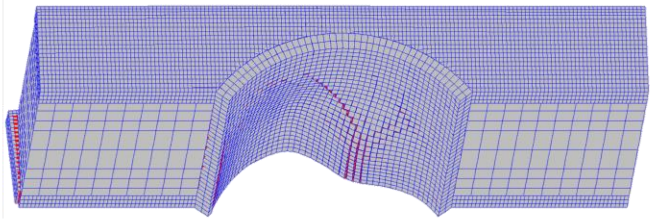

Investigation of 3D Failure Modes

Patch Load

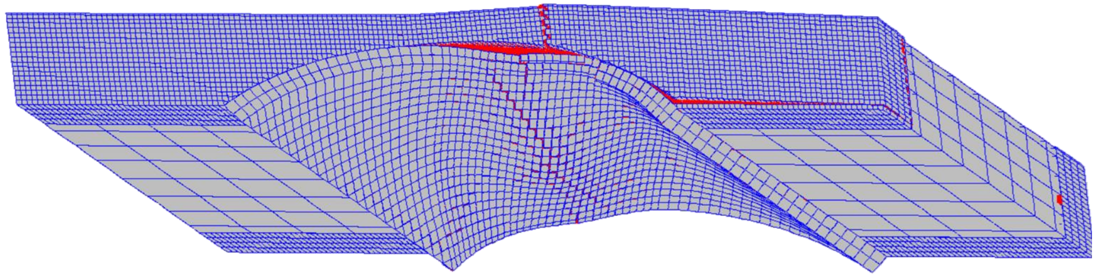

½ Span;
½ Width

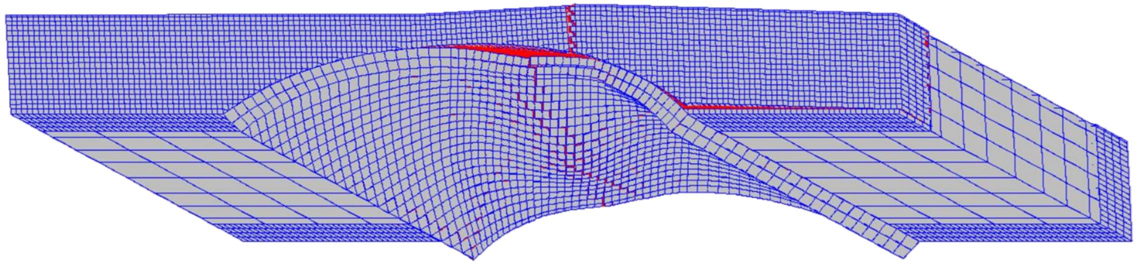

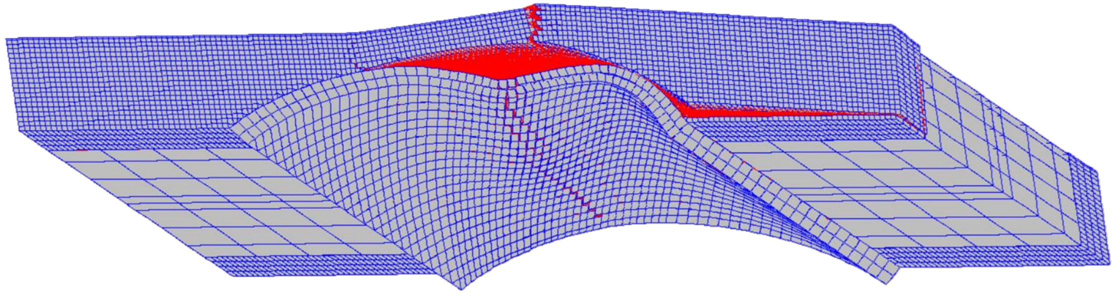

½ Span;
¼ Width

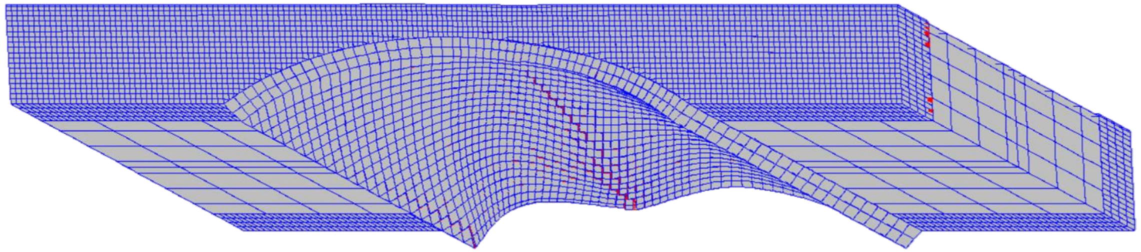

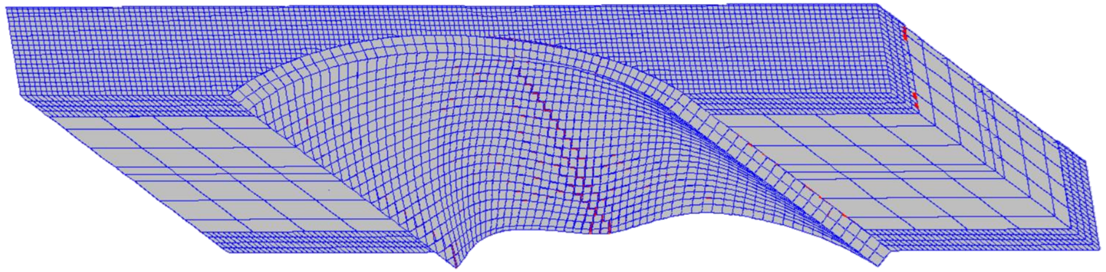

½ Span;
¾ Width

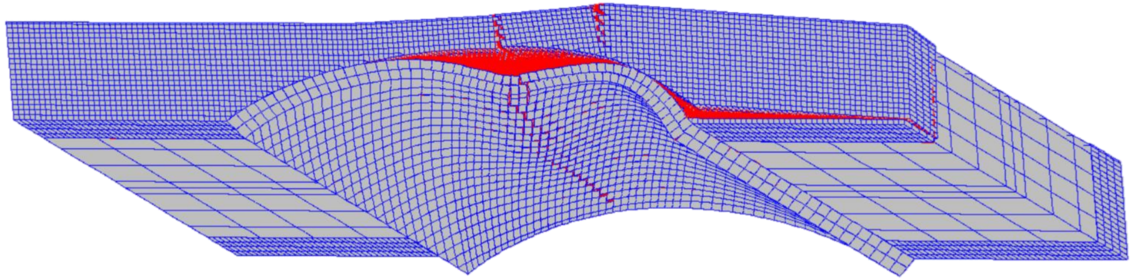

West Elevation

East Elevation

Investigation of 3D Failure Modes

Patch Load

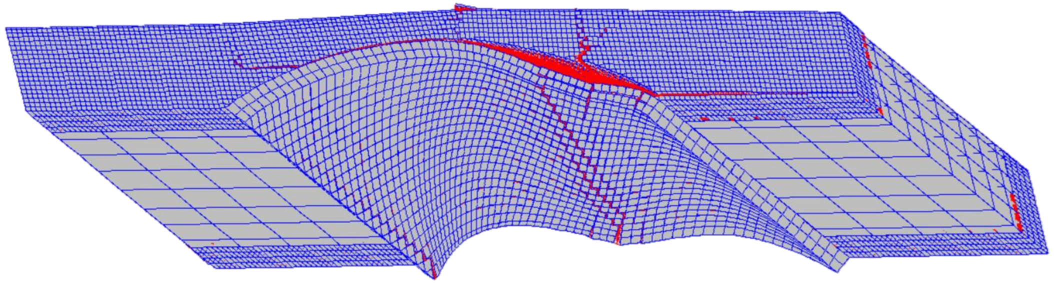

¼ Span;
½ Width

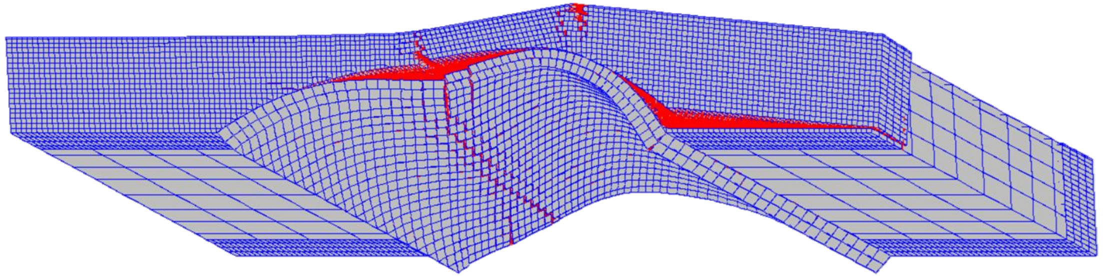

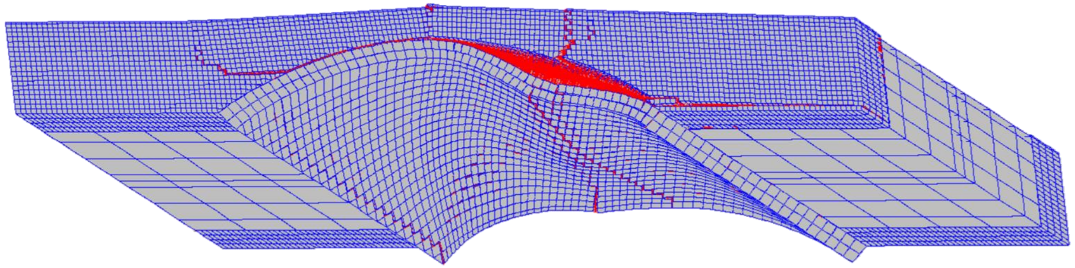

¼ Span;
¼ Width

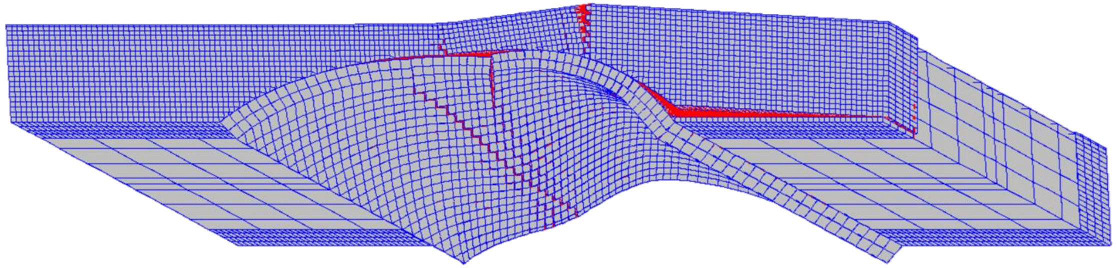

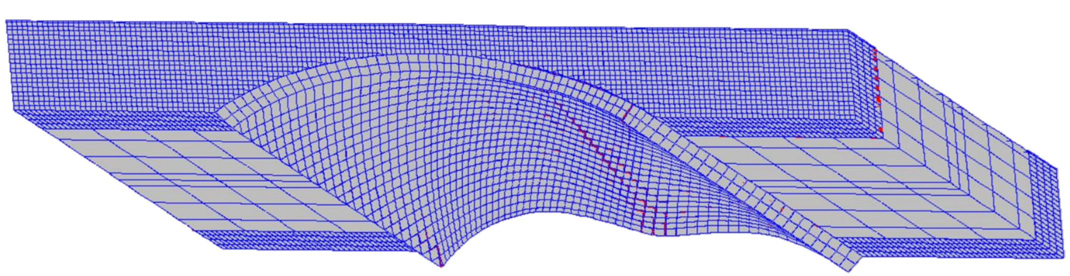

¼ Span;
¾ Width

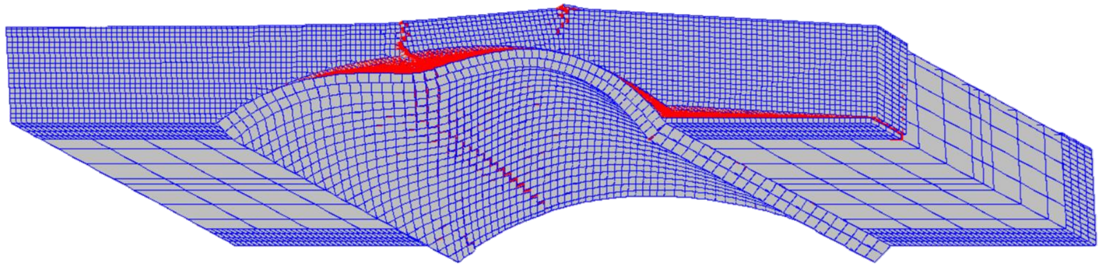

West Elevation

East Elevation

Validation of Numerical Models

Experimental Study

Validation: Experimental Study

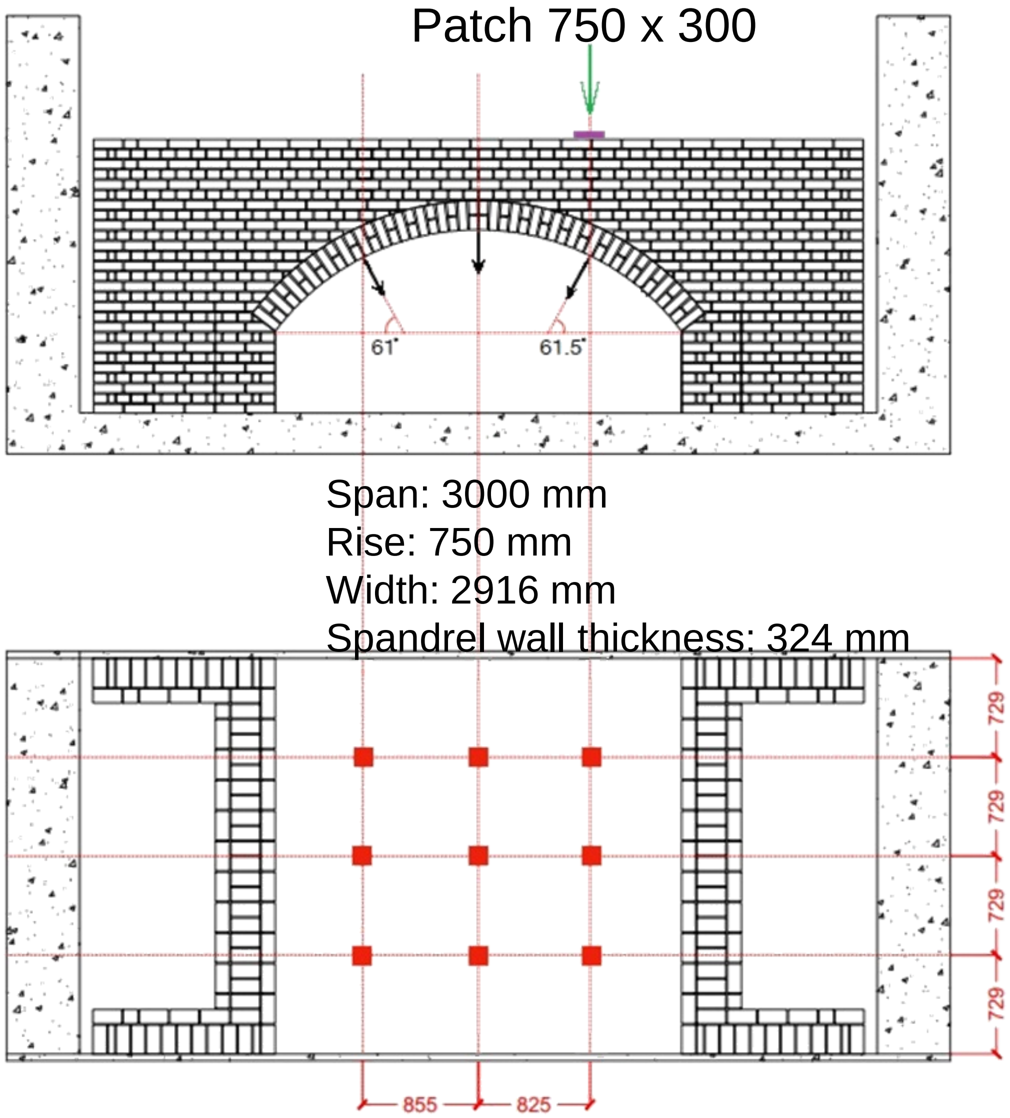

Span: 3000 mm
Rise: 750 mm
Width: 2916 mm
Spandrel wall thickness: 324 mm

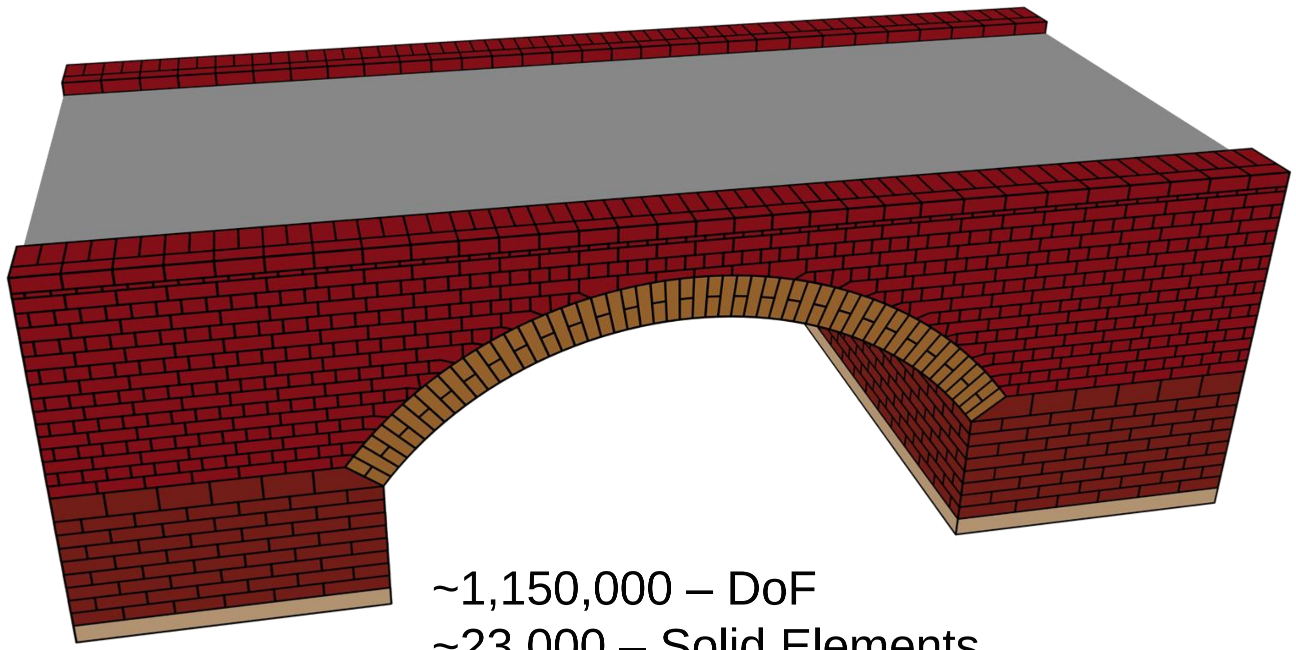

~1,150,000 – DoF
~23,000 – Solid Elements
~45,000 – Interface Elements

Brick unit Young's modulus	N/mm^2	31762
Interface normal stiffness	N/mm^3	72
Interface tensile strength	N/mm^2	0.145
Interface cohesion	N/mm^2	0.31
Interface friction angle		37.8

Validation: Experimental Study

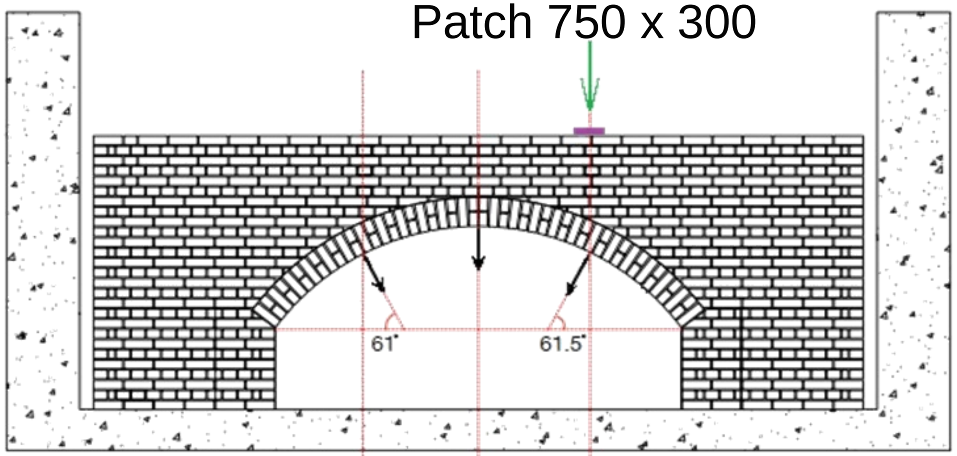

Span: 3000 mm
Rise: 750 mm
Width: 2916 mm
Spandrel wall thickness: 324 mm

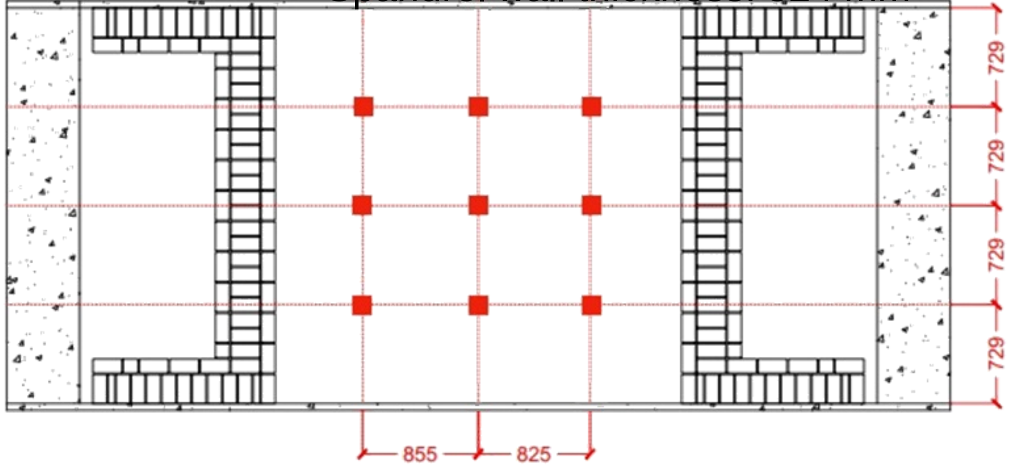

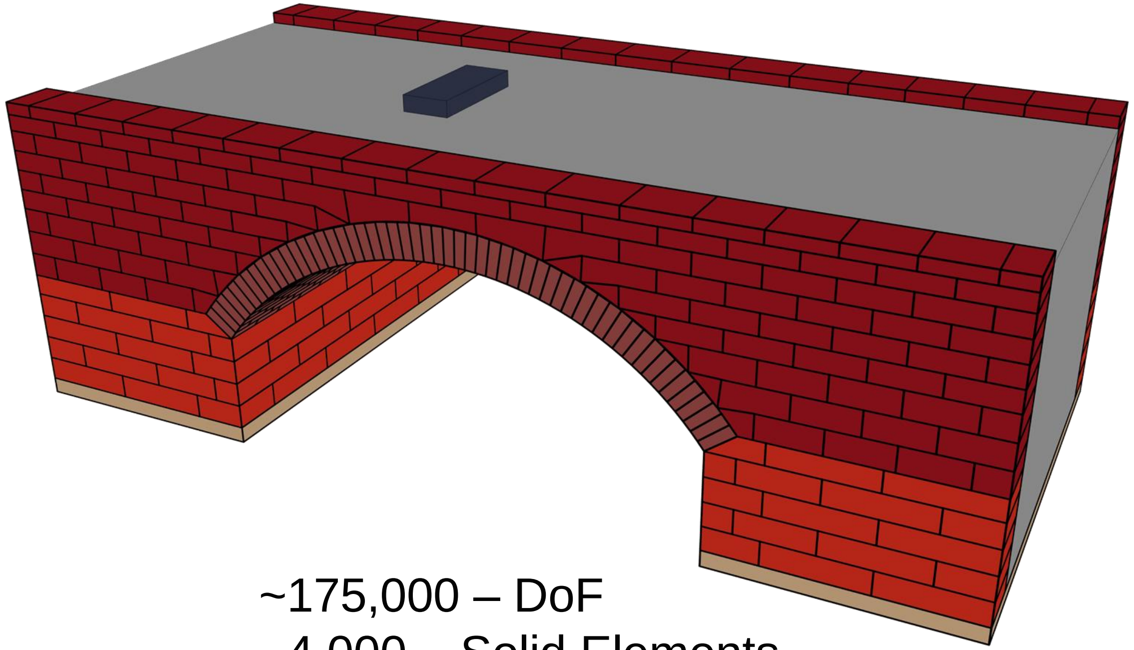

~175,000 – DoF
~4,000 – Solid Elements
~5,000 – Interface Elements

Brick unit Young’s modulus	N/mm^2	31762
Interface normal stiffness	N/mm^3	72
Interface tensile strength	N/mm^2	0.145
Interface cohesion	N/mm^2	0.31
Interface friction angle		37.8

Validation: Experimental Study - Results

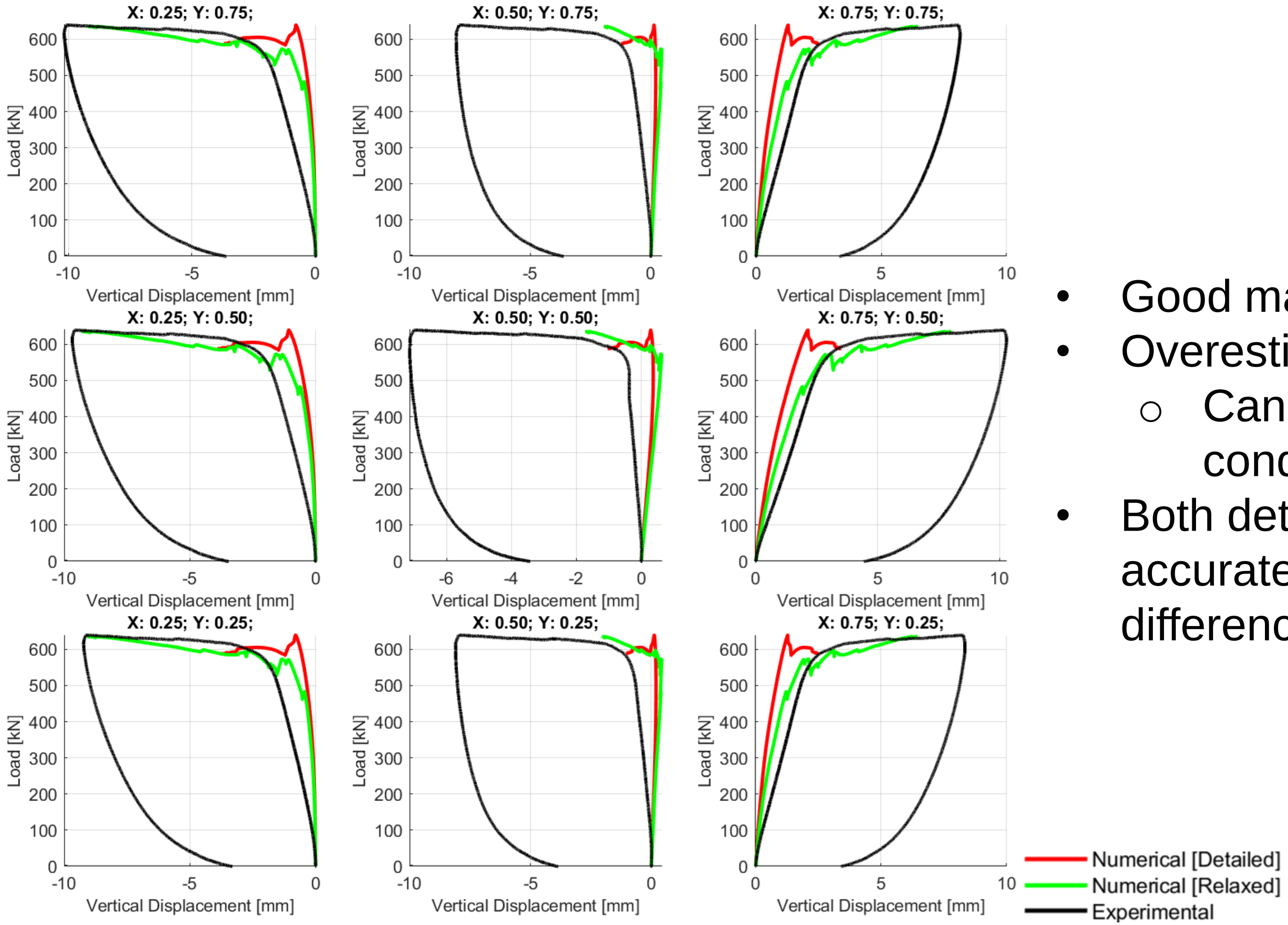

- Good match for the **ultimate load level**
- Overestimation of **initial stiffness**
  - Can be attributed to multiple tests conducted prior to the test to failure
- Both detailed and relaxed models capture accurately the ultimate behaviour with minor differences associated with the SW failure mode

Validation: Experimental Study - Damage

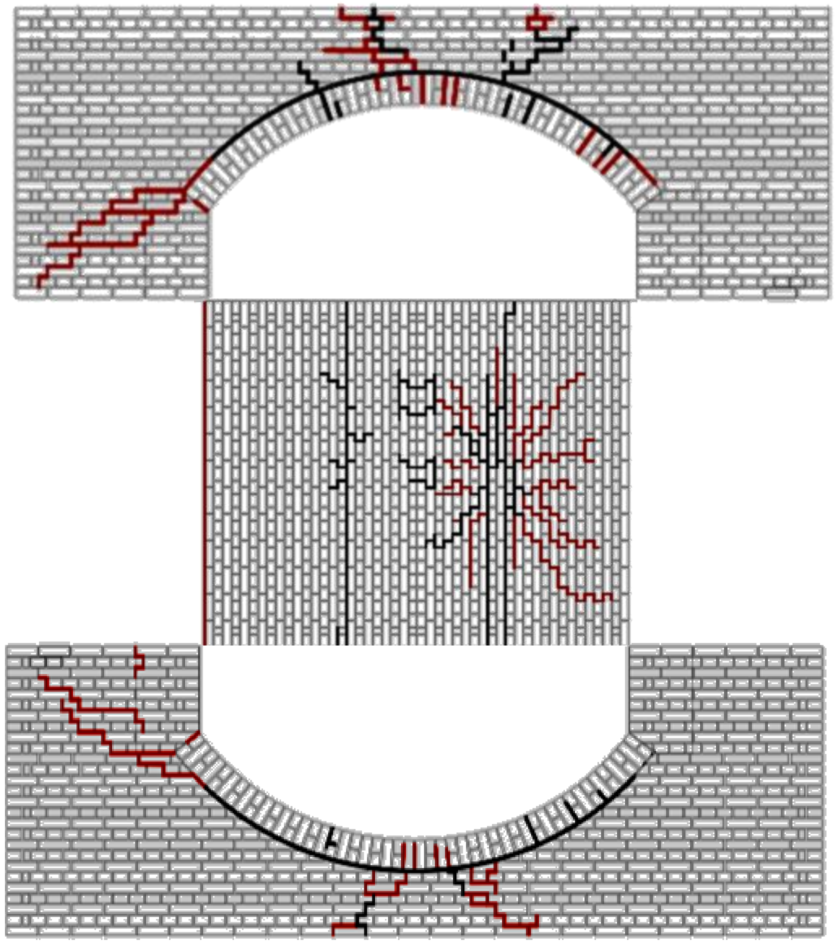

Validation: Experimental Study - Damage

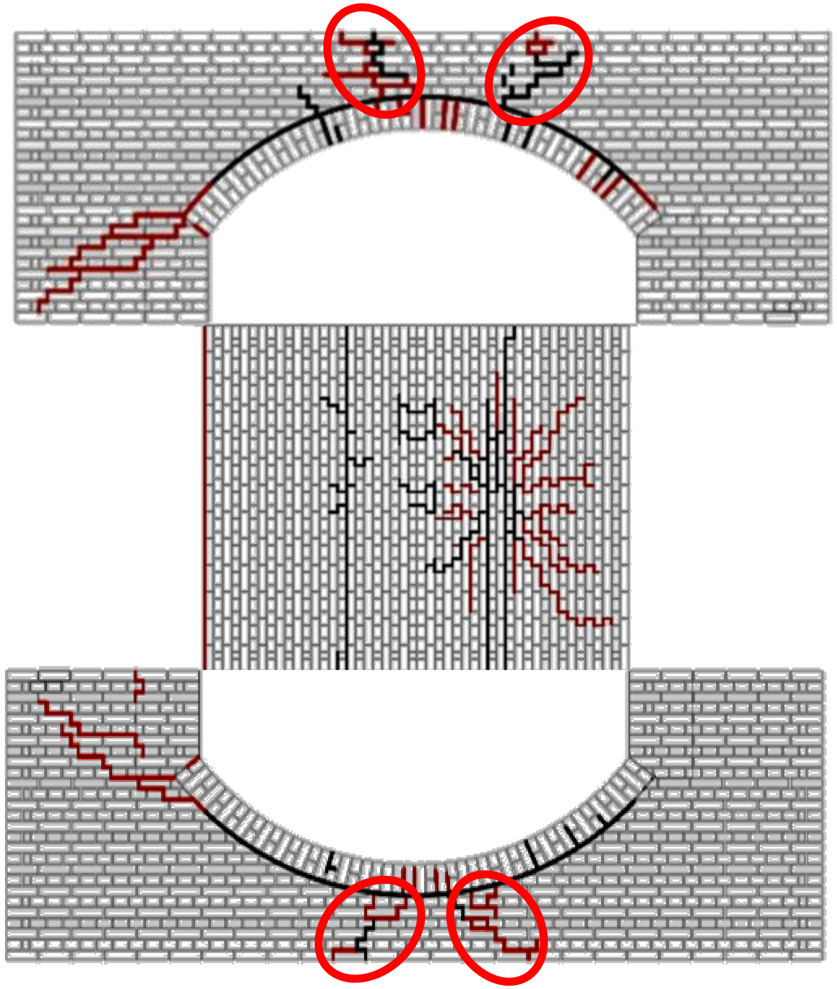

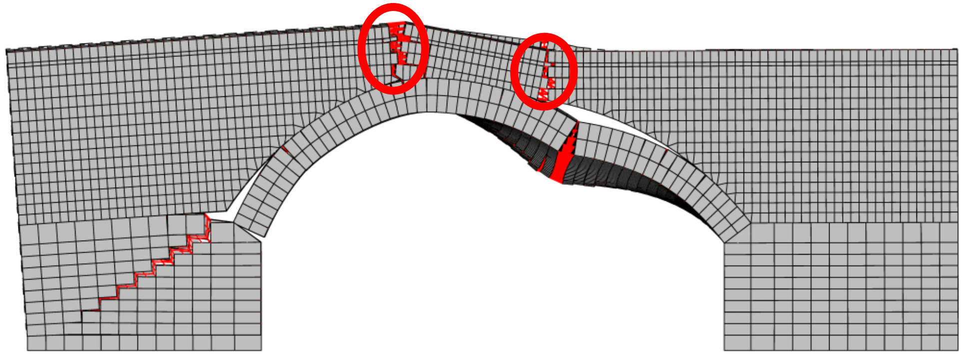

- Accurate prediction of cracks propagation in the SW

Validation: Experimental Study - Damage

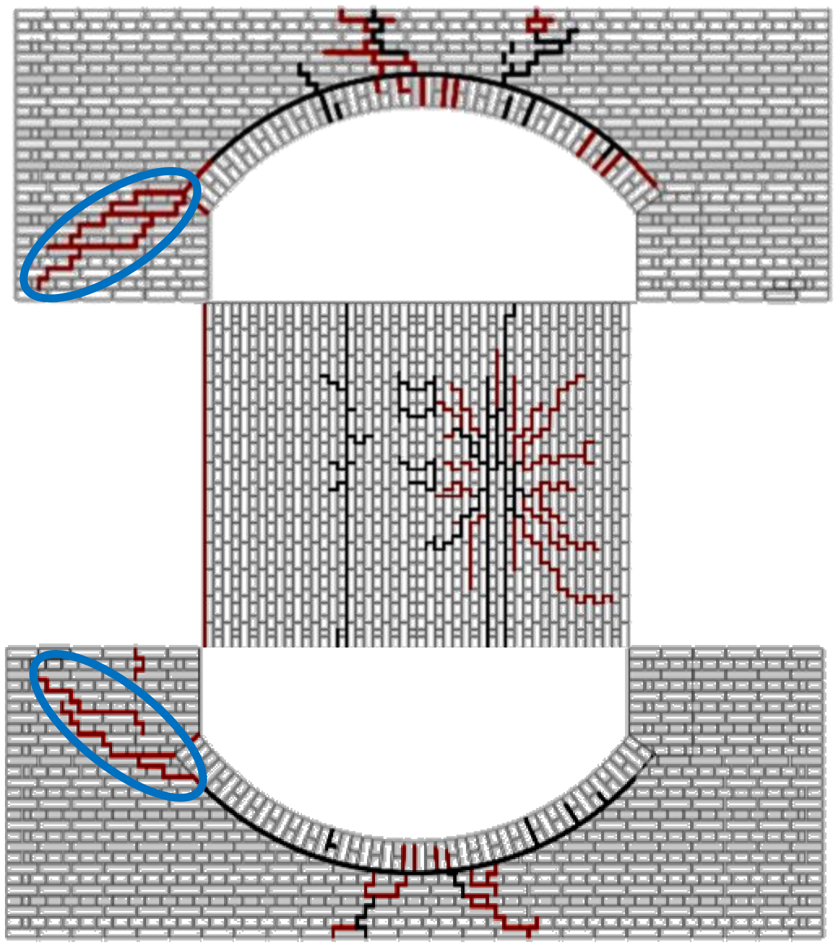

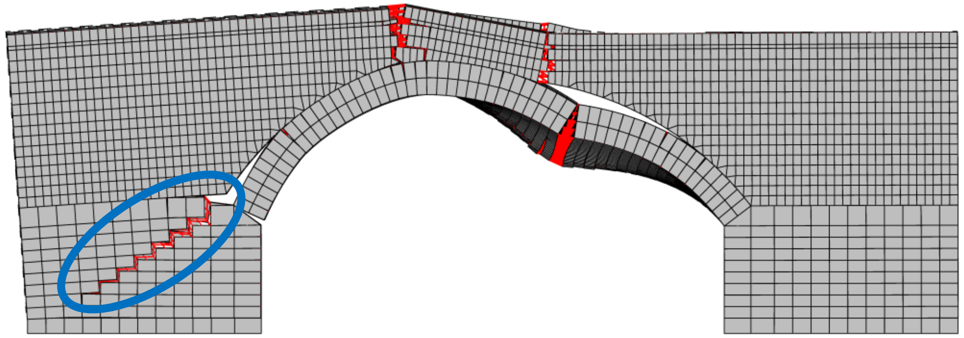

- Accurate prediction of cracks propagation in the SW
- Reasonable prediction of crack propagation through the abutment

Experimental Study Validation: Damage

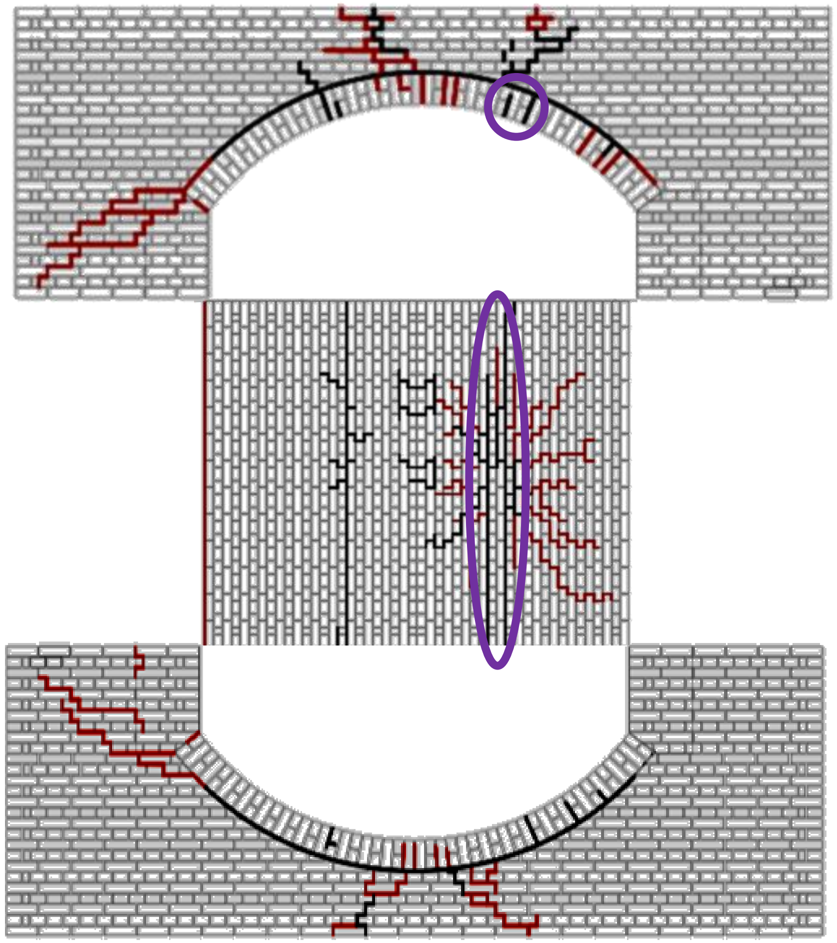

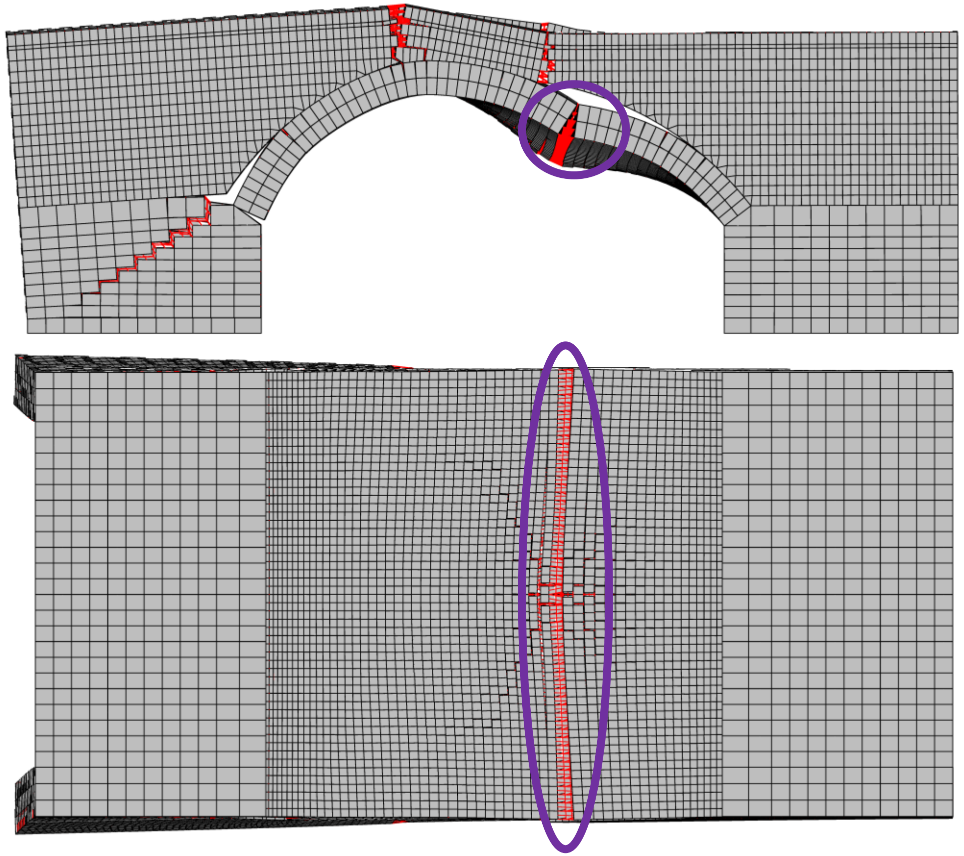

- Accurate prediction of cracks propagation in the SW
- Reasonable prediction of crack propagation through the abutment
- Adequate representation of transversal cracks forming in the arch barrel (AB)

Validation: Experimental Study - Damage

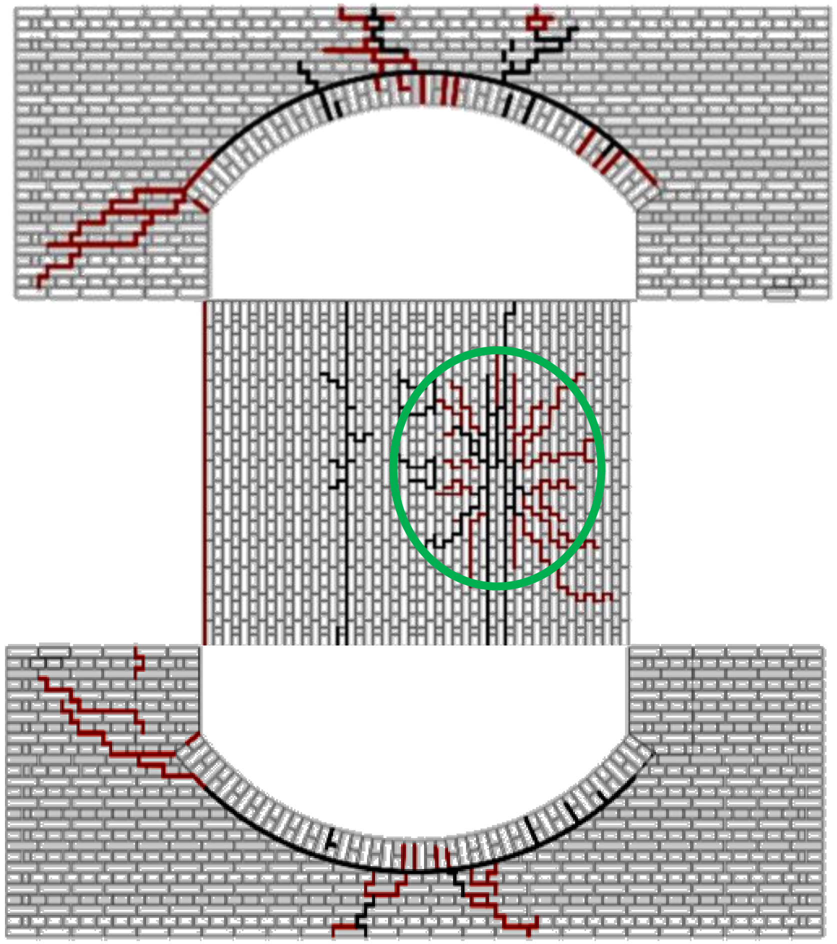

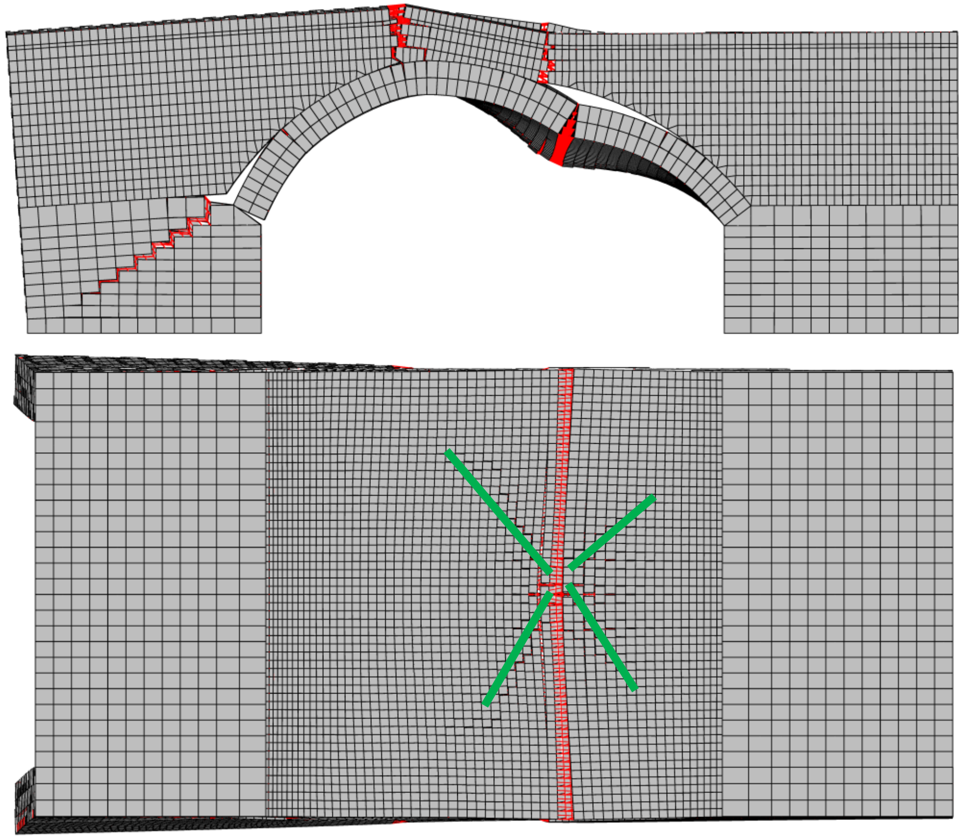

- Accurate prediction of cracks propagation in the SW
- Reasonable prediction of crack propagation through the abutment
- Adequate representation of transversal cracks forming in the arch barrel (AB)
- Diagonal cracks in the AB forming under the loading area

Validation: Experimental Study - Damage

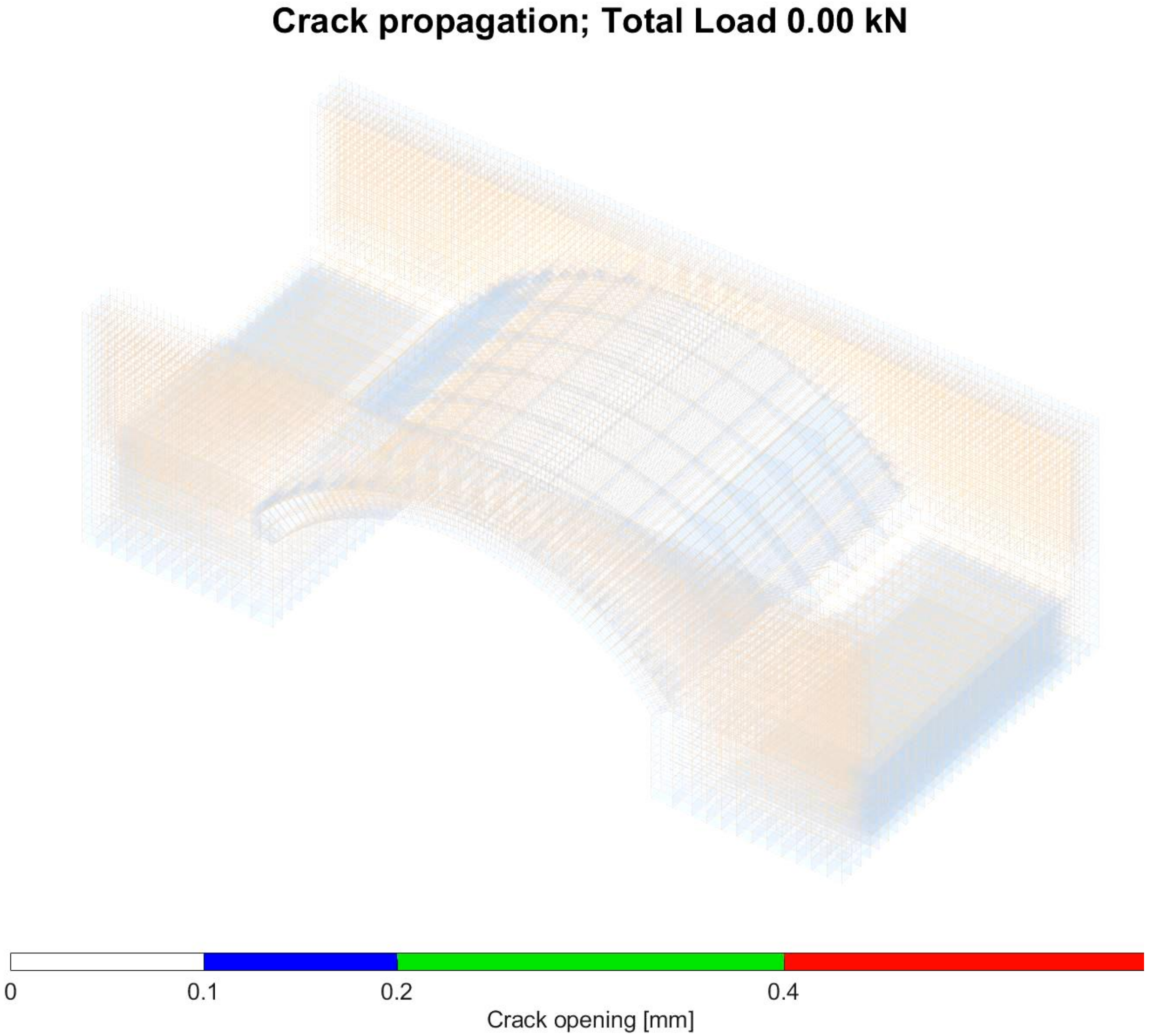

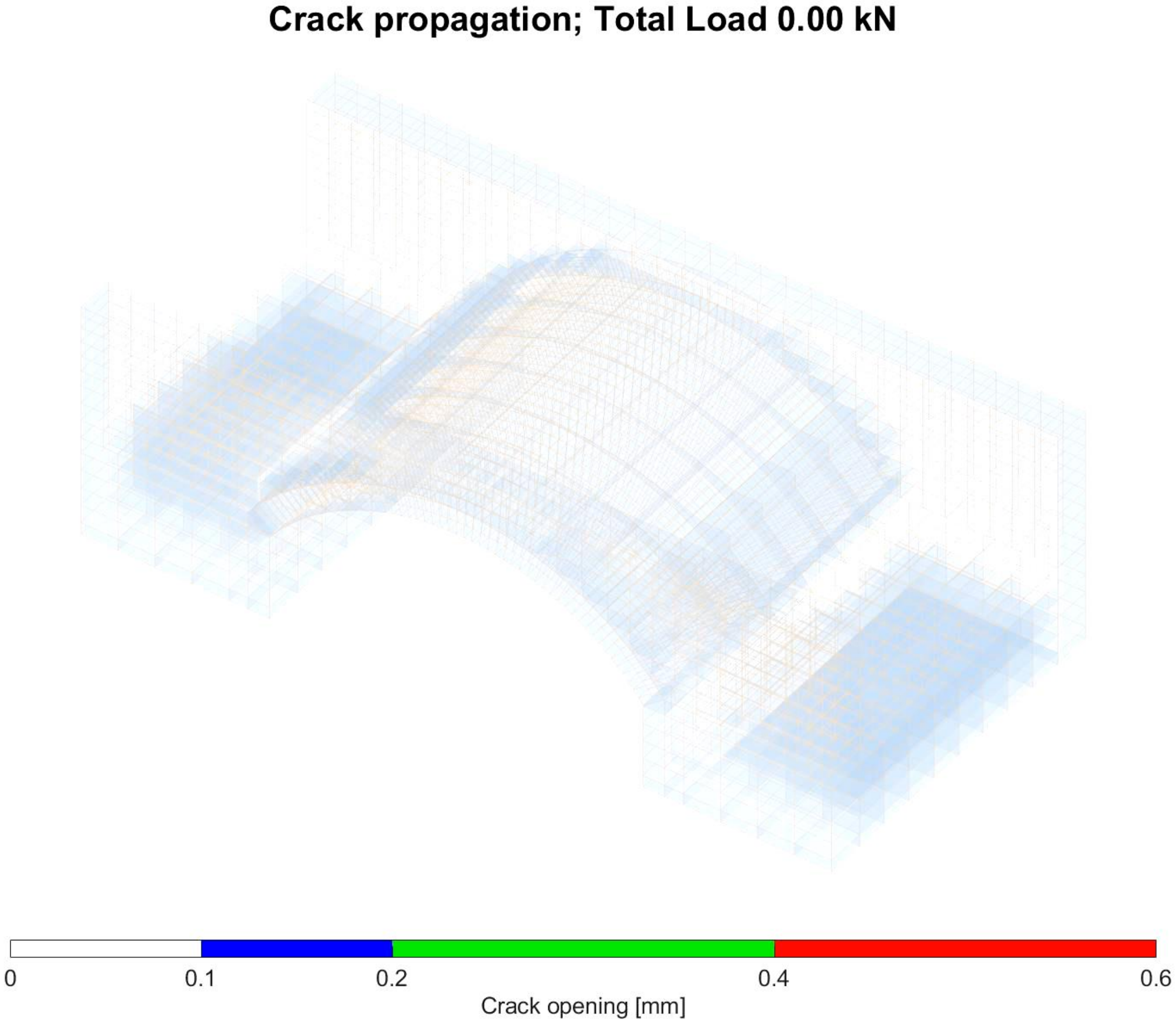

Validation of Numerical Models

Loading History Effects

Validation: Experimental Study - History

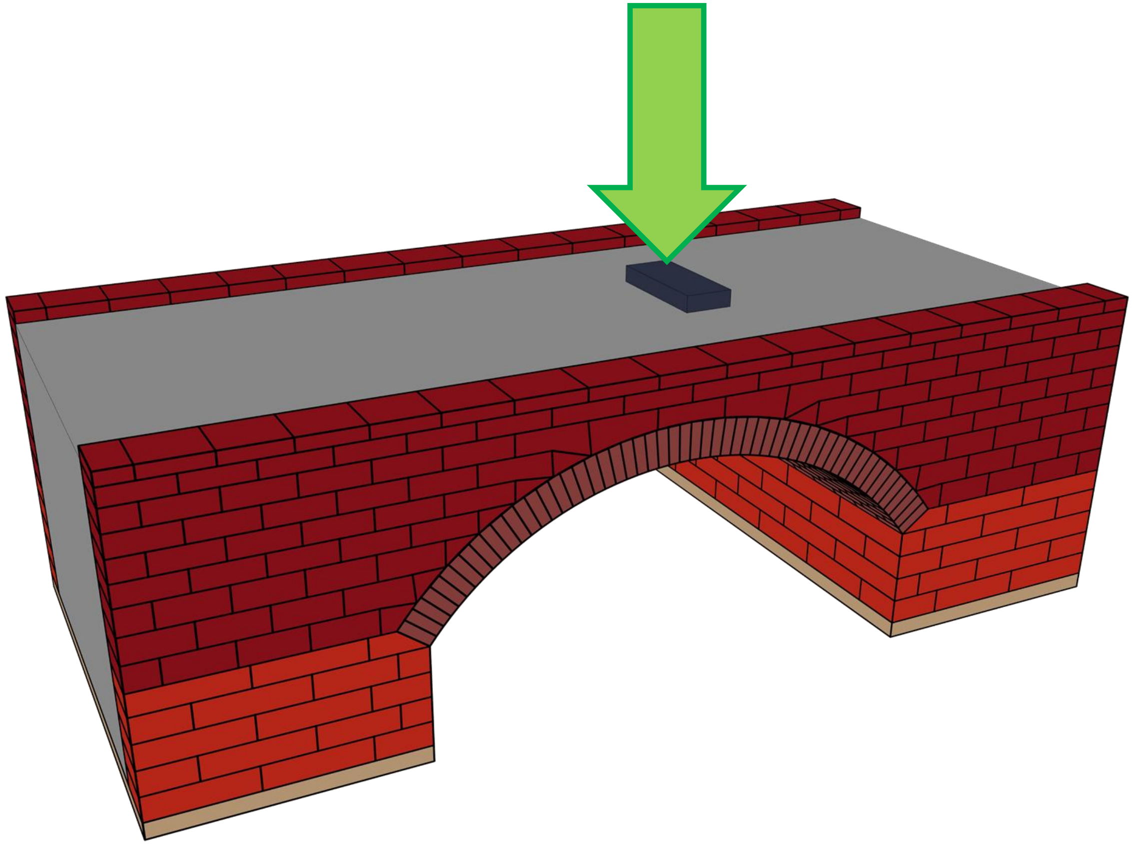

- Influence of prior loading/ unloading cycles was investigated
- Load applied on patch area via displacement control
- Each load level is applied twice

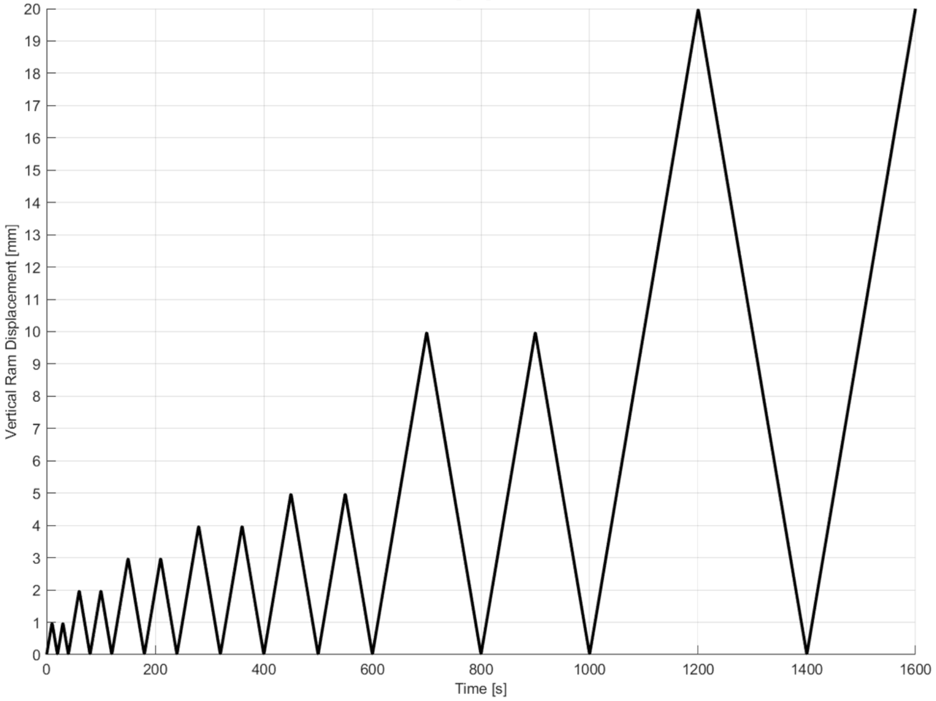

Validation: Experimental Study - History

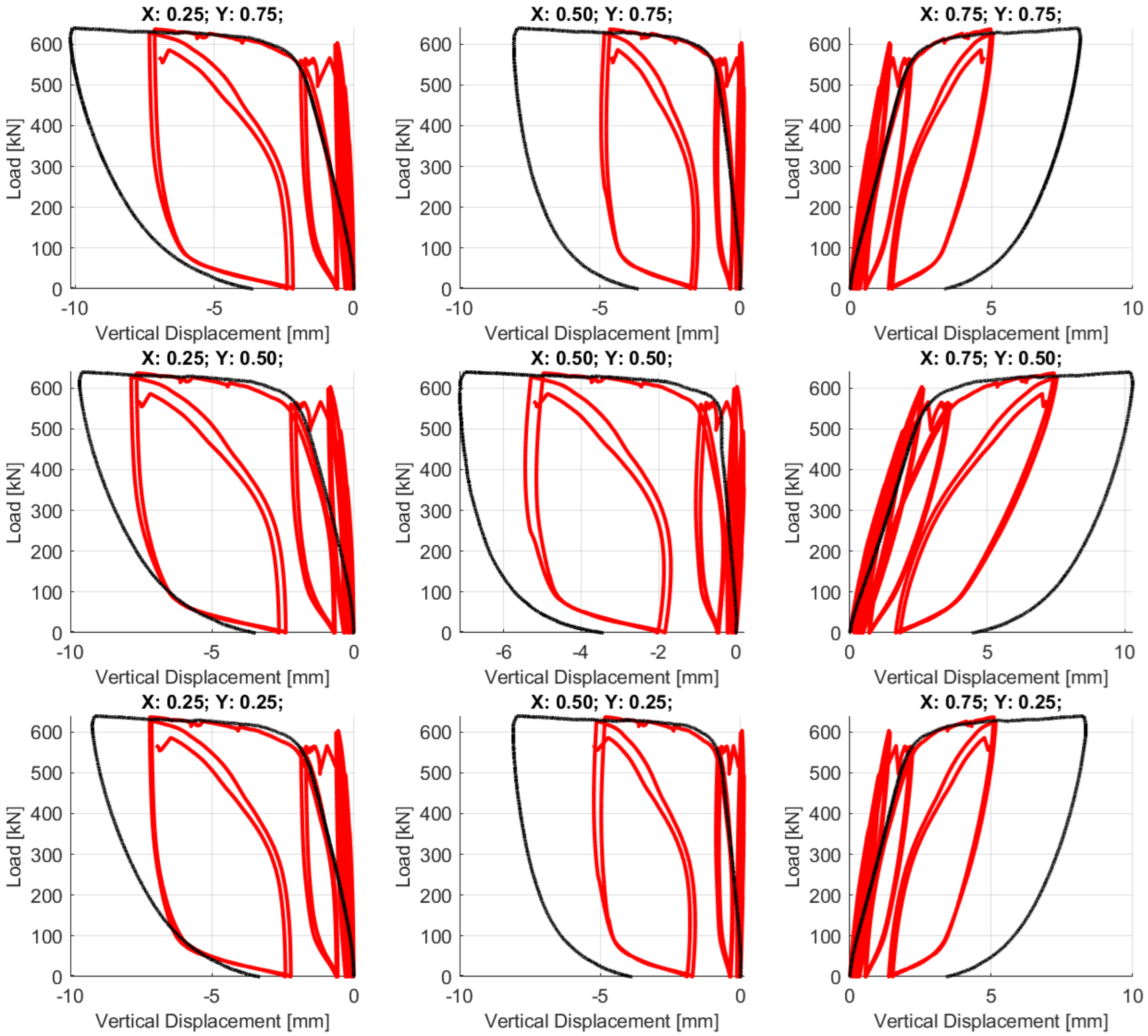

- Consideration of cycling behaviour leads to an improved prediction of the initial stiffness for the ultimate test

Numerical [Quasi-cyclic]
Experimental

UKRI Engineering and Physical Sciences Research Council

Validation: Experimental Study - History

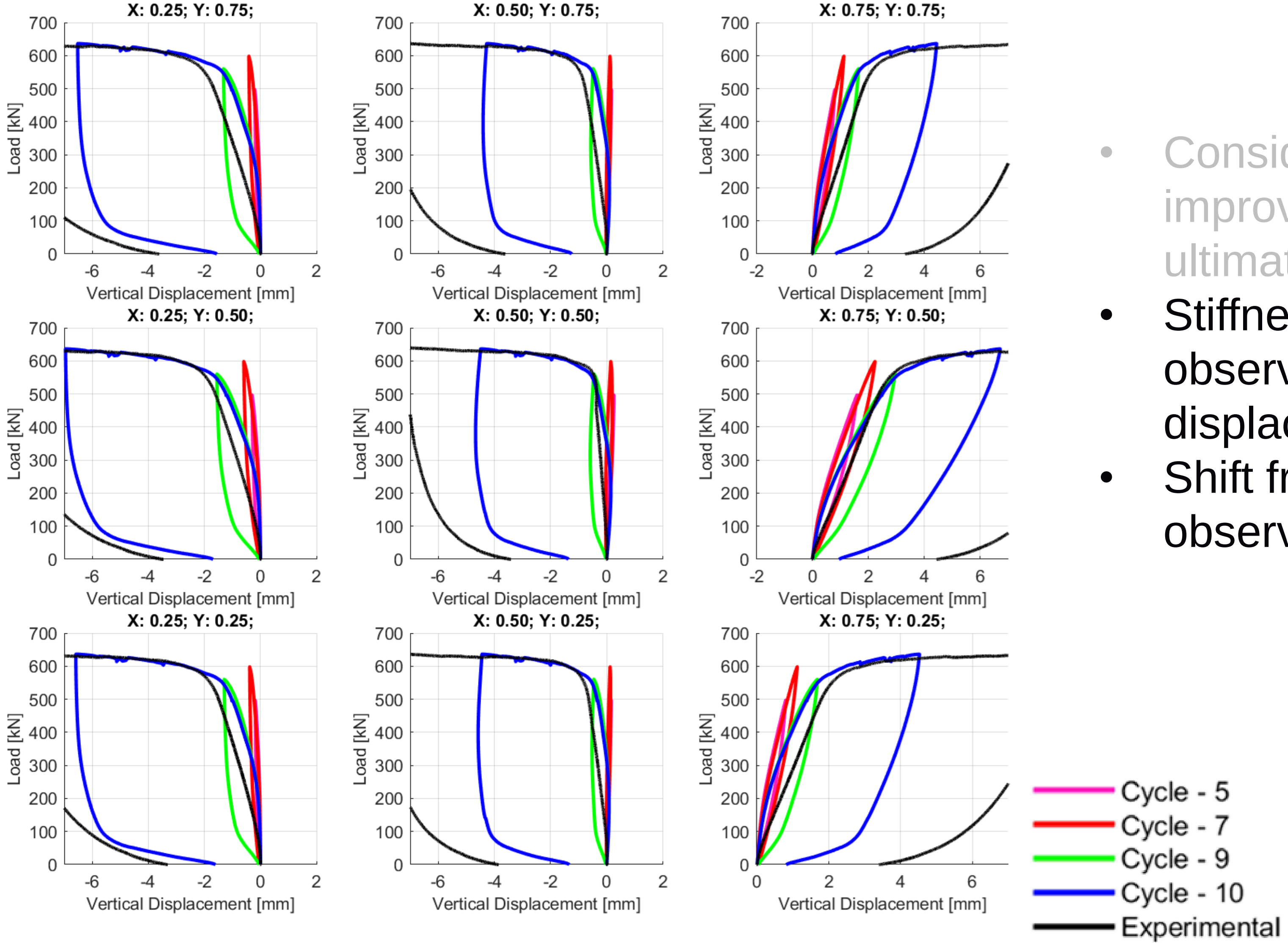

- Consideration of cycling behaviour leads to an improved prediction of the initial stiffness for the ultimate test
- Stiffness deterioration with cycles can be observed by plotting each cycle without displacement accumulation
- Shift from downward to upward displacements is observed at mid-span

Validation: Experimental Study - History

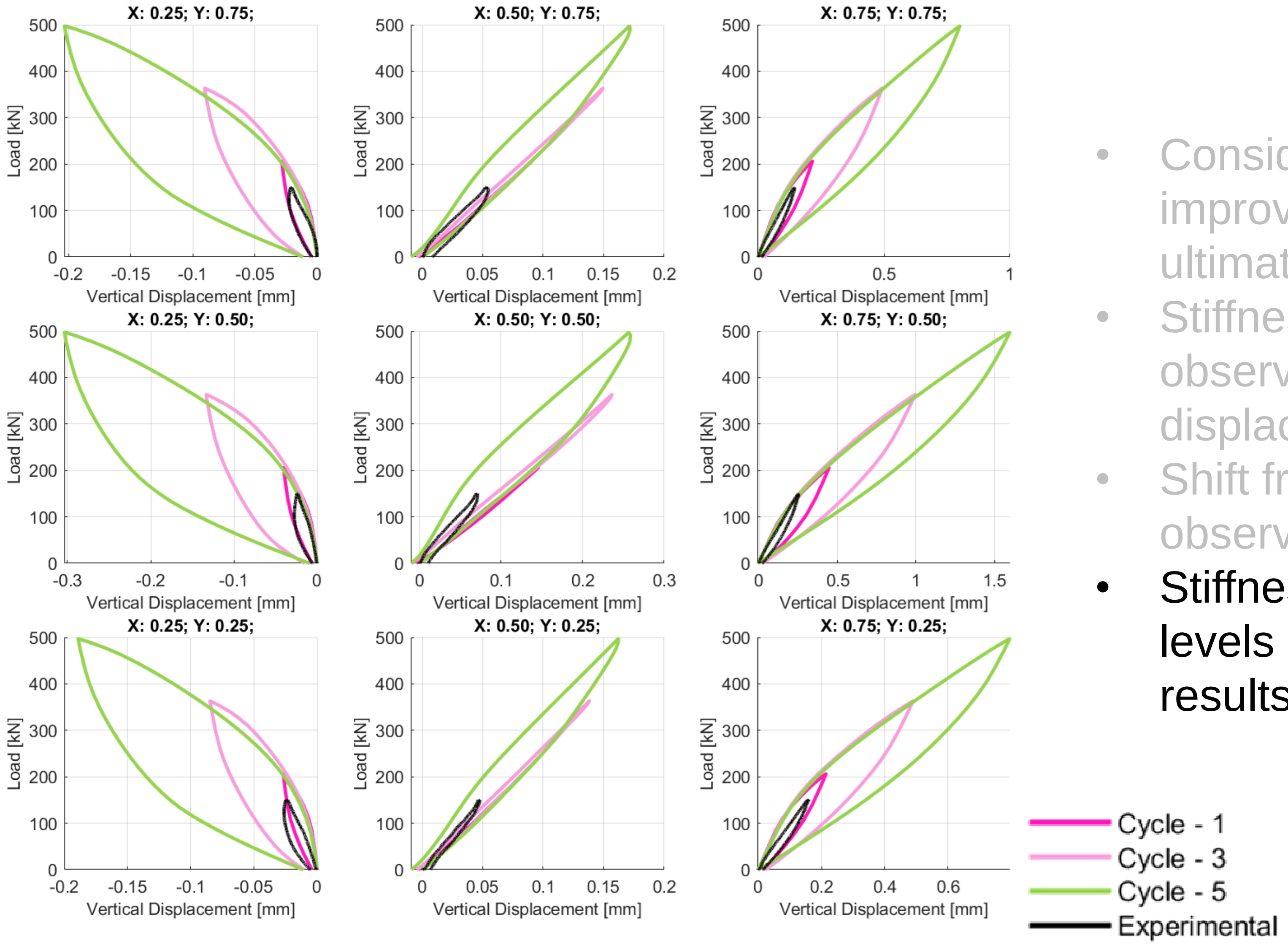

- Consideration of cycling behaviour leads to an improved prediction of the initial stiffness for the ultimate test
- Stiffness deterioration with cycles can be observed by plotting each cycle without displacement accumulation
- Shift from downward to upward displacements is observed at mid-span
- Stiffness predicted when cycling at low loading levels compares well with the experimental results for this loading range

Validation: Experimental Study - History

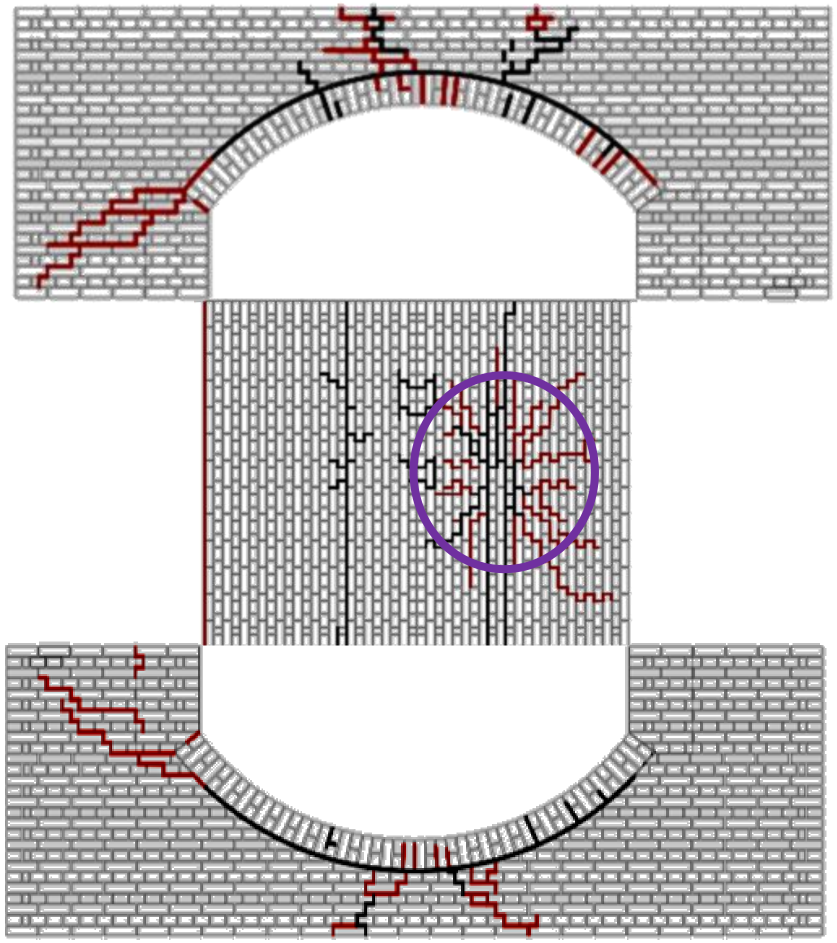

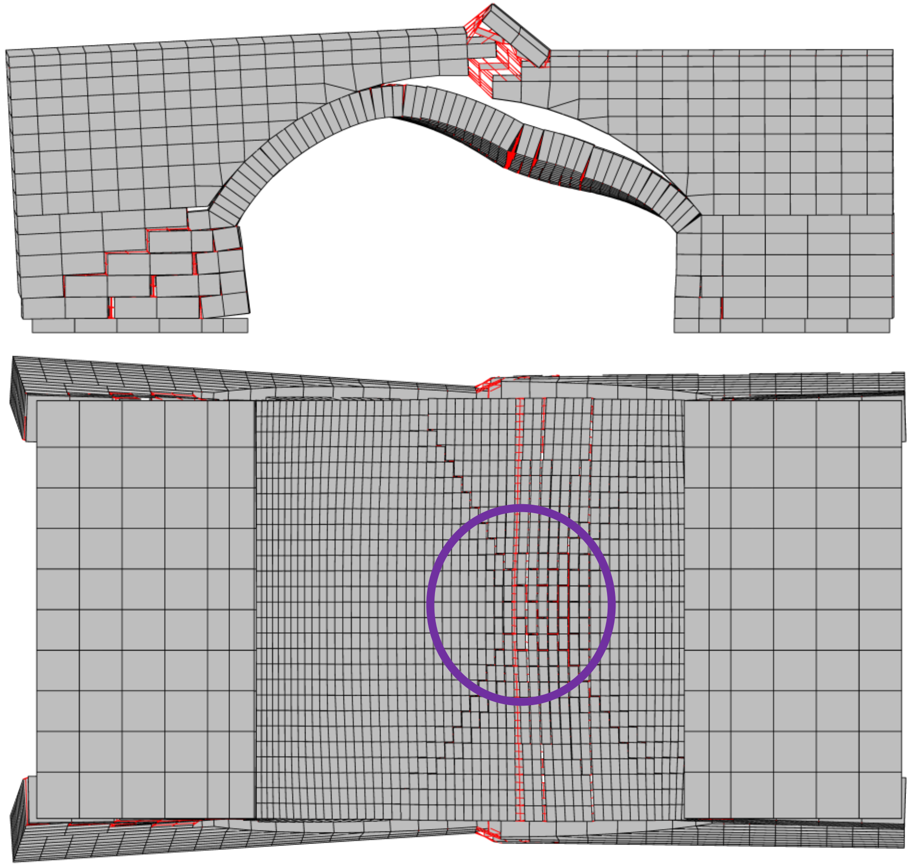

- Cyclic loading increases crack size, especially for diagonal cracks

Validation: Experimental Study - History

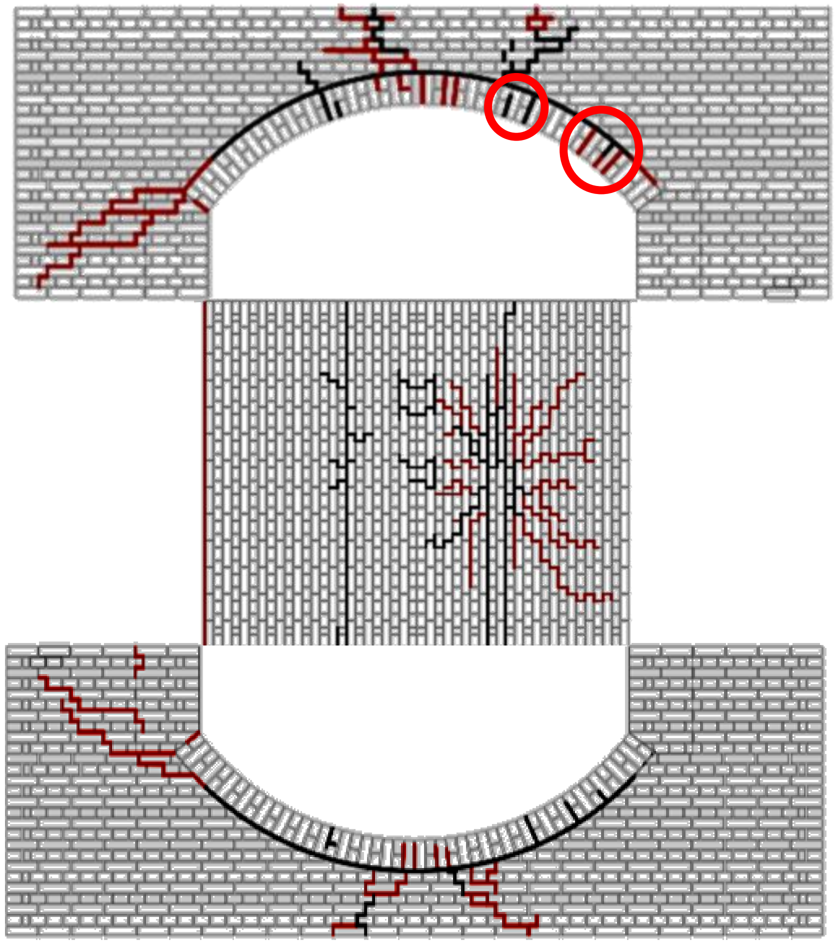

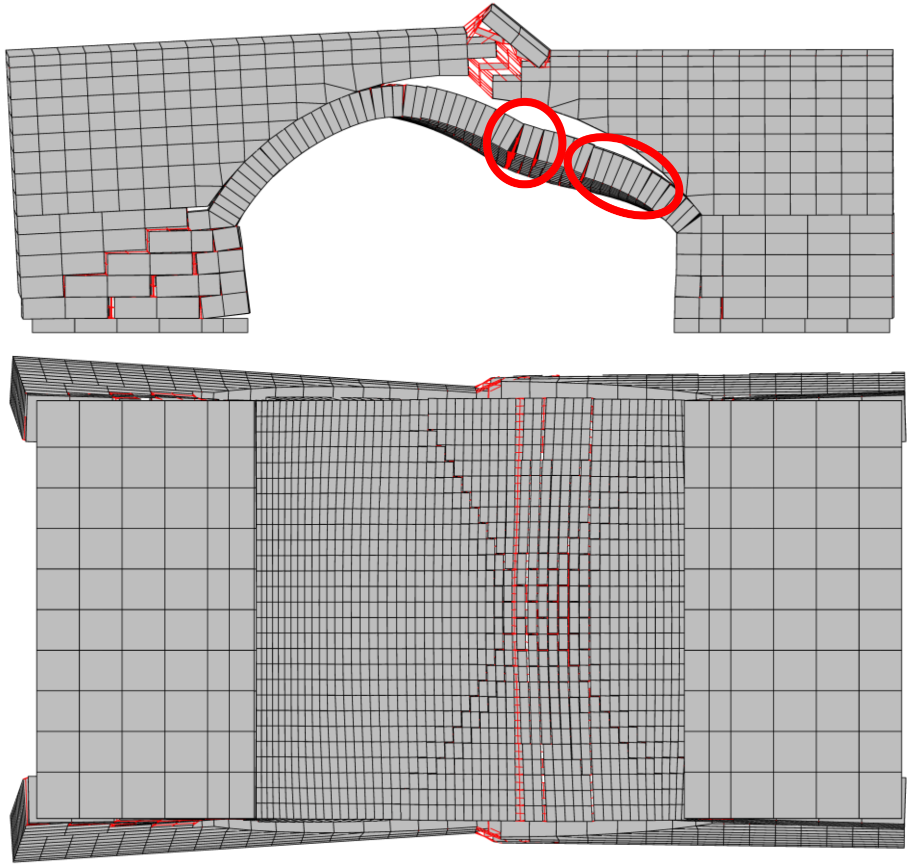

- Cyclic loading increases crack size, especially for diagonal cracks
- Wide transversal crack fully forms at ¾ span
- More partial transversal cracking appears between ¾ span and springing

Validation: Experimental Study - History

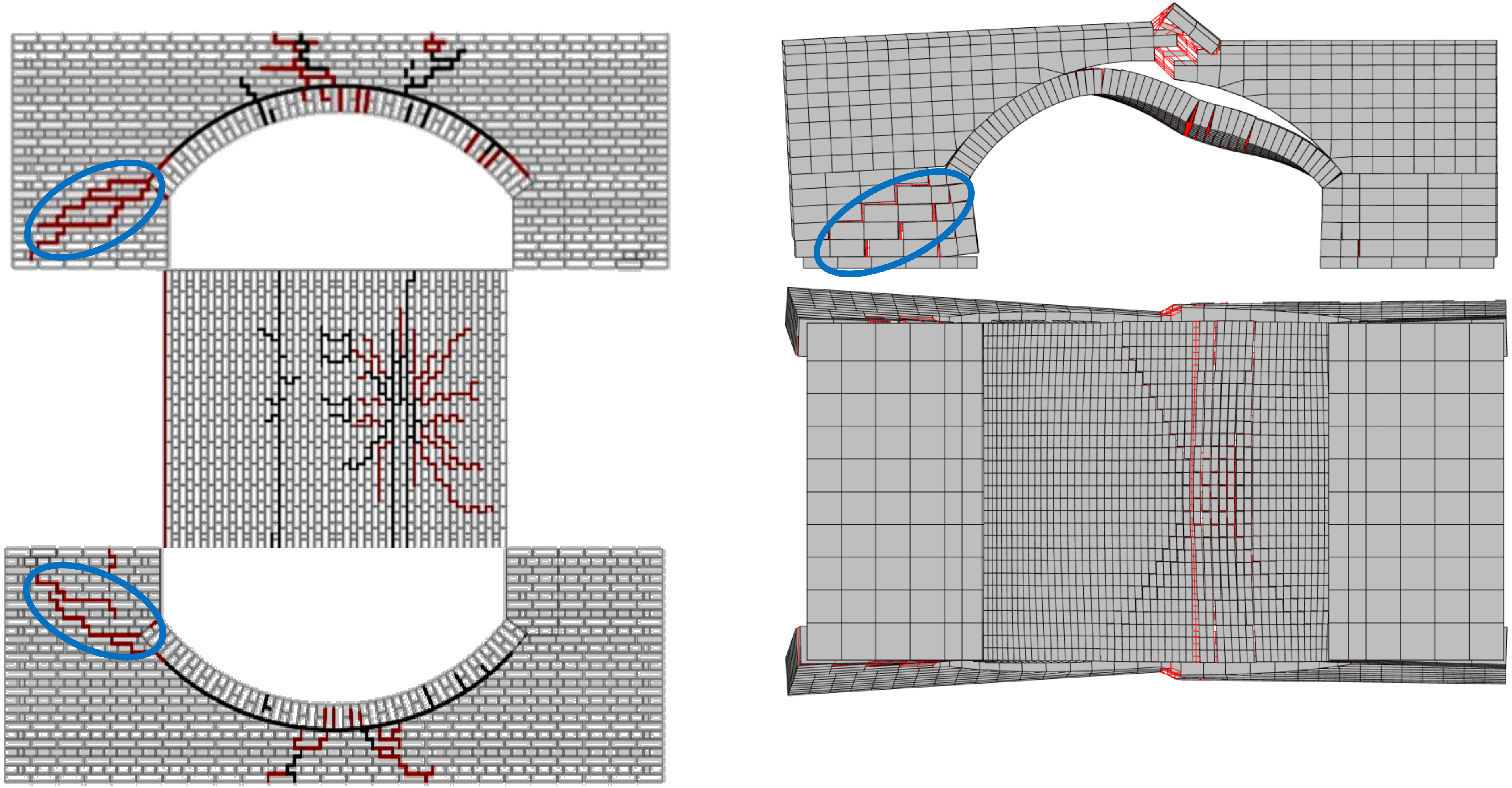

- Cyclic loading increases crack size, especially for diagonal cracks
- Wide transversal crack fully forms at ¾ span
- More partial transversal cracking appears between ¾ span and springing
- Captures formation of the second abutment crack

Validation: Experimental Study - History

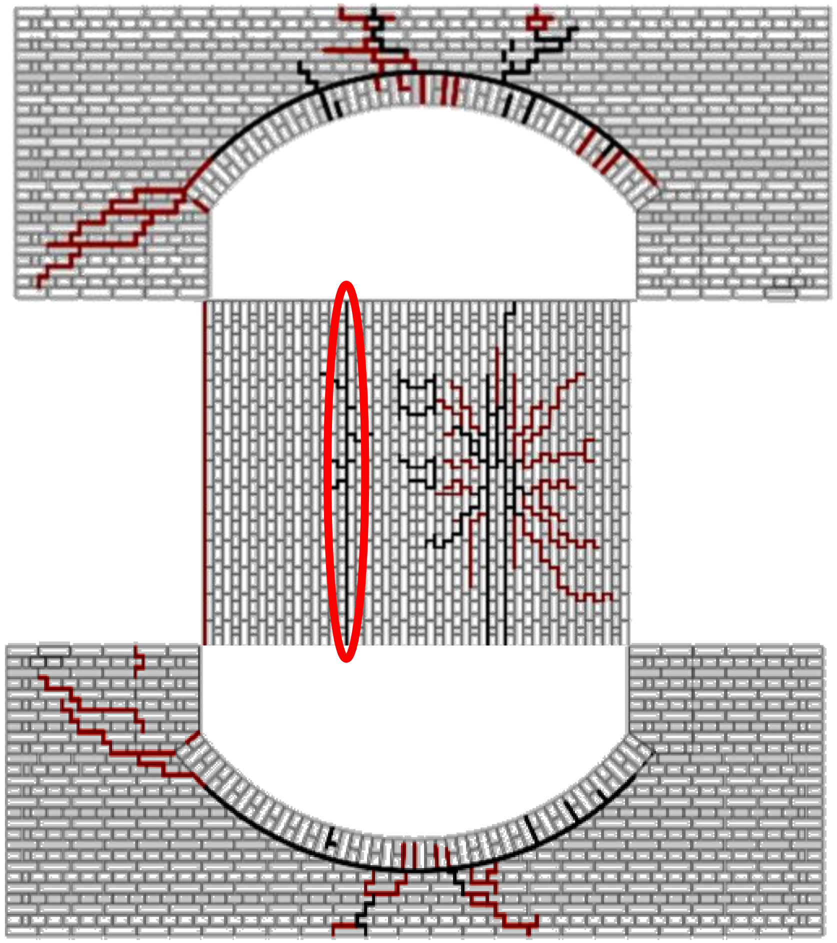

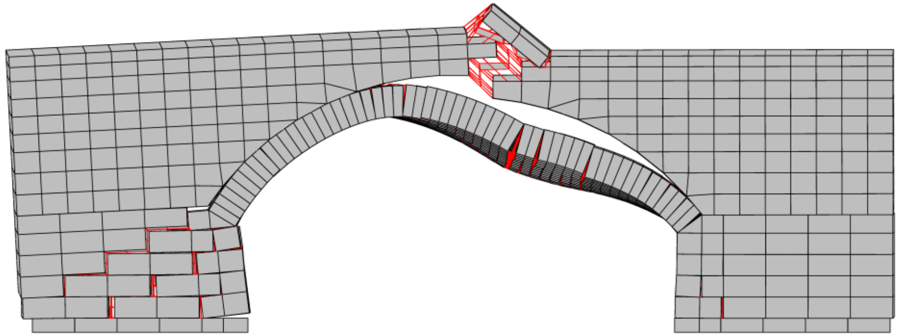

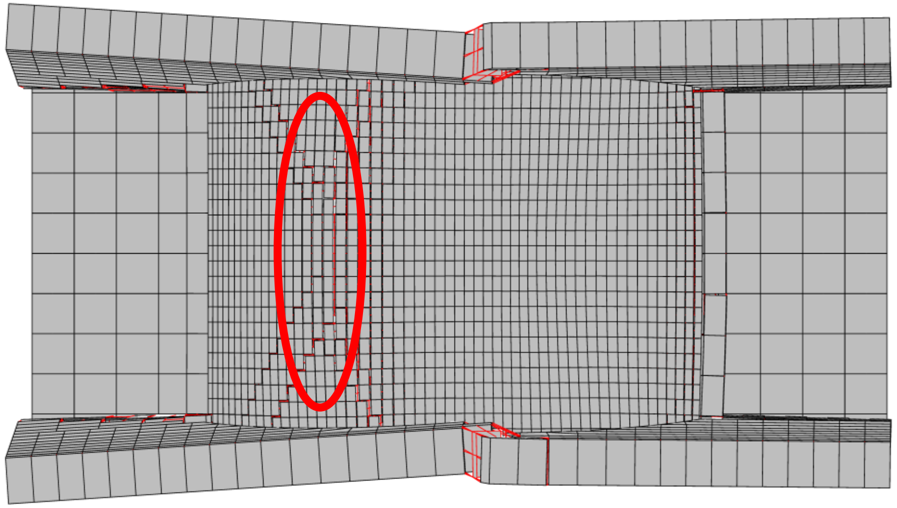

Top view with backfill removed

- Cyclic loading increases crack size, especially for diagonal cracks
- Wide transversal crack fully forms at ¾ span
- More partial transversal cracking appears between ¾ span and springing
- Captures formation of the second abutment crack
- Compressive crushing of mortar combined with multiple loading stages

Validation: Experimental Study - History

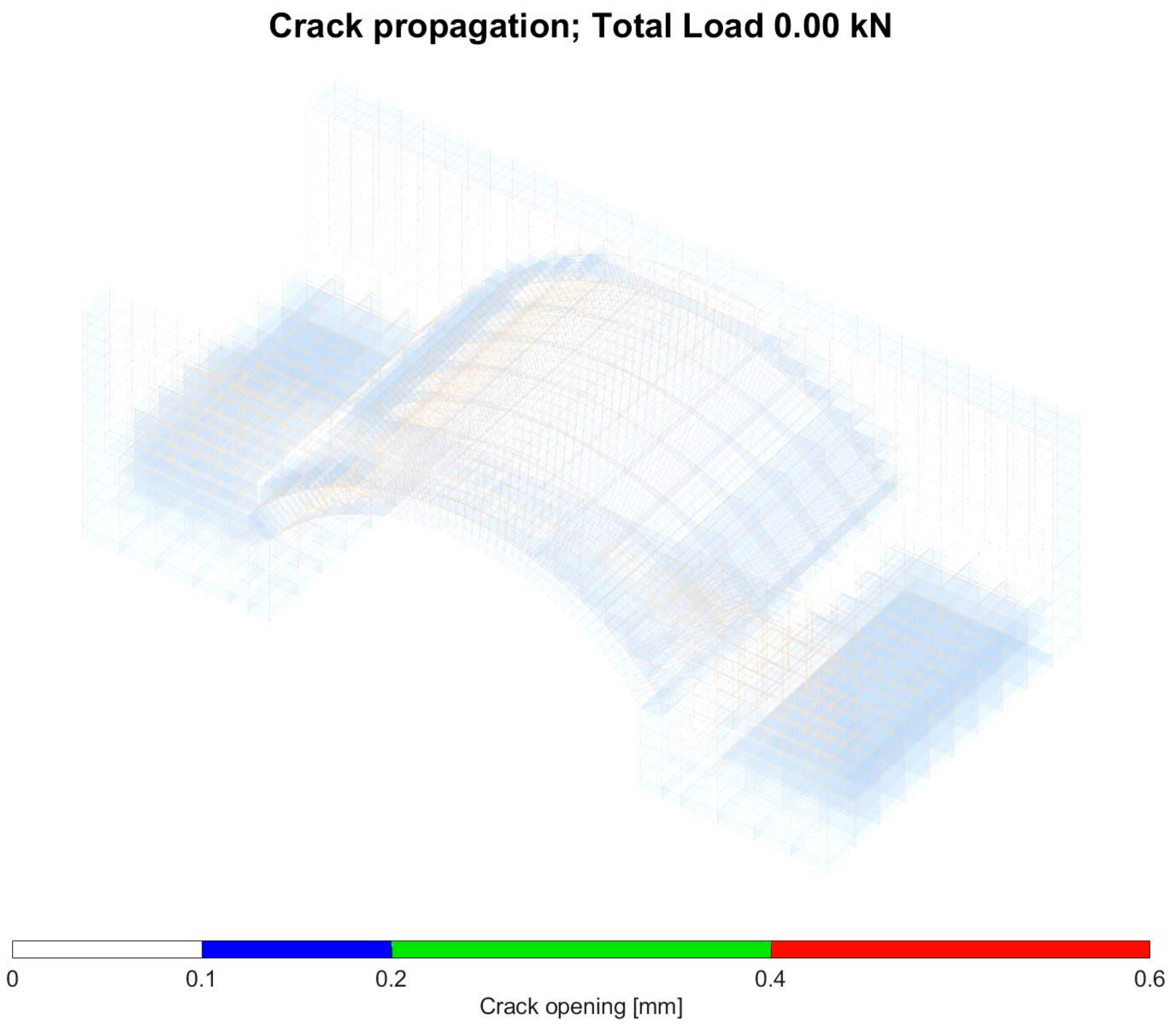

Fatigue in Masonry

Fatigue in Masonry

- Limited research on fatigue behaviour of masonry materials and structures.
- Tests on masonry panels under compression forces revealed a 50% reduction in load capacity under high-cycle (10^5) loading.
- Experimental tests on multi-ring brick-masonry arches showed a change in failure mode under high-cycle loading.

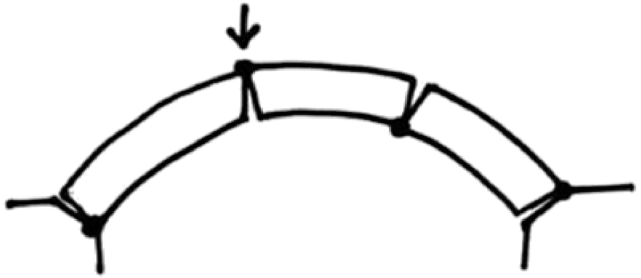

4-hinge mechanism under monotonic loading

Ring separation under cyclic loading

- *Inspections on real masonry bridges confirm notable damage in several structures typically subjected to loading level well below the predicted failure load which may indicate the development of fatigue in the brick/stonework.*

Fatigue in Masonry: Methods

Material model allowing for fatigue damage

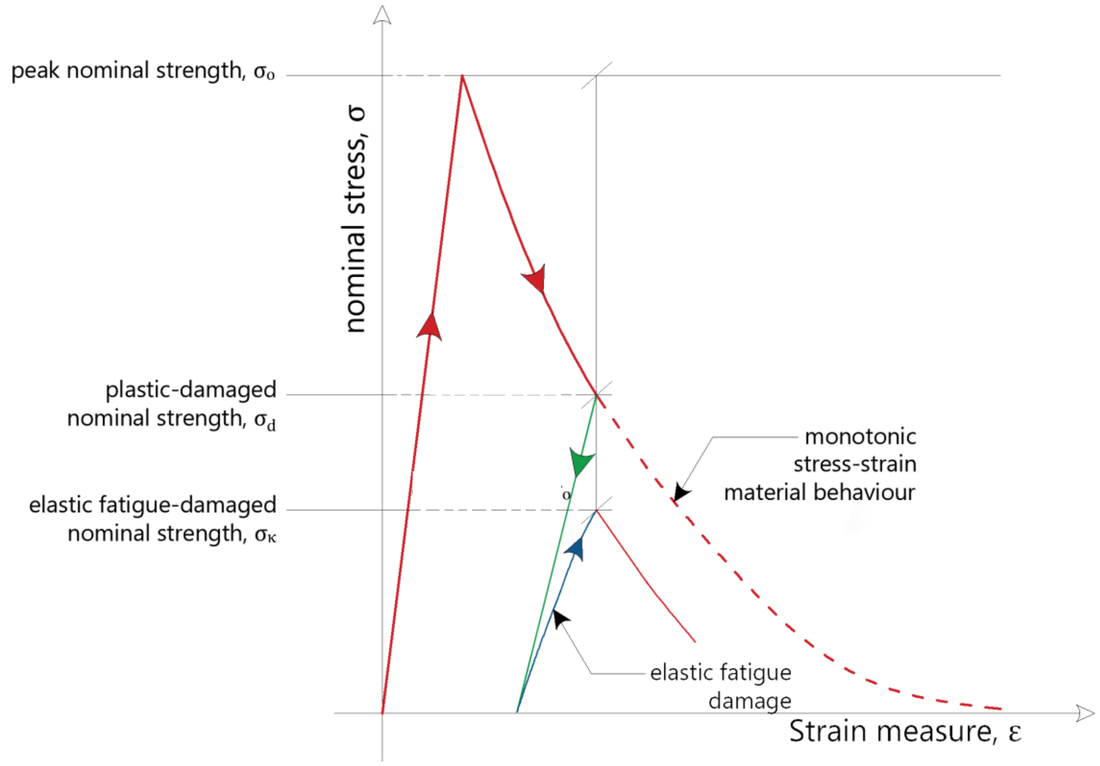

Elastic constitutive law:
The elastic/plastic-damage relation relates the “nominal” stress of the damage material to the effective stress through a damage,variable.

$$\boldsymbol{\sigma} = (\boldsymbol{I} - \boldsymbol{D})\tilde{\boldsymbol{\sigma}}$$

Elastic fatigue damage surface:
Defining an elastic fatigue damage surface as a function of a strain/stress measure and an endurance threshold.

Evolution of fatigue damage:
For each mode of deformation, a vector of fatigue damage evolution is utilised to describe the deterioration due to high cycle fatigue in the material.

Fatigue in Masonry: Methods

Material model allowing for fatigue damage

Fatigue damage evolution is defined as a function of the current level of damage an equivalent loading function weighted by a fatigue damage material parameter $\boldsymbol{\alpha}$*.*

$$\dot{D}_a = \alpha_a \cdot (1 - D_a) \cdot e^{\beta_a \cdot D_a} \cdot \langle \tilde{\sigma}_a - \eta_\alpha \cdot \tilde{\sigma}_{0,a} \rangle \cdot \dot{\varepsilon}_a \qquad [0 < D_a < 1; \quad a = 1,3]$$

Given the increment of the elastic interface opening and effective elastic stress at the current step and the damage in the previous step, the current damage can be obtained by solving the following non-linear equation:

$$f\left(D_a^{n+1}\right) = -D_a^{n+1} + D_a^n + \alpha_a \left(1 - D_a^{n+1}\right) e^{\beta_a D_a^{n+1}} \left\langle \tilde{\sigma}_a^{n+1} - \eta_a \tilde{\sigma}_{o,a} \right\rangle \dot{\varepsilon}_a^{n+1} = 0$$

α_α β_α η_α	material parameters to be derived from fatigue experiments for compression, tension and shear interface opening

Fatigue in Masonry: Static Validation

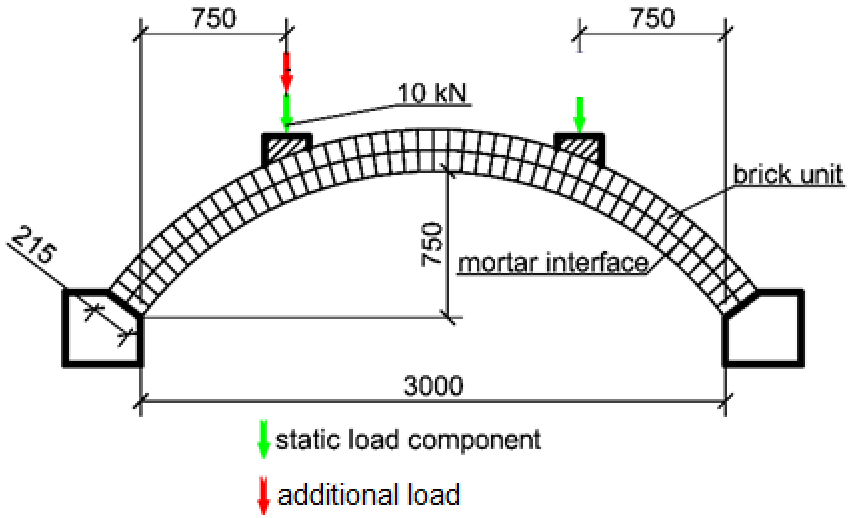

Brick unit Young's modulus	N/mm^2	38500
Interface normal stiffness	N/mm^3	100
Interface tangent stiffness	N/mm^3	40
Interface tensile strength	N/mm^2	0.1
Interface cohesion	N/mm^2	0.14
Fracture energy in tension	N.mm	0.05
Fracture energy in shear	N.mm	0.014

Fatigue in Masonry: Static Validation

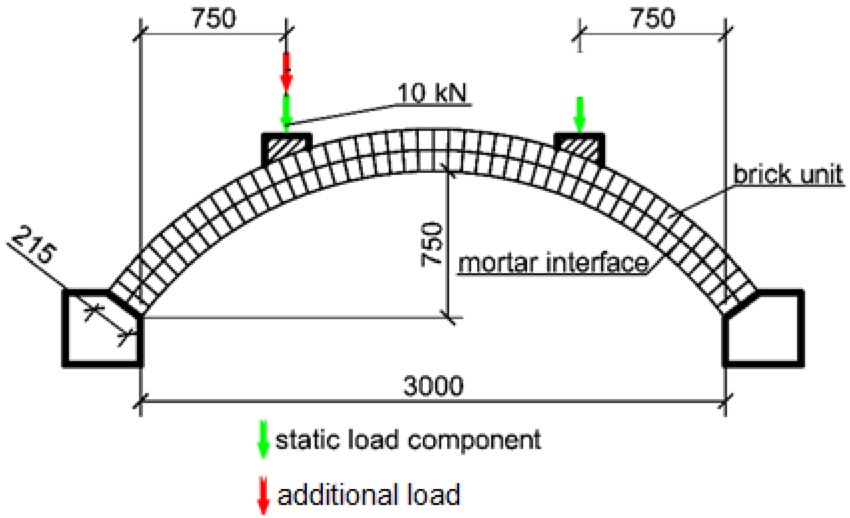

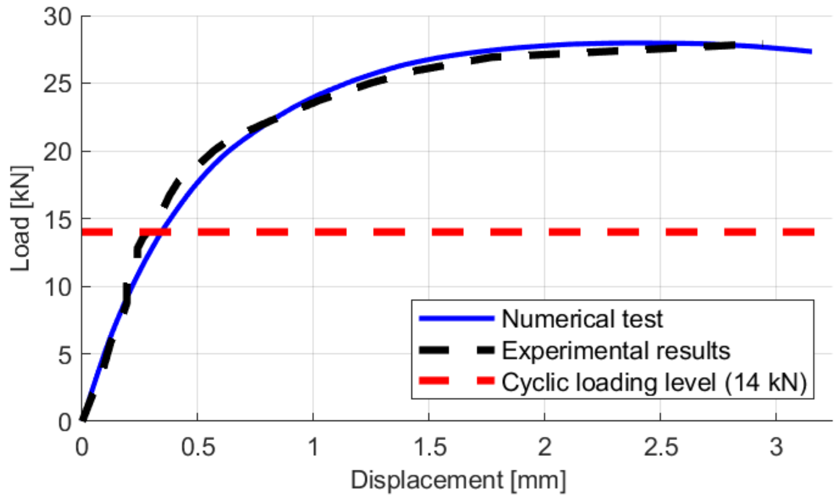

Brick unit Young's modulus	N/mm^2	38500
Interface normal stiffness	N/mm^3	100
Interface tangent stiffness	N/mm^3	40
Interface tensile strength	N/mm^2	0.1
Interface cohesion	N/mm^2	0.14
Fracture energy in tension	N.mm	0.05
Fracture energy in shear	N.mm	0.014

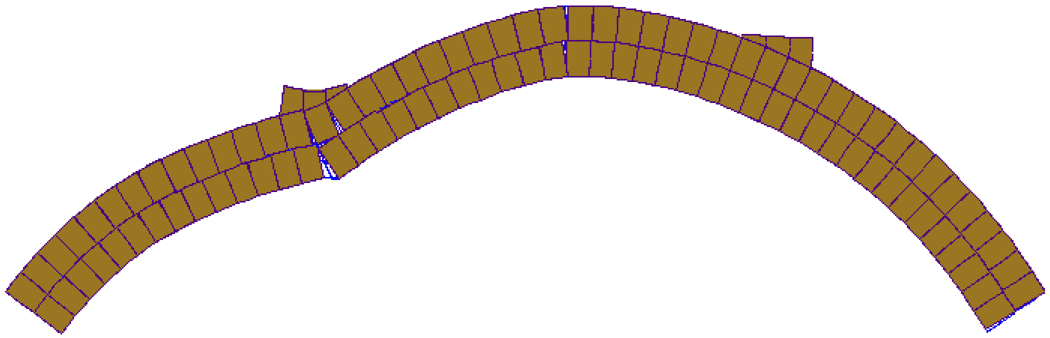

Fatigue in Masonry: Static Validation

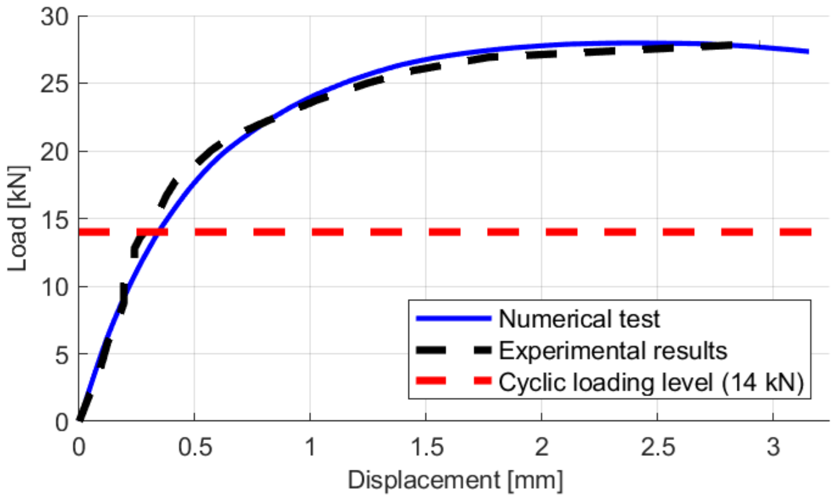

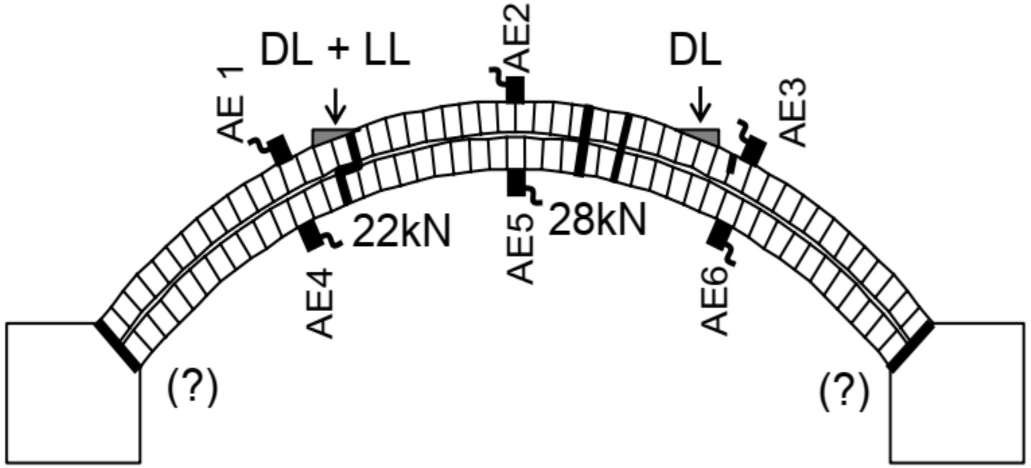

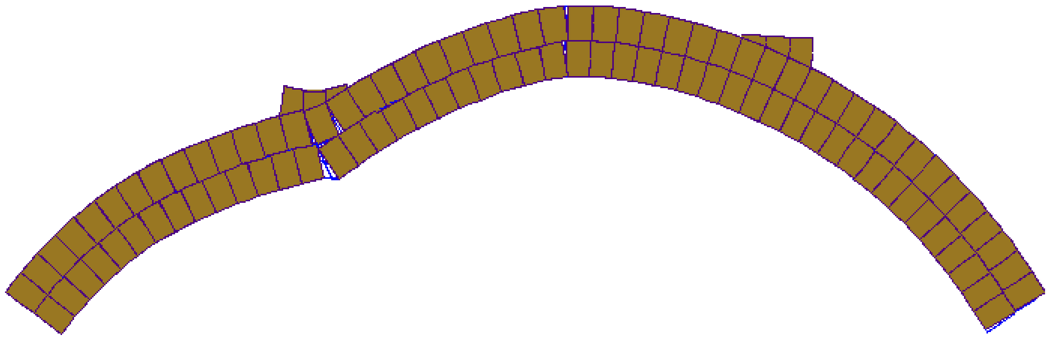

Fatigue in Masonry: Cyclic Validation

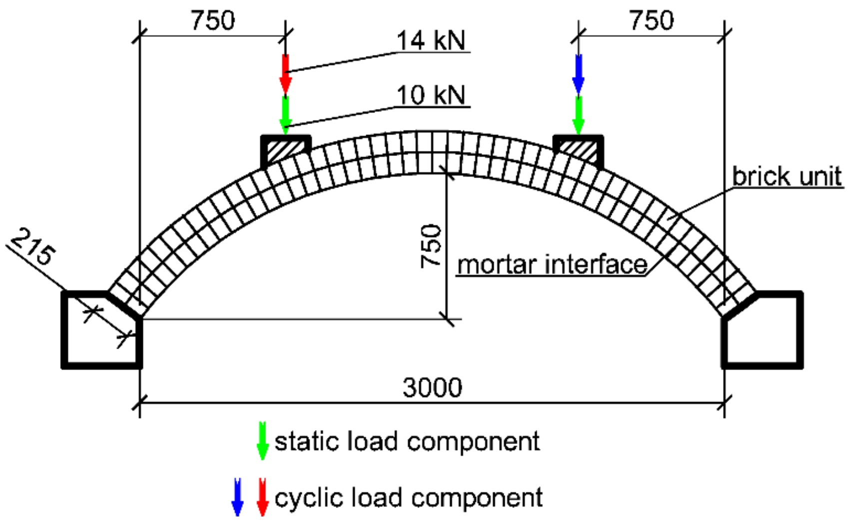

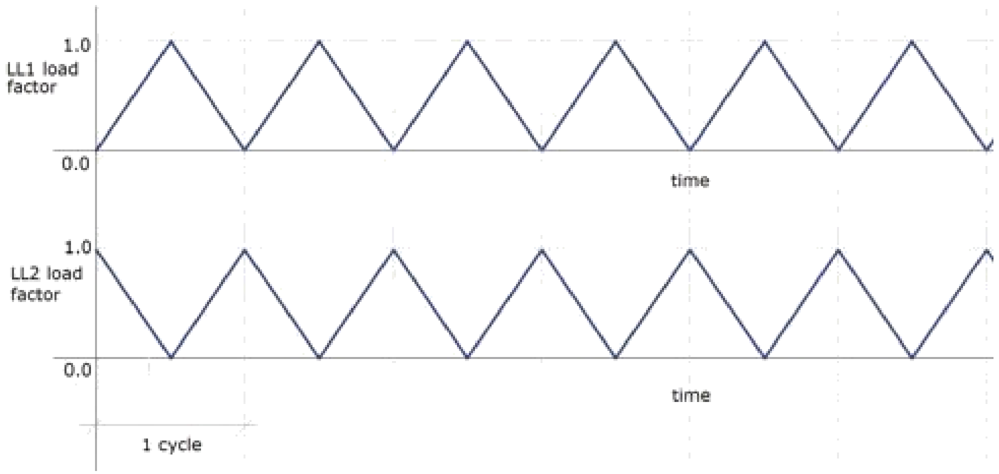

Fatigue in Masonry: Cyclic Validation

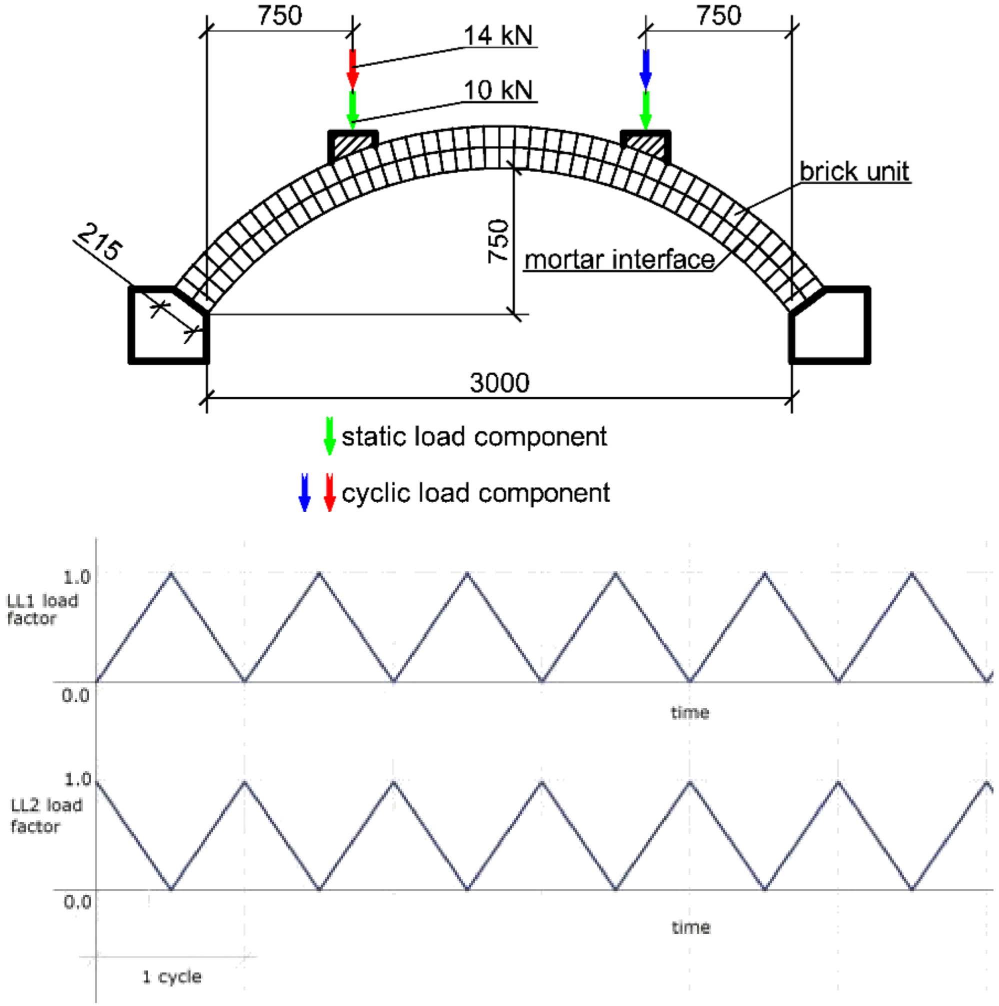

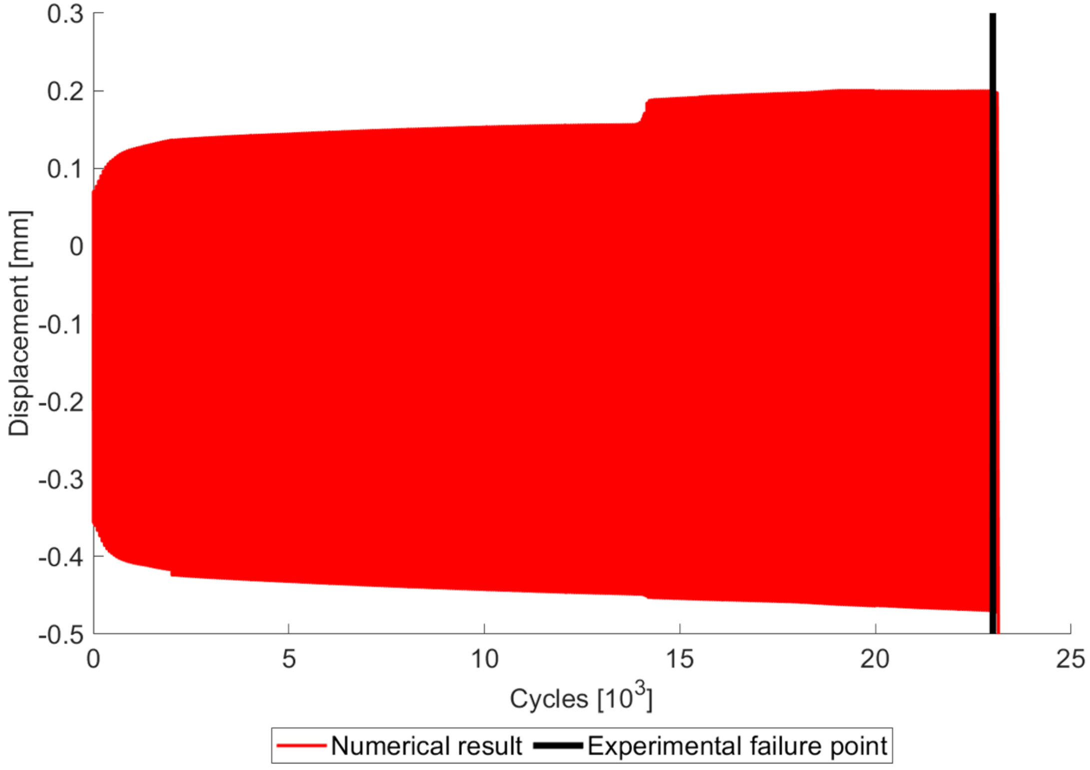

Fatigue in Masonry: Cyclic Validation

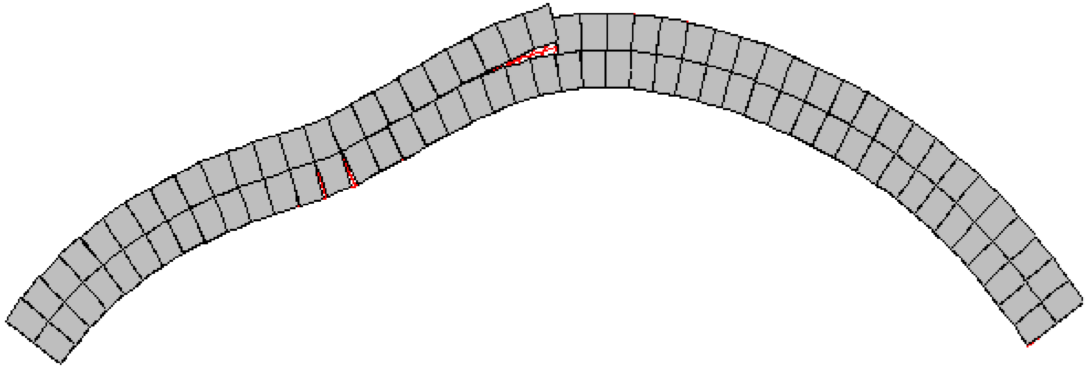

Cycles	Observed damage
48	**Damage initialisation at 1/4 and 3/4 span**
1201	Fully cracked quarter span joints and initialisation of damage at the supports
23101	Development of circumferential cracks, ring sliding and arch failure

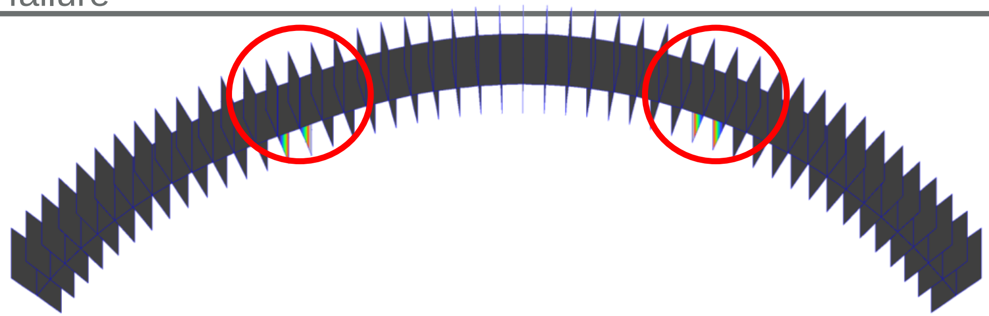

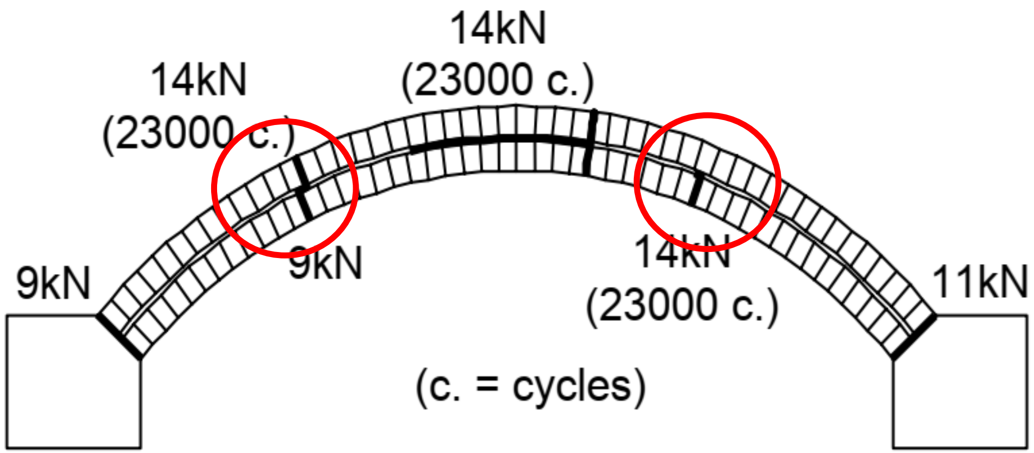

Fatigue in Masonry: Cyclic Validation

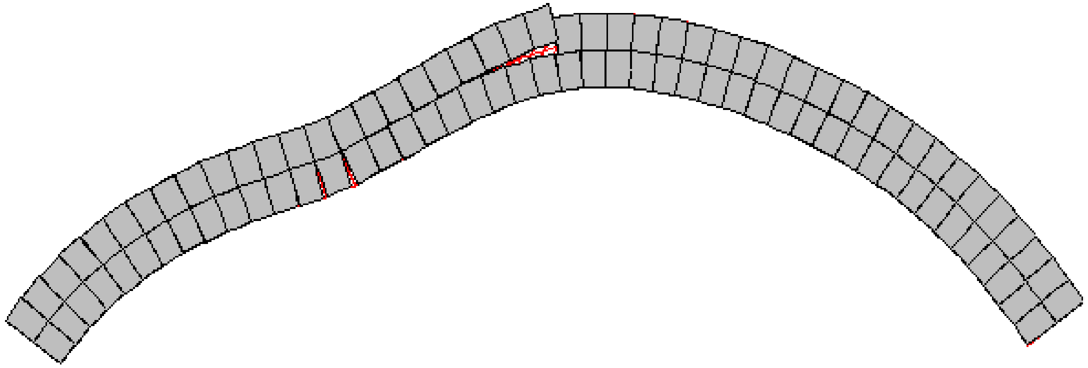

Cycles	Observed damage
48	Damage initialisation at 1/4 and 3/4 span
1201	**Fully cracked quarter span joints and initialisation of damage at the supports**
23101	Development of circumferential cracks, ring sliding and arch failure

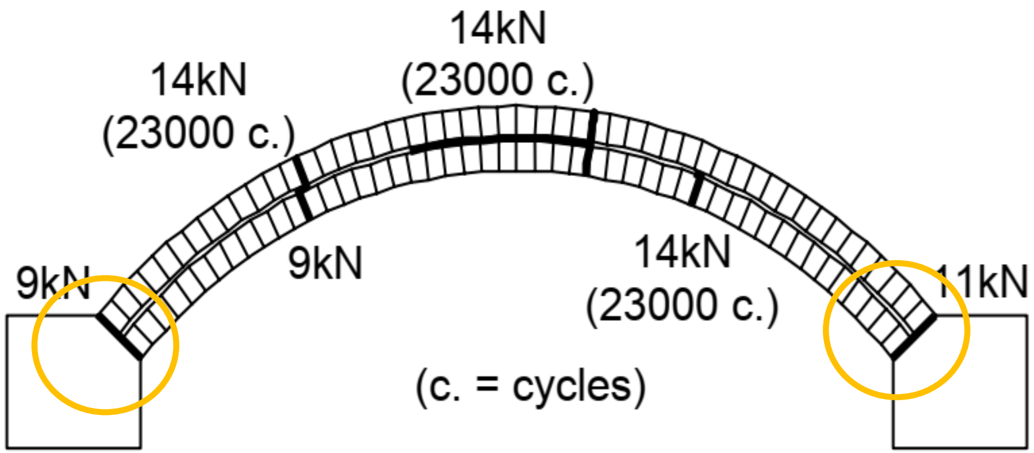

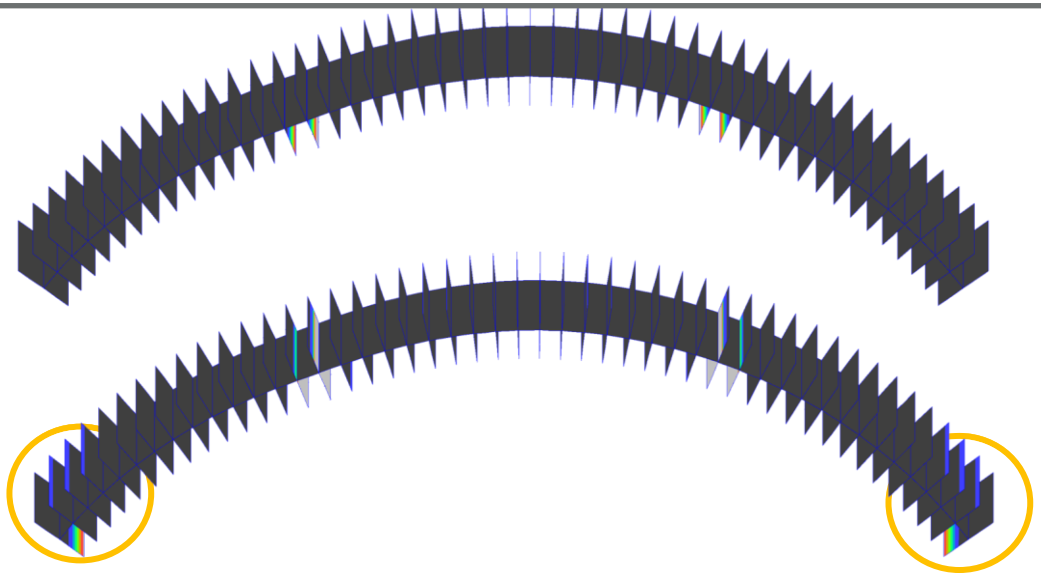

Fatigue in Masonry: Cyclic Validation

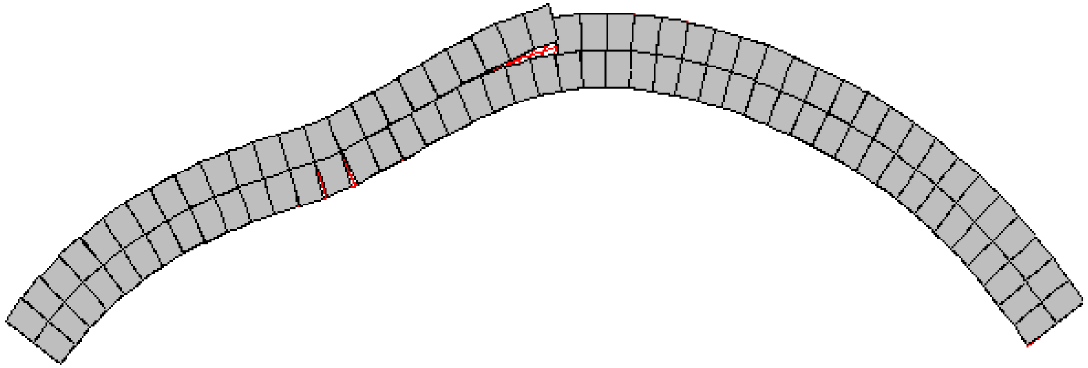

Cycles	Observed damage
48	Damage initialisation at 1/4 and 3/4 span
1201	**Fully cracked quarter span joints and initialisation of damage at the supports**
23101	Development of circumferential cracks, ring sliding and arch failure

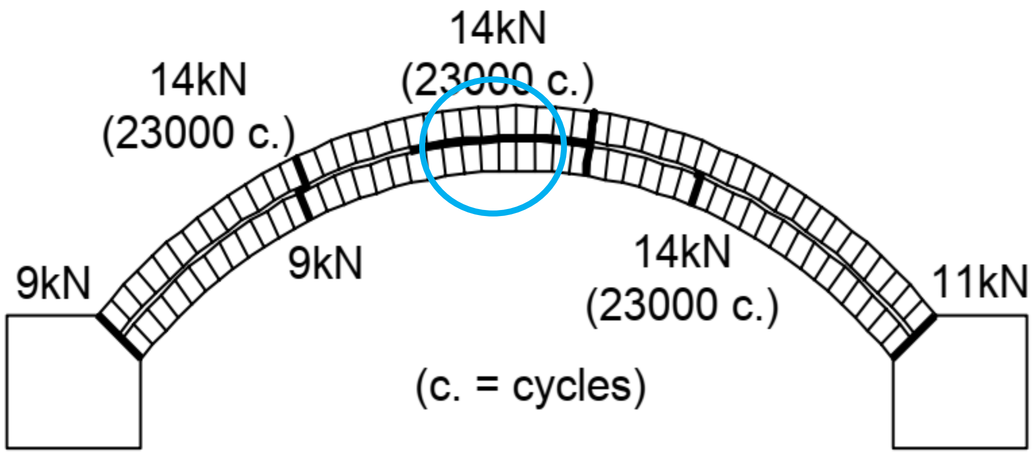

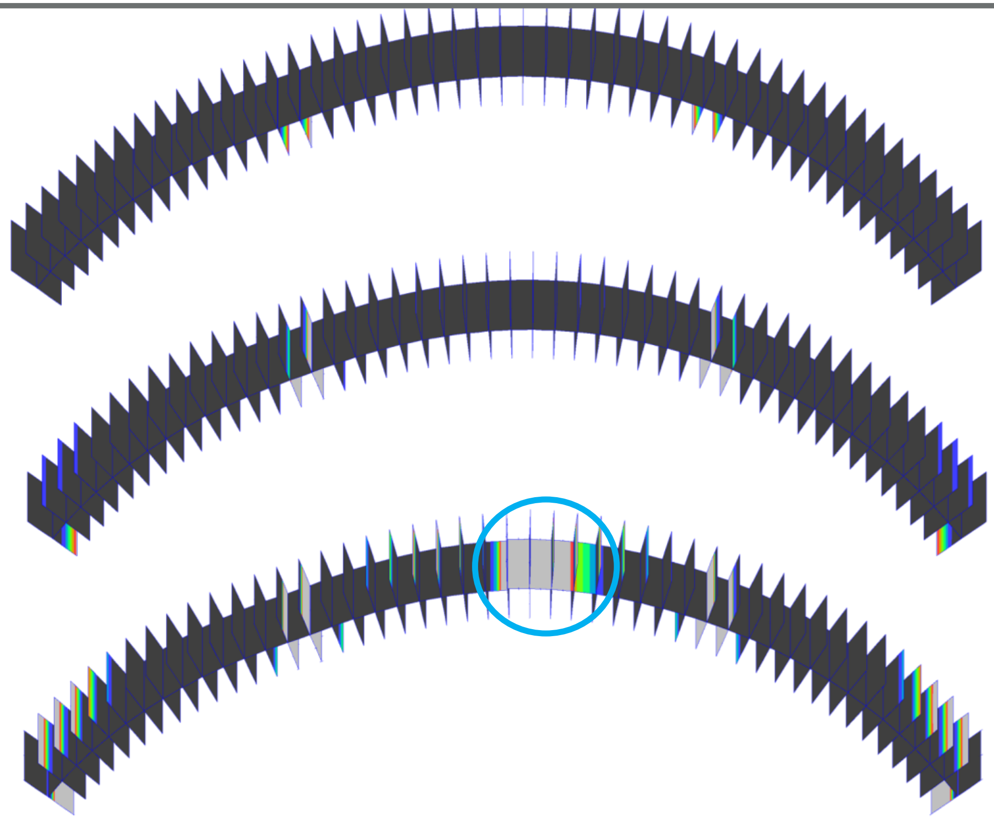

Fatigue in Masonry: Parametric study

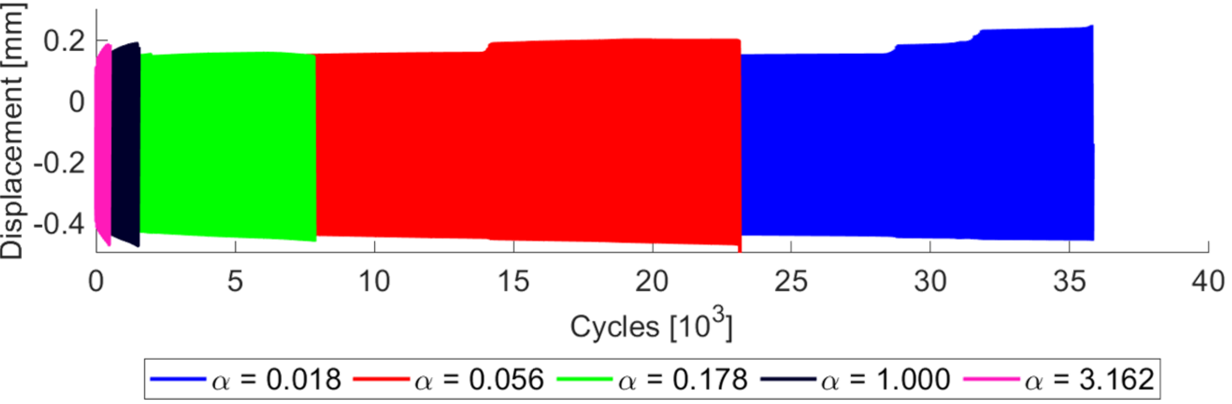

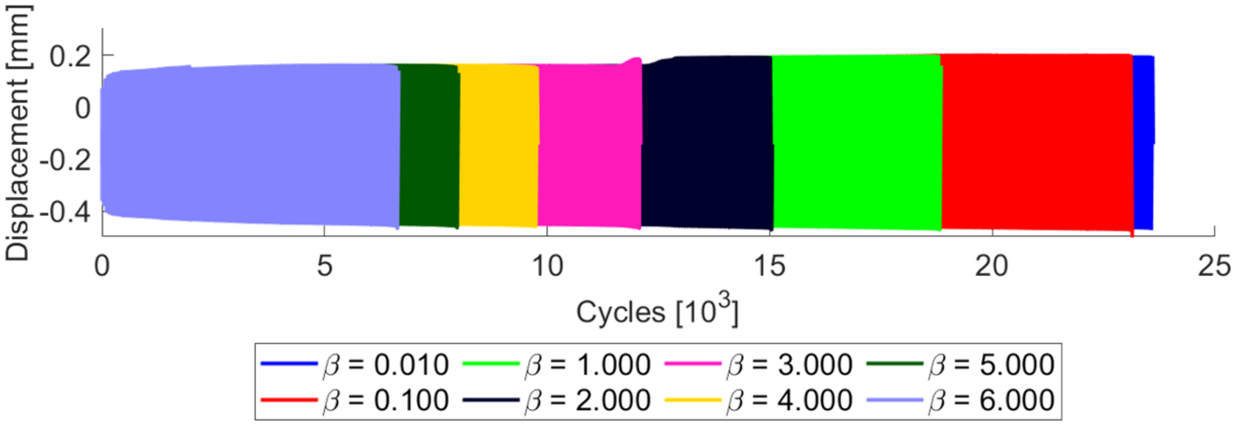

$$\dot{D}_a = \alpha_a \cdot (1 - D_a) \cdot e^{\beta_a \cdot D_a} \cdot \langle \tilde{\sigma}_a - \eta_\alpha \cdot \tilde{\sigma}_{0,a} \rangle \cdot \dot{\varepsilon}_a$$

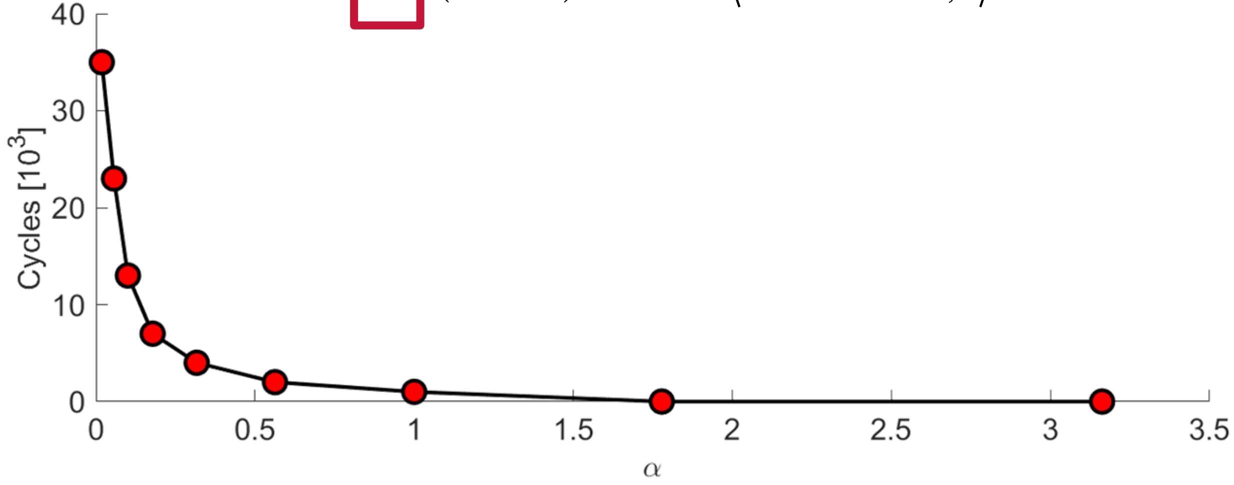

$$\dot{D}_a = \alpha_a \cdot (1 - D_a) \cdot e^{\beta_a \cdot D_a} \cdot \langle \tilde{\sigma}_a - \eta_\alpha \cdot \tilde{\sigma}_{0,a} \rangle \cdot \dot{\varepsilon}_a$$

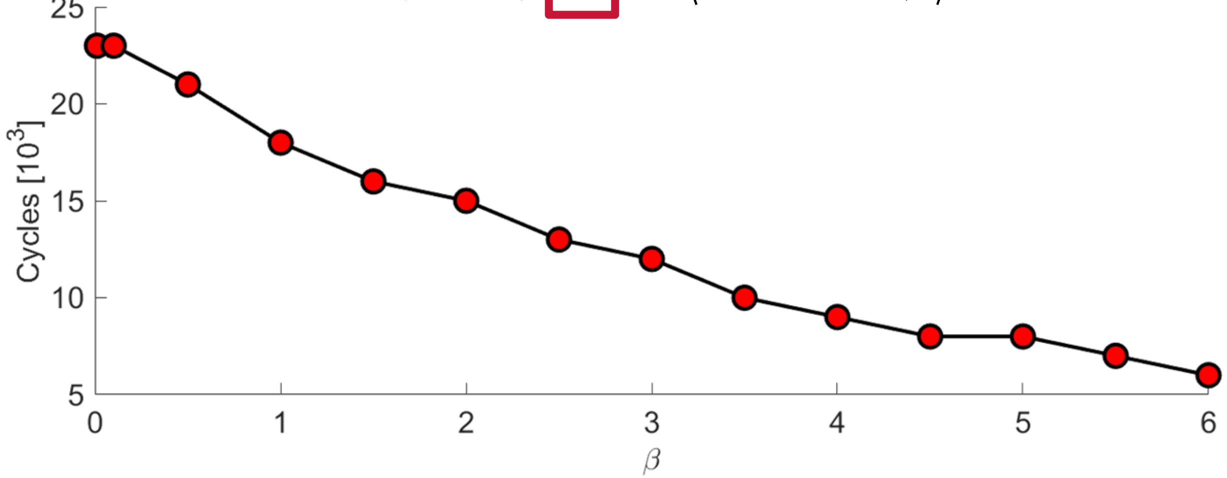

Fatigue in Masonry: Parametric study

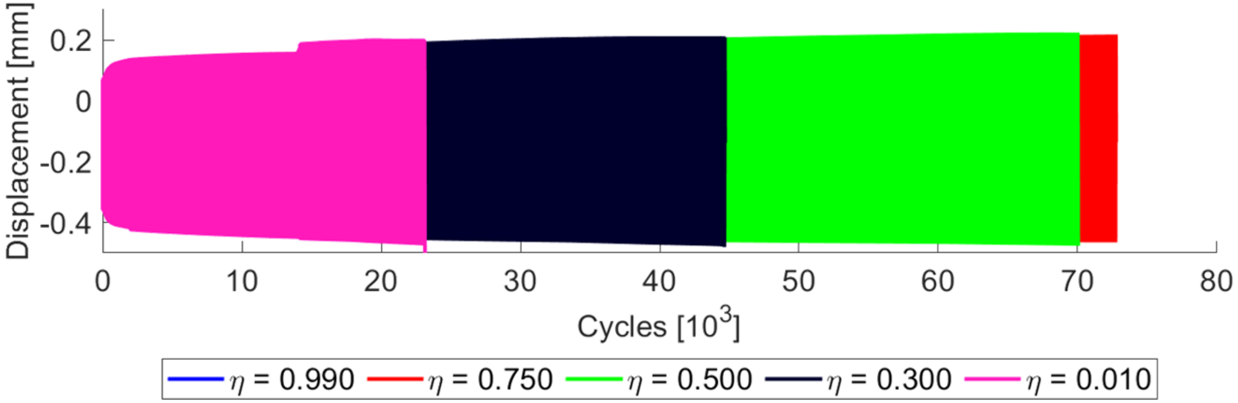

$$\dot{D}_a = \alpha_a \cdot \left(1 - D_a\right) \cdot e^{\beta_a \cdot D_a} \cdot \left\langle \tilde{\sigma}_a - \eta_\alpha \, \tilde{\sigma}_{0,a} \right\rangle \cdot \dot{\varepsilon}_a$$

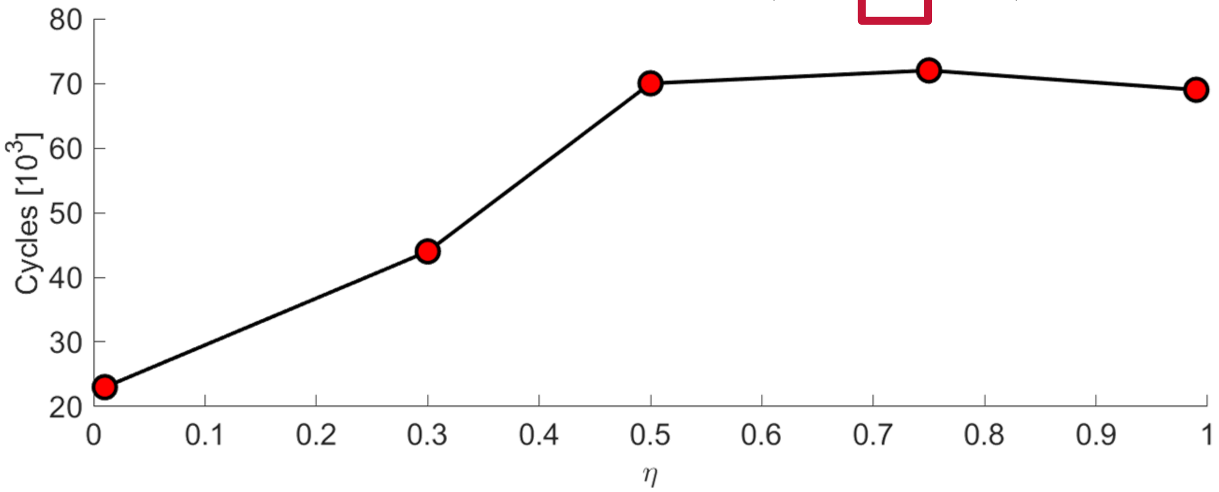

Engineering and Physical Sciences Research Council

Fatigue in Masonry: Parametric study

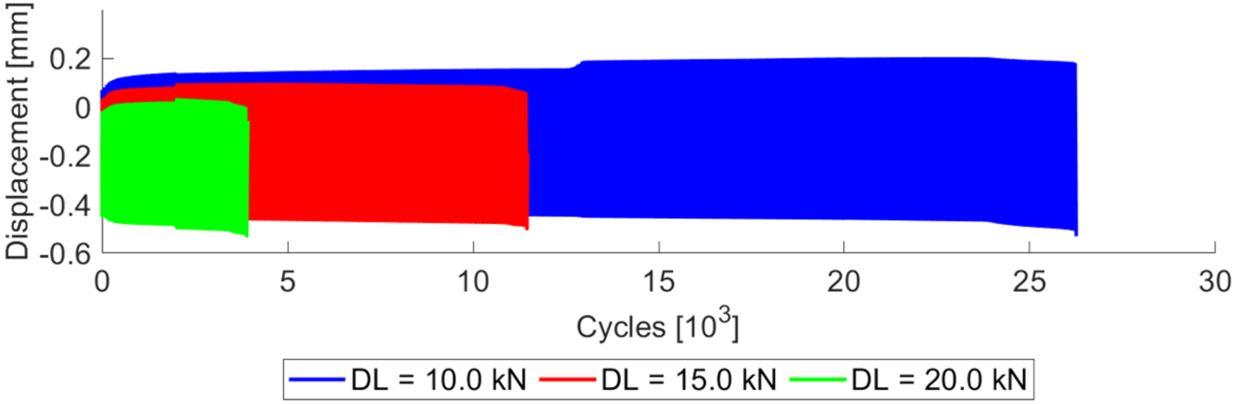

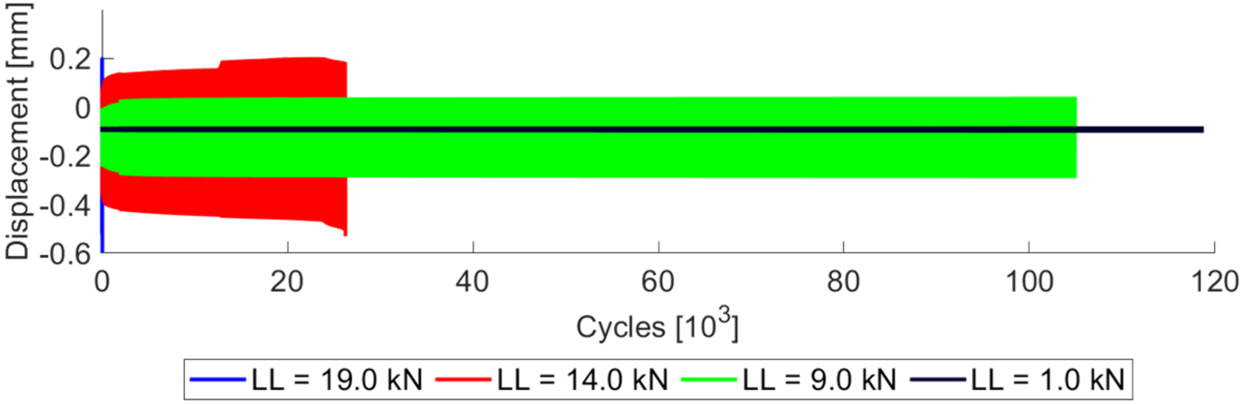

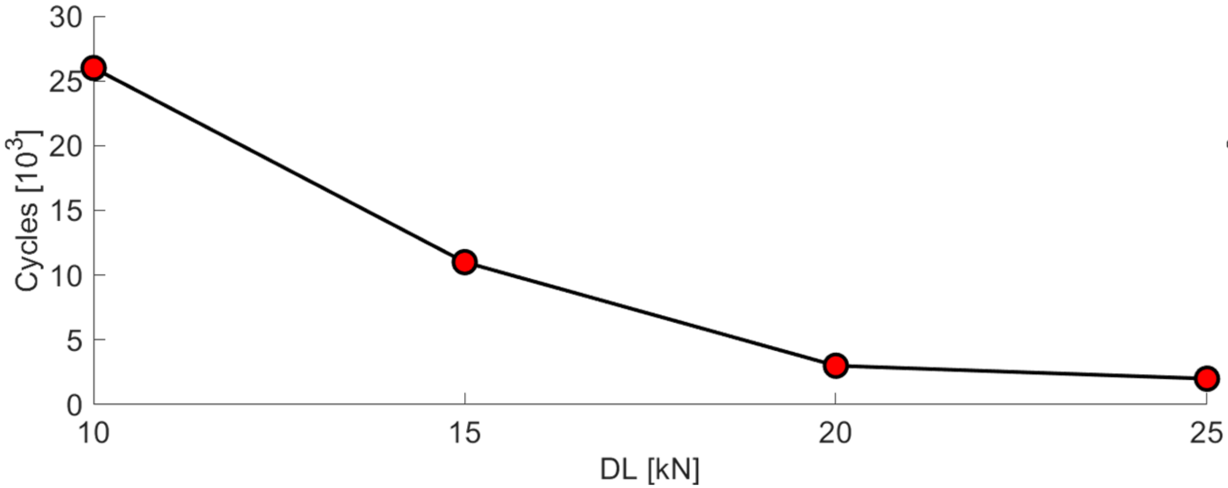

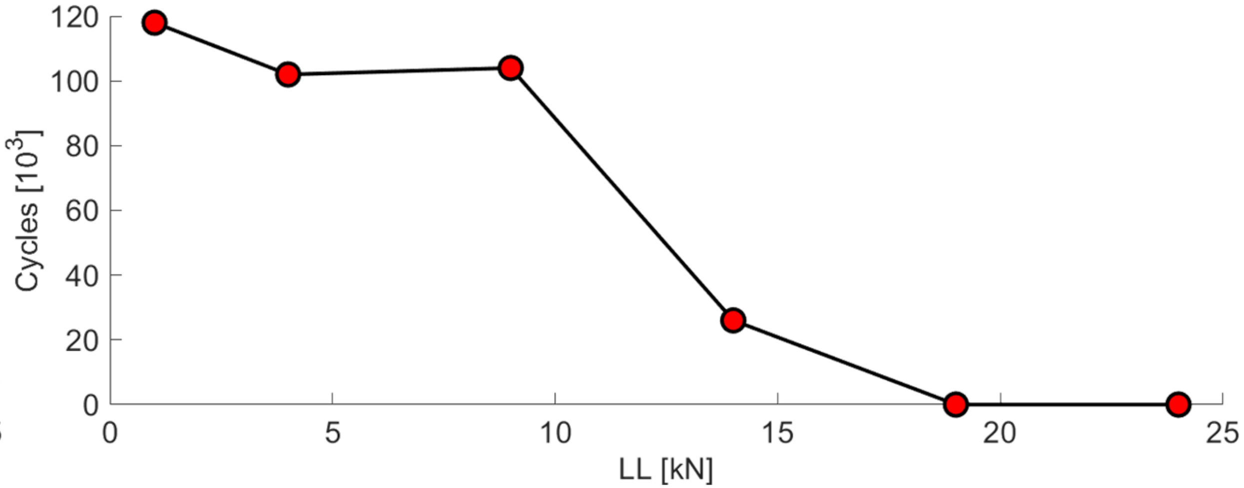

Imperial College London

Engineering and Physical Sciences Research Council

Fatigue in Masonry: Parametric study

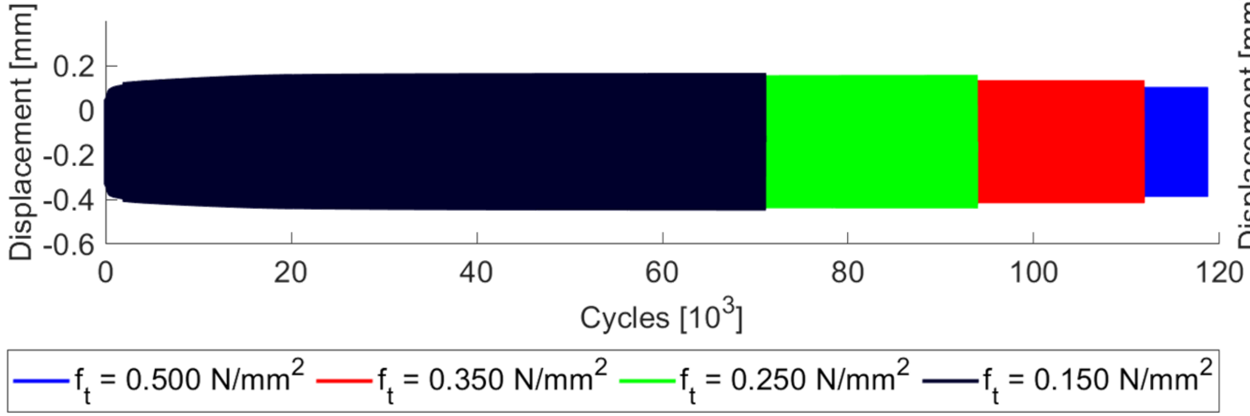

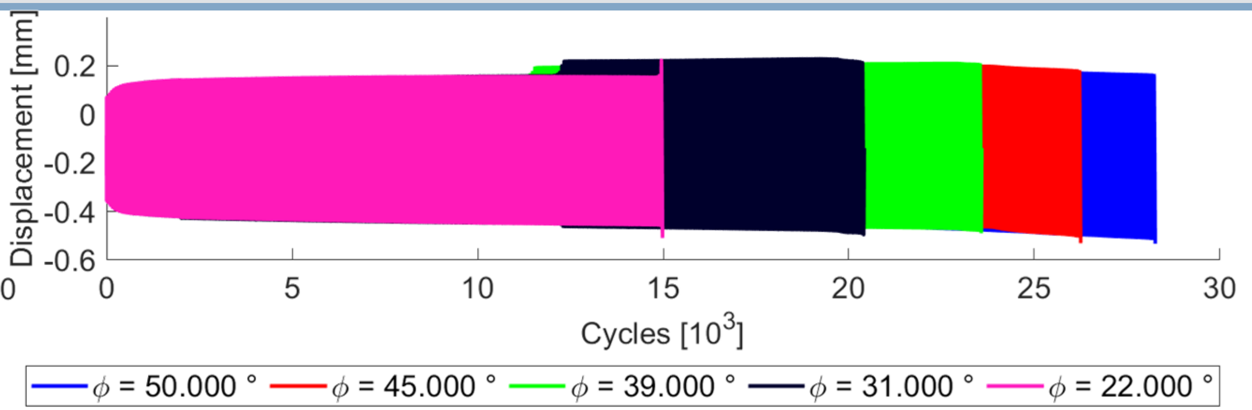

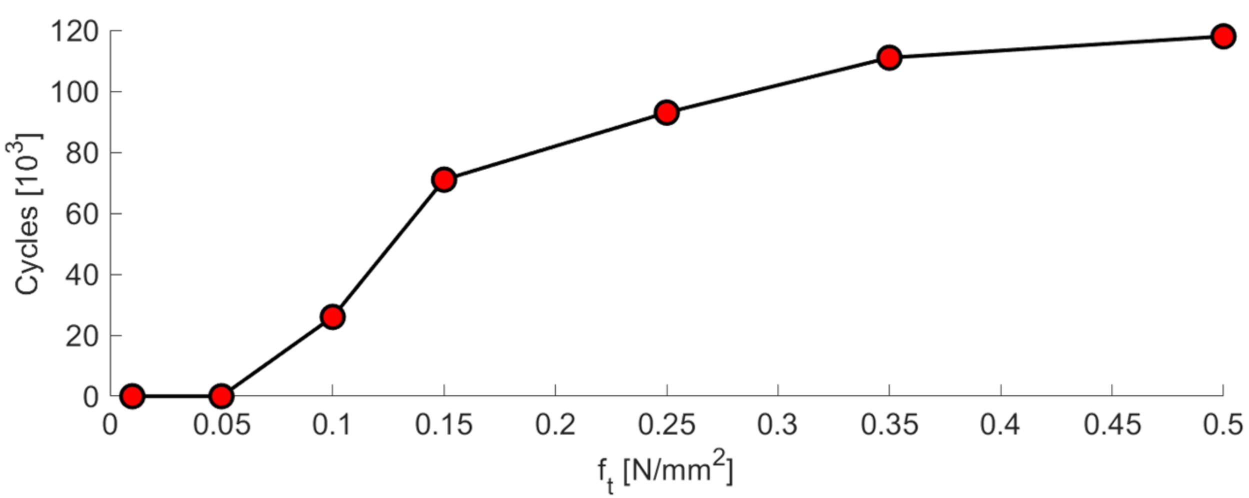

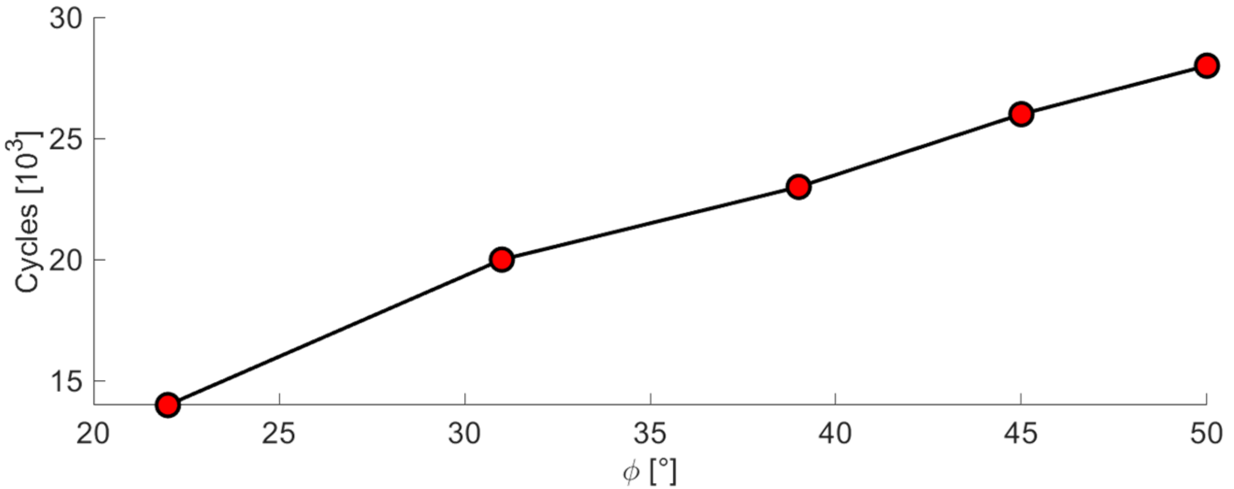

Conclusions

Conclusions

- The developed high-fidelity models for masonry arch bridges enable **accurate response predictions at different loading levels up to collapse;**
- **Damage pattern and propagation** can also be captured with high degree of accuracy;
- **Reduced models** with solid elements and nonlinear interfaces show high potential when assessing the ultimate capacity. Importantly, they also lead to realistic estimates of crack development and propagation in the masonry components;
- Preliminary investigations have showed the potential of the proposed damage fatigue approach in **predicting the fatigue response** of masonry arches subjected to cyclic loading;
- In future research, the developed masonry mesoscale fatigue model will be used to study the behaviour of masonry arch bridges allowing for arch-backfill interaction and 3D effects under repeated loading.